

INFORMATION TO USERS

This manuscript has been reproduced from the microfilm master. UMI films the text directly from the original or copy submitted. Thus, some thesis and dissertation copies are in typewriter face, while others may be from any type of computer printer.

The quality of this reproduction is dependent upon the quality of the copy submitted. Broken or indistinct print, colored or poor quality illustrations and photographs, print bleedthrough, substandard margins, and improper alignment can adversely affect reproduction.

In the unlikely event that the author did not send UMI a complete manuscript and there are missing pages, these will be noted. Also, if unauthorized copyright material had to be removed, a note will indicate the deletion.

Oversize materials (e.g., maps, drawings, charts) are reproduced by sectioning the original, beginning at the upper left-hand corner and continuing from left to right in equal sections with small overlaps.

Photographs included in the original manuscript have been reproduced xerographically in this copy. Higher quality 6" x 9" black and white photographic prints are available for any photographs or illustrations appearing in this copy for an additional charge. Contact UMI directly to order.

Bell & Howell Information and Learning
300 North Zeeb Road, Ann Arbor, MI 48106-1346 USA
800-521-0600

UMI[®]

University of Alberta

OPTIMAL DESIGN OF TRANSMULTIPLEXERS

by

Ting Liu



A thesis submitted to the Faculty of Graduate Studies and Research in partial fulfillment of the requirements for the degree of **Master of Science**.

Department of Electrical and Computer Engineering

Edmonton, Alberta
Fall 1999



**National Library
of Canada**

**Acquisitions and
Bibliographic Services**

**395 Wellington Street
Ottawa ON K1A 0N4
Canada**

**Bibliothèque nationale
du Canada**

**Acquisitions et
services bibliographiques**

**395, rue Wellington
Ottawa ON K1A 0N4
Canada**

Your file Votre référence

Our file Notre référence

The author has granted a non-exclusive licence allowing the National Library of Canada to reproduce, loan, distribute or sell copies of this thesis in microform, paper or electronic formats.

The author retains ownership of the copyright in this thesis. Neither the thesis nor substantial extracts from it may be printed or otherwise reproduced without the author's permission.

L'auteur a accordé une licence non exclusive permettant à la Bibliothèque nationale du Canada de reproduire, prêter, distribuer ou vendre des copies de cette thèse sous la forme de microfiche/film, de reproduction sur papier ou sur format électronique.

L'auteur conserve la propriété du droit d'auteur qui protège cette thèse. Ni la thèse ni des extraits substantiels de celle-ci ne doivent être imprimés ou autrement reproduits sans son autorisation.

0-612-47059-8

Canada

University of Alberta

Library Release Form

Name of Author: Ting Liu

Title of Thesis: Optimal Design of Transmultiplexers

Degree: Master of Science

Year this Degree Granted: 1999

Permission is hereby granted to the University of Alberta Library to reproduce single copies of this thesis and to lend or sell such copies for private, scholarly or scientific research purposes only.

The author reserves all other publication and other rights in association with the copyright in the thesis, and except as hereinbefore provided, neither the thesis nor any substantial portion thereof may be printed or otherwise reproduced in any material form whatever without the author's prior written permission.

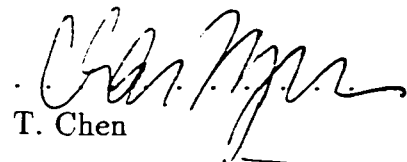
Ting Liu
Ting Liu
CEB 238, Dept. of EE
Univ. of Alberta, AB
Canada, T6G 2C7

Date: *May 20, 1999.*

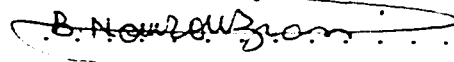
University of Alberta

Faculty of Graduate Studies and Research


The undersigned certify that they have read, and recommend to the Faculty of Graduate Studies and Research for acceptance, a thesis entitled **Optimal Design of Transmultiplexers** submitted by Ting Liu in partial fulfillment of the requirements for the degree of **Master of Science**.



T. Chen



B. Nowrouzian



B. Huang

Date: *May 20, 1999*

To my parents...

Abstract

Optimal designs of multi-channel, uniform- and nonuniform-band transmultiplexers are considered. For uniform transmultiplexers, a measure based on 2-norm of transfer matrices is proposed to quantify the degree of closeness to perfect reconstruction; connections of this error measure to the traditional cross-talk, magnitude, and phase distortions are established. An optimal design procedure for FIR analysis filters is developed and applied to two design examples.

In the nonuniform case, it is well known that using traditional building blocks — up- and downsamplers and linear time-invariant (LTI), causal filters — nonuniform transmultiplexers typically do not achieve perfect reconstruction. To alleviate this, we propose to build nonuniform transmultiplexers using general dual-rate structures which provide more design freedom and hence perfect reconstruction can be achieved. Such general transmultiplexers have a new source of error called *aliasing distortion*, in addition to the traditional cross-talk, magnitude, and phase distortions. Similarly, we propose a new composite error criterion based on the 2-norm of the *blocked* error system which captures all four distortions in one. Using this error criterion as reconstruction performance measure, we develop an iterative optimal design procedure and apply it to a three-channel nonuniform example, yielding an FIR transmultiplexer which has good frequency limiting properties in the synthesis end and is very close to perfect reconstruction.

Acknowledgements

I would like to thank my supervisor Tongwen Chen. Dr. Chen gave me a lot of grateful help in my research and many helpful suggestions in the preparation of this thesis. I also want to thank him for his help with proof reading this thesis. Finally, I want to thank Dr. Horacio J. Marquez for his advice during my graduate course study.

Contents

1	Introduction	1
1.1	Applications of Multirate Systems	1
1.1.1	Digital Time Division Multiplexing (TDM) to Frequency Division Multiplexing (FDM) Translation	1
1.1.2	Short-Time Spectral Analysis and Synthesis	2
1.1.3	Application in Communications	3
1.2	Organization of the Thesis	3
2	Filter Banks and Transmultiplexers	6
2.1	Decimation and Interpolation	6
2.1.1	The M -fold Decimator	6
2.1.2	The L -fold Expander	7
2.1.3	Decimation Filters and Interpolation Filters	9
2.1.4	The Noble Identities	11
2.2	Filter Banks and Transmultiplexers	12
2.3	Errors Created By Filter Bank Systems	15
2.4	Polyphase Decomposition	16
2.5	Perfect Reconstruction of Filter Banks	20
2.6	\mathcal{H}_2 Norm	21
2.6.1	Norms of Signals	21
2.6.2	Norms of SISO Systems	21
2.6.3	Norms of Multivariable Systems	22
3	Optimal Design of Uniform Transmultiplexers	24
3.1	Applications of Transmultiplexers	25

3.2	Input-Output Relation for Uniform Transmultiplexers	27
3.3	Polyphase Decomposition	29
3.4	Perfect Reconstruction	30
3.4.1	The Conditions for Perfect Reconstruction	30
3.4.2	Relation to Perfect Reconstruction (PR) Filter Banks	31
3.5	Distortion Measures	34
3.6	Optimal Design Procedures	39
3.7	Design Examples	41
4	Optimal Design of Nonuniform Transmultiplexers Using General Building Blocks	48
4.1	Introduction	48
4.2	Blocked Models	51
4.2.1	Blocking Signals	52
4.2.2	Blocking Systems	53
4.2.3	Blocking Analysis Subsystems	54
4.2.4	Blocking Synthesis Subsystems	55
4.2.5	Blocking the Transmultiplexer System	56
4.3	Realization of Dual-Rate Systems via Linear Switching Time-Varying Structures	57
4.4	Perfect Reconstruction	61
4.5	Distortion Measures	62
4.6	Design Procedures	65
4.7	A Design Example	67
5	Conclusions	76

List of Figures

1.1	Illustration of (a) a TDM-FDM translator; (b) an FDM-TDM translator.	2
1.2	Spectral interpretation of TDM-FDM signal translation.	3
1.3	(a) Example of a short-time spectral analysis/synthesis system with spectral modification; and (b) an illustration of the sliding window framework of this process.	4
2.1	Decimator.	6
2.2	Demonstration of decimation for $M = 3$	7
2.3	Frequency-domain effects of decimator for $M = 2$	7
2.4	Expander.	7
2.5	Demonstration of expander for $L = 2$	8
2.6	Frequency-domain effects of expander for $L = 2$	8
2.7	The complete decimation circuit.	9
2.8	The complete interpolation circuit.	9
2.9	Scheme for A/D stage of a digital audio system.	10
2.10	Fractional sampling rate alteration.	10
2.11	The noble identities for multirate systems.	11
2.12	An M -channel filter bank.	12
2.13	Typical frequency responses of the analysis filters.	13
2.14	Splitting a signal into subband signals $x_0(n)$ and $x_1(n)$	14
2.15	The two channel filter bank for subband coding.	14
2.16	An M -channel uniform-band transmultiplexer.	15
2.17	Polyphase representation of the M -channel filter bank in Figure 2.12.	19
2.18	Rearrangement using noble identities.	19
2.19	The polyphase identity.	20

2.20	A SISO system.	21
2.21	An MIMO system.	22
3.1	An M -channel uniform-band transmultiplexer.	24
3.2	M -band transmultiplexer structure for CDMA communications	25
3.3	A basic structure of a DMT modulation-based digital ADSL transceiver. . .	26
3.4	The relation between $\hat{x}_k(n)$ and $x_m(n)$	28
3.5	Polyphase decomposition of the transmultiplexer in Figure 3.1.	30
3.6	Rearrangement using noble identities.	30
3.7	The equivalent form of Figure 3.6.	31
3.8	The error system between the transmultiplexer and the ideal system. . . .	37
3.9	$\sin^{-1} A_i$	38
3.10	Example 1: The magnitude responses for F_0 (solid) and F_1 (dotted): dB versus $\omega/2\pi$	42
3.11	Example 1: J_{opt} versus the reconstruction delay d	43
3.12	Example 1: The simulation results of the error system with inputs (solid) and outputs (dotted).	44
3.13	Example 1: The magnitude responses for the optimal H_0 (solid) and H_1 (dotted): dB versus $\omega/2\pi$	45
3.14	Example 2: The magnitude responses for F_0 (solid), F_1 (dotted) and F_2 (dashed): dB versus $\omega/2\pi$	46
3.15	Example 2: The simulation results of the error system with inputs (solid) and outputs (dashed).	46
3.16	Example 1: The magnitude responses for the optimal H_0 (solid), H_1 (dotted) and H_2 (dashed): dB versus $\omega/2\pi$	47
4.1	A nonuniform transmultiplexer using traditional building blocks.	48
4.2	A sample-rate changer.	49
4.3	A dual-rate system.	50
4.4	A nonuniform transmultiplexer using general building blocks.	51
4.5	An analysis subsystem.	54
4.6	A synthesis subsystem.	55
4.7	An $[r, s]$ -LSTV system.	57

4.8	The structure of an $[r, s]$ -LSTV system.	58
4.9	Implementation of a (p, q) -shift invariant system via an LSTV structure.	59
4.10	A three-channel nonuniform transmultiplexer using traditional building blocks.	68
4.11	The magnitude responses for the initial F_0 (solid), F_1 (dotted) and F_2 (dash-dot): dB versus $\omega/2\pi$	69
4.12	The magnitude responses for the designed F_0 (solid), F_1 (dotted) and F_2 (dash-dot): dB versus $\omega/2\pi$	71
4.13	The magnitude responses for the designed H_0 (solid), H_1 (dotted) and H_2 (dash-dot): dB versus $\omega/2\pi$	72
4.14	A three-channel nonuniform transmultiplexer using general analysis building blocks.	72
4.15	The magnitude responses for the designed F_0 (solid), F_1 (dotted) and F_2 (dash-dot): dB versus $\omega/2\pi$	74
4.16	The magnitude responses for the designed $H_{0,0}$ (solid), $H_{0,1}$ (dotted): dB versus $\omega/2\pi$	74
4.17	The magnitude responses for the designed $H_{1,0}$: dB versus $\omega/2\pi$	75
4.18	The magnitude responses for the designed $H_{2,0}$ (solid), $H_{2,1}$ (dotted) and $H_{2,2}$ (dash-dot): dB versus $\omega/2\pi$	75

Chapter 1

Introduction

1.1 Applications of Multirate Systems

The area of multirate digital signal processing is basically concerned with problems in which more than one sampling rates are required in a digital system. It is an especially important part of modern (digital) telecommunications theory in which digital transmission systems are required to handle data at several rates.

Multirate techniques have been in use for many years. The use of multiple sampling rates offers many advantages, such as reduced computational complexity for a given task, reduced transmission rate (i.e. bits per second), and/or reduced storage requirement, depending on the application. In summary, the multirate techniques have been applied in a wide variety of areas in signal processing [11, 19, 27]. Some of the applications are discussed below.

1.1.1 Digital Time Division Multiplexing (TDM) to Frequency Division Multiplexing (FDM) Translation

An application of multirate digital systems is the translation of signals in a telephone system between time division multiplexed (TDM) and frequency division multiplexed (FDM) formats [17, 42, 16]. The FDM format is often used for long distance transmission, whereas the TDM format is more convenient for digital switching.

Figure 1.1 illustrates the basic process of translating a series of 12 TDM digital speech signals, $s_1(n)$, $s_2(n)$, \dots , $s_{12}(n)$, to a single FDM signal $r(m)$ and the reverse (FDM to TDM) translation process. The sampling rate of the TDM speech signals is 8kHz. In each channel of the TDM-to-FDM translator the sampling rate is

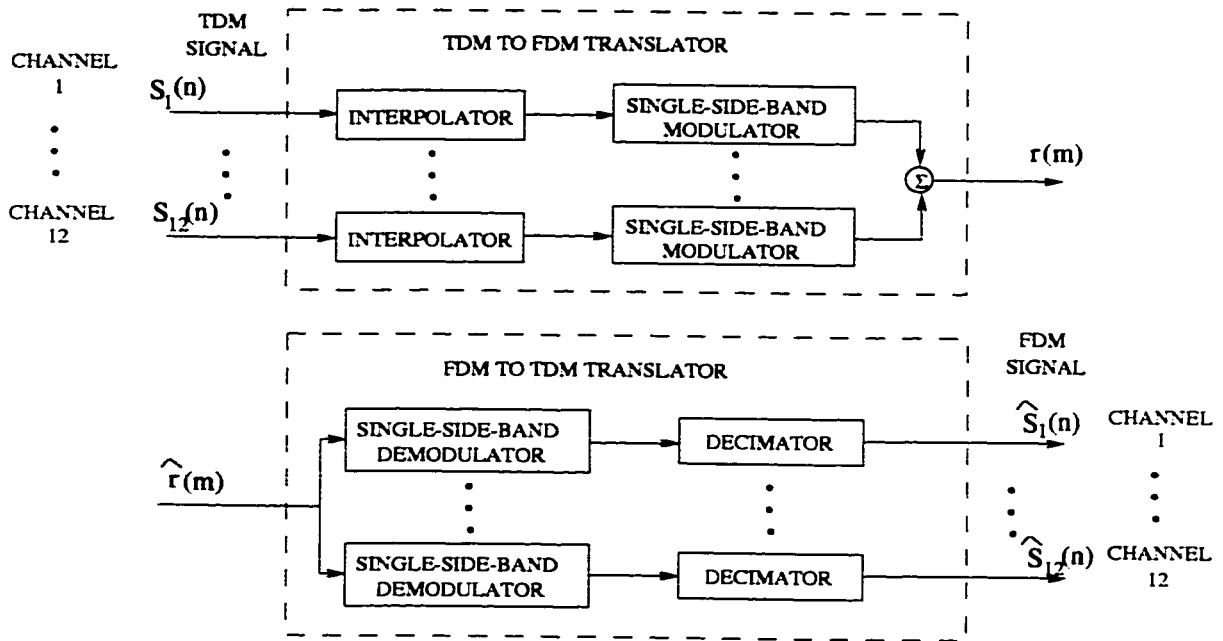


Figure 1.1: Illustration of (a) a TDM-FDM translator; (b) an FDM-TDM translator.

effectively increased (by interpolation) to the higher FDM sampling rate. The signal is then modulated to its appropriate frequency band location in the range 56kHz to 112kHz as illustrated in Figure 1.2. The interpolated and modulated channel signals are then digitally summed to give the desired FDM signal. In the FDM-to-TDM translator the reverse process takes place.

As seen from Figure 1.1, the process of translation between TDM and FDM formats involves sampling rate conversion and therefore these systems are inherently multirate systems.

1.1.2 Short-Time Spectral Analysis and Synthesis

Another example of multirate signal processing systems is a short-time spectral analysis and synthesis system [31]. Such systems are widely used in the areas of speech processing, antenna, and radar systems. Figure 1.3 gives a simplified explanation of a spectrum analysis-synthesis system. The signal $s(n)$ is periodically windowed with a sliding window (shown in Figure 1.3) to form a short-time, finite duration piece of signal at each time slot. This short-time signal is then transformed with a fast DFT (discrete Fourier transform) algorithm to form a short-time spectral estimate of the signal for that time slot. Then the signal may be modified in a variety of ways (or

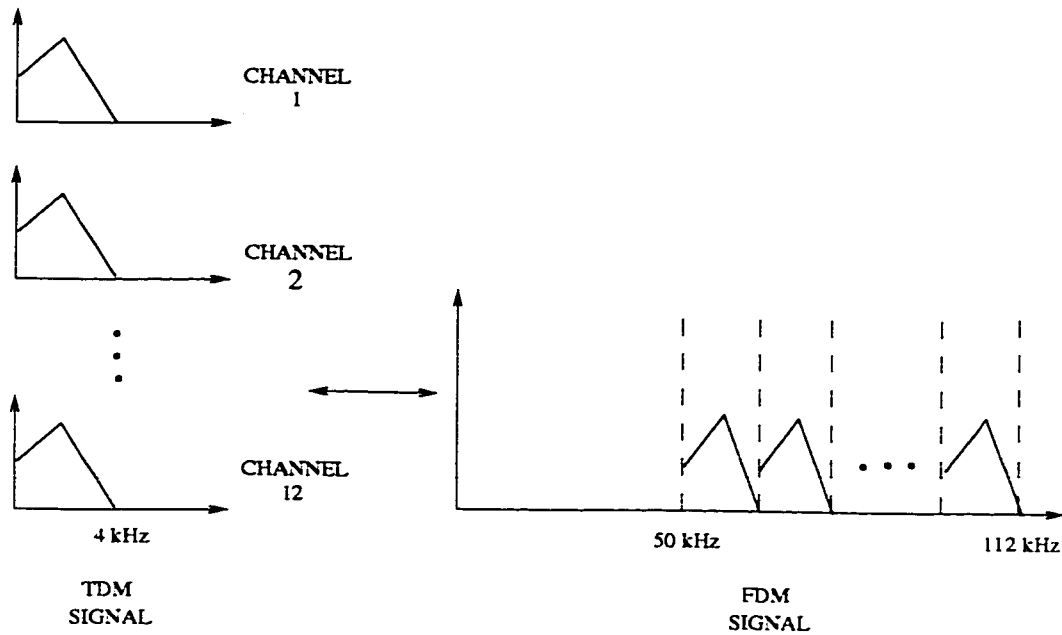


Figure 1.2: Spectral interpretation of TDM-FDM signal translation.

the short-time spectrum may be an end result in itself). The modified short-time spectrum is then inverse transformed to form a modified short-time segment of the signal. Finally, a reconstructed, modified signal $\hat{s}(n)$ is obtained by appropriately overlapping and summing the modified signal segments from each time slot.

1.1.3 Application in Communications

A third application of multirate sampling techniques is in the area of digital communications [18]. In communication networks a variety of different coding formats may be used in different parts of the network to achieve flexibility and efficiency. Conversion between these coding formats often involves a conversion of the basic sampling rate.

Other applications of multirate systems such as sampling rate conversion in digital audio systems and subband coding will be discussed later.

1.2 Organization of the Thesis

Our work focuses on the optimal design of uniform and nonuniform transmultiplexers. The thesis is organized as follows. In Chapter 2 we introduce some basic ideas of

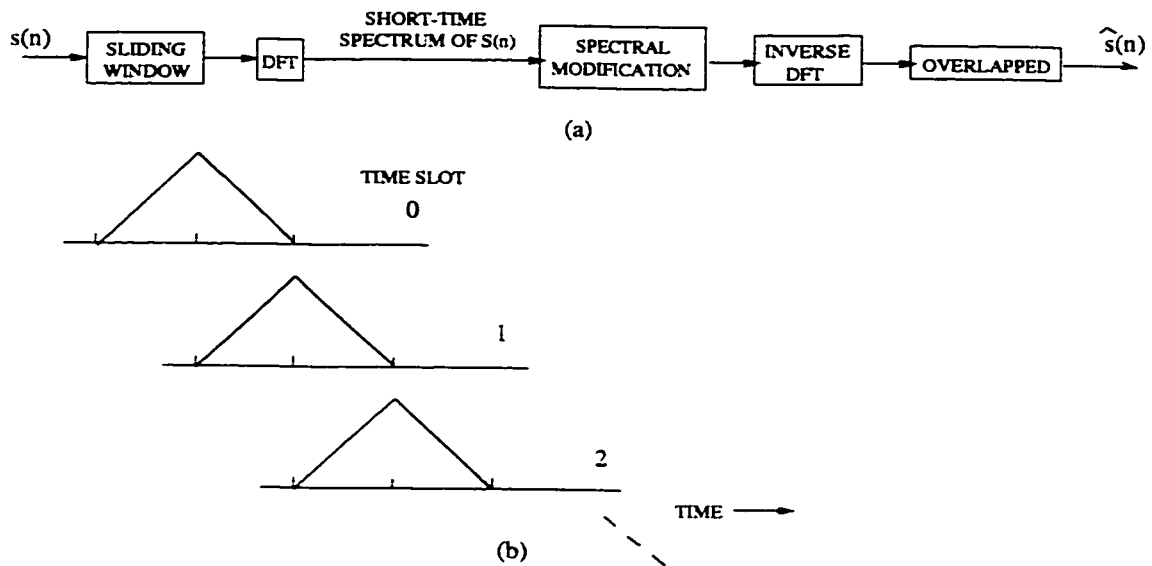


Figure 1.3: (a) Example of a short-time spectral analysis/synthesis system with spectral modification; and (b) an illustration of the sliding window framework of this process.

filter banks and transmultiplexers. Chapter 3 and Chapter 4 propose the optimal design methods of uniform and nonuniform transmultiplexers, respectively, with design examples. Chapter 5 concludes the thesis, and points out some future work.

Briefly, the contributions of this thesis are as follows.

- A single error criterion using the 2-norm of transfer matrices for the uniform case (or the nonuniform case) is introduced, which is relatively easy to be optimized and can capture the distortions (such as cross-talk, magnitude and phase distortions) all in one.
- We propose ways to measure the distortions associated with a non-perfect reconstruction transmultiplexer: cross-talk, magnitude and phase distortions, and a new aliasing distortion in the nonuniform case.
- Employing the blocking technique, we derive a blocked LTI model for nonuniform transmultiplexers; based on the blocked model, we give conditions for perfect reconstruction.
- We develop an optimal iterative design procedure for FIR subsystems. By fixing the synthesis or analysis subsystems in each step, the optimization problems are

finite-dimensional, convex optimization with a quadratic cost function, whose global optimal solution can be computed.

Chapter 2

Filter Banks and Transmultiplexers

2.1 Decimation and Interpolation

The most basic operations in multirate signal processing are *decimation* and *interpolation*. In order to describe these, two building blocks, called *decimator* and *expander*, are introduced.

2.1.1 The M -fold Decimator

Figure 2.1 shows the M -fold decimator – see [38] for details, which takes an input sequence $x(n)$ and produces the output sequence

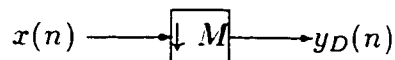


Figure 2.1: Decimator.

$$y_D(n) = x(Mn),$$

where M is an integer. Only those samples of $x(n)$ which occur at times equal to multiples of M are retained by the decimator. Figure 2.2 shows the idea of this operation. The decimator is also called a *downsampler*. It is easy to see that it may not be possible to recover $x(n)$ from $y_D(n)$ because of loss of information.

Using z -transforms, we can derive an expression for the output $Y_D(z)$ in terms of $X(z)$ [38]:

$$Y_D(z) = \frac{1}{M} \sum_{k=0}^{M-1} X(z^{1/M} W^k), \quad (2.1)$$

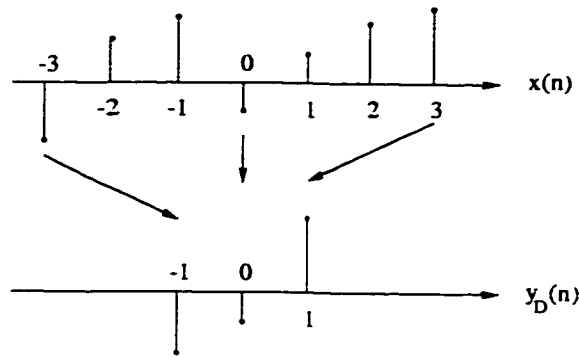


Figure 2.2: Demonstration of decimation for $M = 3$.

here $W_M = e^{-j2\pi/M}$. The changes in the frequency domain can be seen in Figure 2.3 [38], which can be graphically interpreted as follows: (a) stretch $X(e^{j\omega})$ by a factor M to obtain $X(e^{j\omega/M})$, (b) create $M - 1$ copies of this stretched version by shifting it uniformly in successive amounts of 2π , and (c) add all these shifted and stretched versions to the unshifted but stretched version $X(e^{j\omega/M})$, and divide by M . It is easy to see that if $x(n)$ is not a signal bandlimited to the region $|\omega| < \pi/M$, the stretched version $X(e^{j\omega/M})$ can overlap with its shifted replicas, which means we can not recover $x(n)$ from $y_d(n)$. This overlapping effect is called *aliasing*.

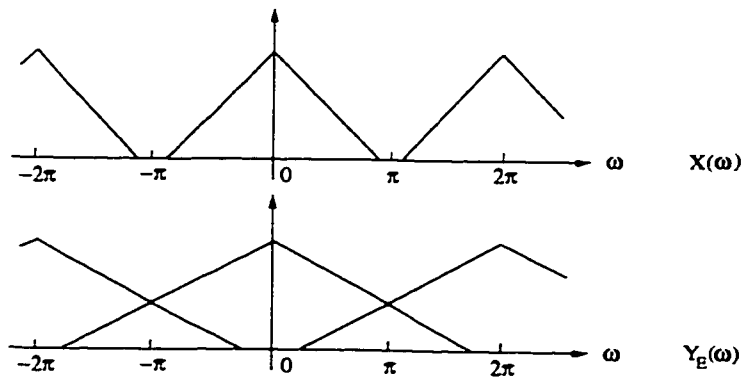


Figure 2.3: Frequency-domain effects of decimator for $M = 2$.

2.1.2 The L -fold Expander

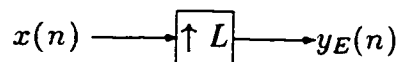


Figure 2.4: Expander.

Figure 2.4 shows the L -fold expander, where L is an integer. This device takes an input $x(n)$ and produces an output sequence [38, 11]:

$$y_E(n) = \begin{cases} x(n/L), & \text{if } n \text{ is integer multiple of } L, \\ 0, & \text{otherwise.} \end{cases} \quad (2.2)$$

Figure 2.5 shows this operation in the time domain when $L = 2$.

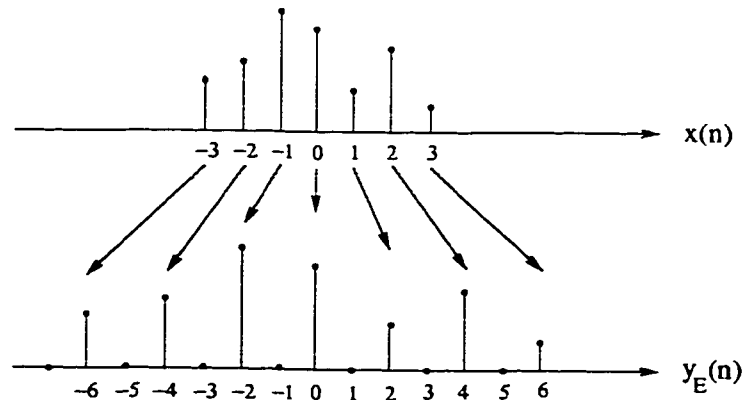


Figure 2.5: Demonstration of expander for $L = 2$.

The z -transform of $Y_E(z)$ is [38]:

$$Y_E(z) = X(z^L). \quad (2.3)$$

The frequency domain operation is shown in Figure 2.6. From (2.3) we know $Y_E(e^{j\omega}) = X(e^{j\omega L})$, which means $Y_E(e^{j\omega})$ is an L -fold compressed version of $X(e^{j\omega})$. In Figure 2.6 the other $L - 1$ copies of the compressed spectrum are called *images*.

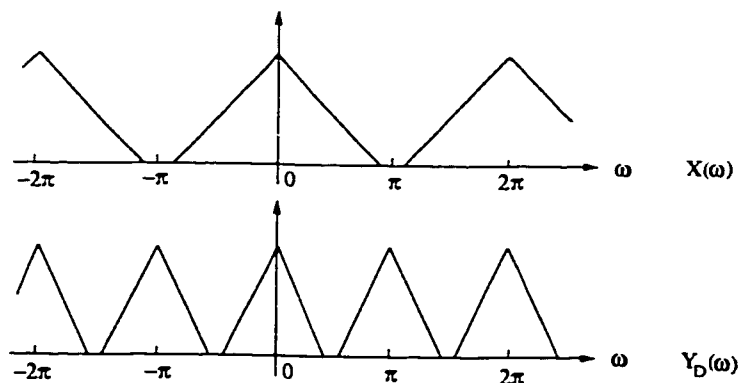


Figure 2.6: Frequency-domain effects of expander for $L = 2$

2.1.3 Decimation Filters and Interpolation Filters

Often, a decimator is preceded by a lowpass digital filter called the decimation filter, see Figure 2.7. The filter ensures that the signal being decimated is bandlimited to avoid aliasing. The exact passband of the filter depends on how much aliasing is permitted. In filter bank applications, a certain degree of aliasing is permitted because this can eventually be cancelled out [38].

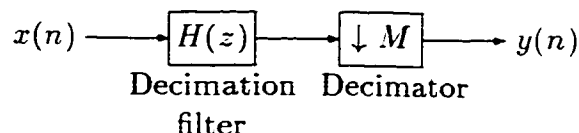


Figure 2.7: The complete decimation circuit.

An interpolation filter (see Figure 2.8) is a digital filter that follows an expander. The typical purpose is to suppress all the images. Typically the interpolation filter is lowpass with cutoff frequency π/L . Thus, it retains only the compressed spectrum, not the images (see Figure 2.6).

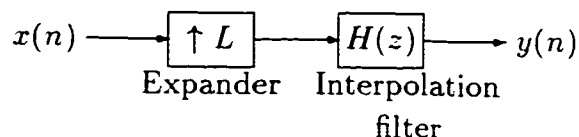


Figure 2.8: The complete interpolation circuit.

In the digital audio industry, it is a common requirement to change the sampling rates of bandlimited sequences. So the decimation and interpolation filters are widely used. For example, suppose we want to digitize an analog music waveform $x_a(t)$. Assuming that the significant information is in the band $0 \leq |\Omega|/2\pi \leq 22\text{kHz}$, a minimum sampling rate of 44kHz is suggested (Figure 2.9). It is necessary to perform analog filtering before sampling to eliminate out-of-band noise. Now the requirements on the analog filter $H_a(j\Omega)$ are stringent: It should have a fairly flat passband and a narrow transition band. Optimal filters for this purpose have a very nonlinear phase response around the bandedge, that is, around 22kHz. In high quality music this is considered to be objectionable. A method to solve this problem is to oversample

$x_a(t)$ by a factor of two. The filter $H_a(j\Omega)$ now has a much wider transition band, so that the phase-response nonlinearity is acceptably low. Such filters are sufficient to provide the required stopband attenuation to avoid aliasing. The sequence $x_1(n)$ obtained by the above oversampling method is then lowpass filtered by a digital filter $H(z)$ and then decimated by the same factor of two to obtain the final digital signal $x(n)$.

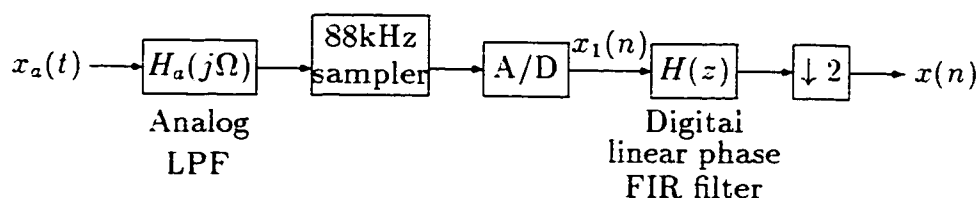


Figure 2.9: Scheme for A/D stage of a digital audio system.

A similar problem can arise after the A/D conversion stage, where the digital music signal $x(n)$ should be converted to an analog signal by lowpass filtering. To eliminate the images of $X(e^{j\omega})$ in the region higher than 22kHz, a sharp cutoff (hence nonlinear phase) analog lowpass filter is required. This problem is avoided by using an expander and a digital interpolation filter.

Decimation and interpolation techniques permit us to alter the sampling rate of a signal by an integer factor. In some applications, however, it is necessary to change the rate by a rational fraction. Figure 2.10 is a fractional sampling rate alteration. The rate is changed from $x(n)$ to $y(n)$ by a rational fraction L/M .

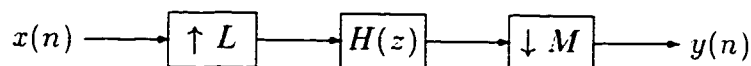


Figure 2.10: Fractional sampling rate alteration.

Fractional sampling rate alterations are very useful in communications. In digital audio, there are several applications which require fractional sampling rate alterations. This is because at least three sampling rates coexist: For most studio work, the sampling rate is 48kHz, whereas for CD mastering the rate is 44.1kHz. For broadcasting of digital audio, a sampling rate of 32kHz is expected to become the standard. To convert from studio frequency to CD mastering standards, one would use the arrangement of Figure 2.10 with $L = 441$ and $M = 480$. Such large values of L normally

imply that $H(z)$ has very high order. A multistage design (see Sec. 4.4 in [38]) is more convenient in such cases.

2.1.4 The Noble Identities

After seeing cascades of decimators and expanders with LTI systems, a different type of cascade is shown in Figure 2.11, where a filter $G(z)$ follows a decimator, and $H(z)$ precedes an expander. Such interconnections arise when we try to use the polyphase representation (discussed later) for decimation and interpolation filters. If the transfer functions $G(z)$ and $H(z)$ are rational we can redraw them as in the Figure 2.11 [38]. These are called *noble identities* and are very useful in the theory and implementation of multirate systems [38, 11].

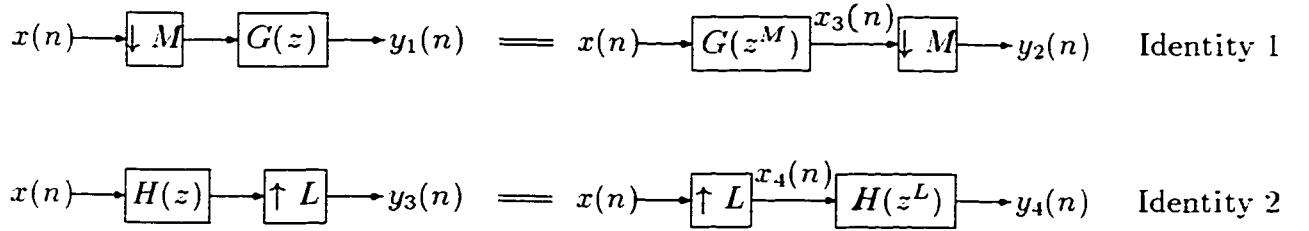


Figure 2.11: The noble identities for multirate systems.

The noble identities can be verified easily [38]. Note that

$$X_3(z) = G(z^M)X(z). \quad (2.4)$$

Substituting (2.1) into (2.4) gives

$$Y_2(z) = \frac{1}{M} \sum_{k=0}^{M-1} X(z^{1/M}W^k)G((z^{1/M}W^k)^M) = \frac{1}{M} \sum_{k=0}^{M-1} X(z^{1/M}W^k)G(z)$$

which agrees with $Y_1(z)$. Also

$$Y_4(z) = G(z^L)X_4(z) \quad (2.5)$$

Substitute (2.3) into (2.5) to get

$$Y_4(z) = G(z^L)X_4(z) = G(z^L)X(z^L) = Y_3(z),$$

this proves identity 2.

2.2 Filter Banks and Transmultiplexers

A multirate filter bank is shown in Figure 2.12. If the decimation and expansion ratio n_k are the same for all the channels, it is called a uniform Quadrature Mirror Filter (QMF) bank. Here a discrete-time signal $x(n)$ is passed through a group of digital filters $H_k(z)$ called analysis filters. All the filters in the analysis bank are frequency selective. The typical frequency responses of analysis filters are sketched in Figure 2.13. The filtered signals $x_k(n)$ (subband signals) are thus approximately band limited: x_0 is lowpass, x_{M-1} is highpass and the others are bandpass corresponding to their analysis filters H_i . They are then decimated by M , so that the number of samples per unit time (counting $v_k(n)$) is the same as that for $x(n)$. The decimated subband signals, $v_k(n)$, are then quantized and transmitted. At the received end, they are recombined by using expanders and synthesis filters $F_k(z)$. In this manner, an approximation $\hat{x}(n)$ of the signal $x(n)$ is generated.

If the decimation and expansion ratio n_k are not the same for all channels, it is called a nonuniform filter bank.

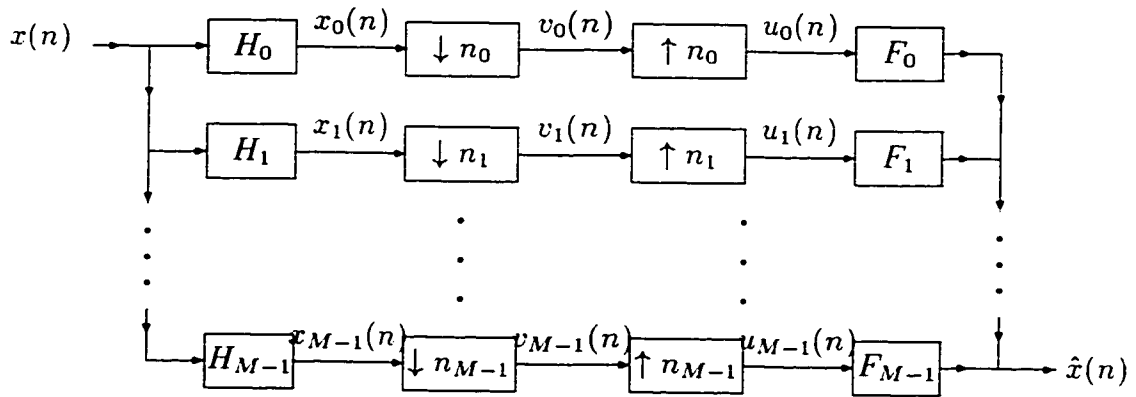


Figure 2.12: An M -channel filter bank.

Filter banks are very useful in subband coding [11, 38, 19]. In practice one often encounters signal with energy dominantly concentrated in a particular region of frequency. But it is more common to encounter signals that are not band limited, and still have dominant frequency bands. An example is shown in Figure 2.14. The frequency component in $|\omega| > \pi/2$ is not small enough to be discarded, and we can not decimate $x(n)$ without causing aliasing either. It seems that we can not obtain

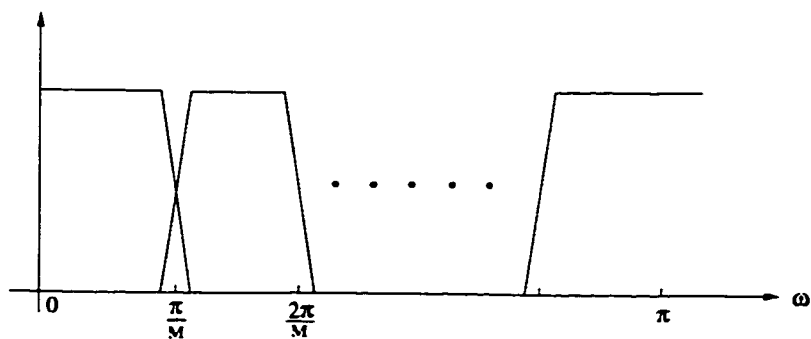


Figure 2.13: Typical frequency responses of the analysis filters.

any kind of signal compression at all. But we can use subband coding to get around this difficulty. In view of Figure 2.15, we can split the signal into two frequency bands by using an analysis bank with frequency responses as in Figure 2.14. The subband signal $x_1(n)$ has less energy than $x_0(n)$ and so can be encoded with fewer bits than $x_0(n)$. For example, suppose that $x(n)$ is a 10kHz signal (10000samples/sec) and requires 16 bits per sample for coding, so that the data rate is 160 Kbits/sec. Let us assume that the subband signals $x_0(n)$ and $x_1(n)$ can be represented with 16 bits and 8 bits per sample, respectively. Because these signals are also decimated by a factor of two, the data rate now works out to be $80 + 40 = 120$ Kbits/sec, which is a reduction by 4/3. The basic principle of subband coding is: Split the signal into two or more subbands, decimate each subband signal, and allocate bits for samples in each subband depending on the energy content. This is a very effective way for coding and transmitting signals which are not bandlimited.

From (2.1) and (2.3), the expressions of decimator and expander in Sections 2.11 and 2.12, we can obtain an expression for $\hat{X}(z)$ in terms of $X(z)$ in Figure 2.12, by ignoring the presence of coding and quantization errors. Each subband signal is given by

$$X_k(z) = H_k(z)X(z);$$

thus the decimated signals $v_k(n)$ have z -transform

$$V_k(z) = \frac{1}{M} \sum_{l=0}^{M-1} H_k(z^{1/M}W^l)X(z^{1/M}W^l),$$

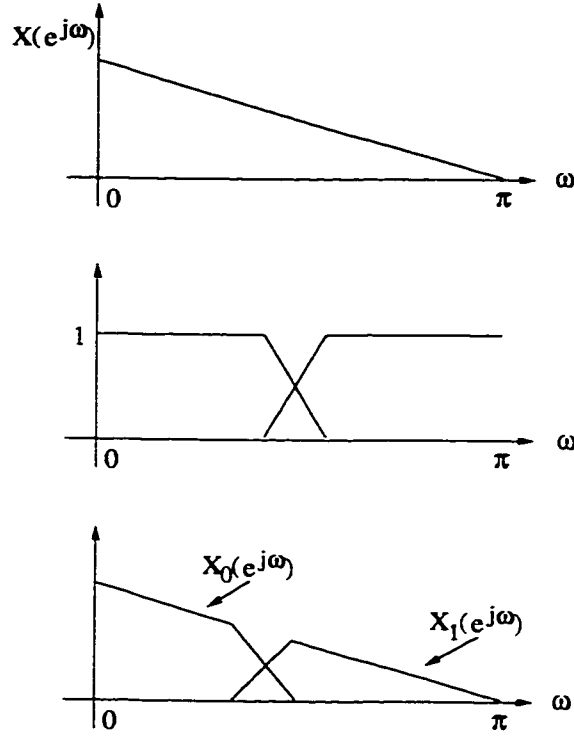


Figure 2.14: Splitting a signal into subband signals $x_0(n)$ and $x_1(n)$

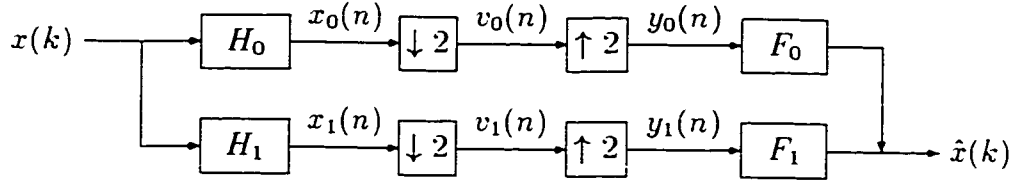


Figure 2.15: The two channel filter bank for subband coding.

where $W = W_M = e^{-j2\pi/M}$. The outputs of the expanders are therefore given by

$$U_k(z) = V_k(z^M) = \frac{1}{M} \sum_{l=0}^{M-1} H_k(zW^l)X(zW^l).$$

Hence the reconstructed signal is

$$\hat{X}(z) = \sum_{k=0}^{M-1} F_k(z)U_k(z) = \frac{1}{M} \sum_{l=0}^{M-1} X(zW^l) \sum_{k=0}^{M-1} H_k(zW^l)F_k(z).$$

We can rewrite this in the more convenient form

$$\hat{X}(z) = \sum_{l=0}^{M-1} A_l(z)X(zW^l), \quad (2.6)$$

where

$$A_l(z) = \frac{1}{M} \sum_{k=0}^{M-1} H_k(zW^l)F_k(z), \quad 0 \leq l \leq M-1. \quad (2.7)$$

The Fourier transform of $X(zW^l)$ can be written for $z = e^{j\omega}$ as

$$X(e^{j\omega}W^l) = X(e^{j(\omega - \frac{2\pi l}{M})}).$$

For $l \neq 0$, $X(e^{j\omega}W^l)$ represents a shifted version of the spectrum $X(e^{j\omega})$. So $\hat{X}(e^{j\omega})$ is a linear combination of $X(e^{j\omega})$ and its $M-1$ uniformly shifted versions.

Transmultiplexers, used for interconversion between the time division multiplexing (TDM) and the frequency division multiplexing (FDM) formats, have very similar architectures as filter banks by switching the analysis part and synthesis part, whose diagram is shown in Figure 2.16 [38]. So the F_i and H_i are synthesis filters and analysis filters respectively. Similar to filter banks, if all the decimation and expansion ratios of all the channels are equal to M , it is called a uniform transmultiplexer; otherwise, it is called a nonuniform transmultiplexer. For the uniform case, the typical frequency responses of synthesis filters are also frequency selective, see in Figure 2.13.

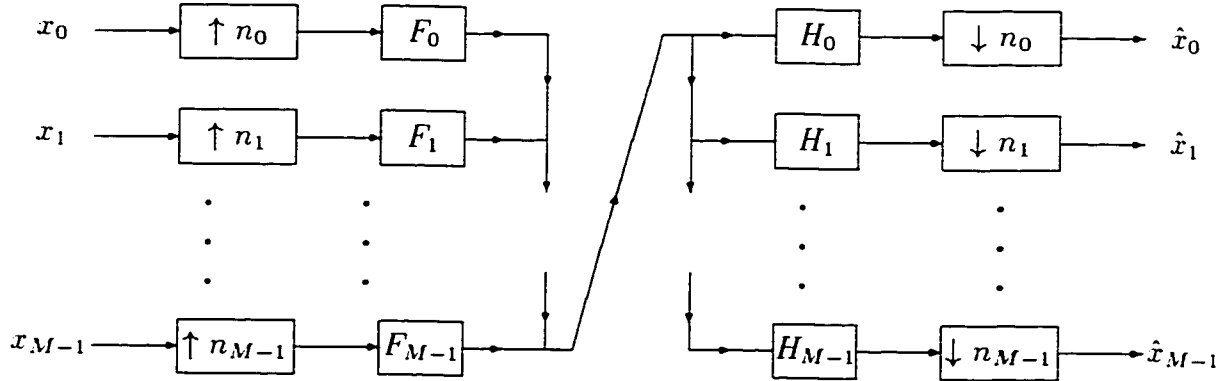


Figure 2.16: An M -channel uniform-band transmultiplexer.

The main use of transmultiplexers is simultaneous transmission of several data signals through a single channel [39, 38] – some conventional and emerging applications in communications are discussed in Section 3.1.

2.3 Errors Created By Filter Bank Systems

In Equation (2.6), the presence of shifted versions $X(zW^l)$, $l \neq 0$, is due to the decimation and interpolation operations. From Figure 2.13 we can see that all the

analysis filters are frequency selective [38, 11]. But in practice, the filters have nonzero transition bandwidths and stopband gains. Therefore, the signals filtered by the analysis filters, $x_i(k)$, are not bandlimited. Based on the discussion in Section 2.1.3, if the signal $x_i(k)$ is not bandlimited to the desired region (lowpass or bandpass), after the decimator n_i , the stretched version $X_i(e^{j\omega/n_i})$ can in general overlap with its shifted replicas.

In view of (2.6), we say that $X(zW^l)$ is the l th aliasing term. It is clear that aliasing can be eliminated for every possible input $x(n)$, if and only if

$$A_i(z) = 0, \quad 1 \leq i \leq M - 1.$$

From (2.7) we know that we can choose the proper synthesis filters to make A_i zero. That is, aliasing is cancelled out.

Suppose the filter bank is free from aliasing. We then have

$$\hat{X}(z) = T(z)X(z).$$

Thus even after aliasing is cancelled, the signal $\hat{x}(n)$ suffers from a linear shift invariant distortion $T(z)$. Letting $T(e^{j\omega}) = |T(e^{j\omega})|e^{j\phi(\omega)}$, we have

$$\hat{X}(e^{j\omega}) = |T(e^{j\omega})|e^{j\phi(\omega)}X(e^{j\omega}).$$

Unless $T(z)$ is allpass: $|T(e^{j\omega})| = d \neq 0$ for all ω , we say that $\hat{X}(e^{j\omega})$ suffers from amplitude distortion. Similarly unless $T(z)$ has linear phase (that is, $\phi(\omega) = a + b\omega$ for constant a, b), $\hat{X}(e^{j\omega})$ suffers from phase distortion. We say the uniform filter banks have the perfect reconstruction if and only if all the three distortions are zero.

In summary, there are three distortions in uniform filter bank: aliasing, magnitude and phase distortions. We say the uniform filter bank achieves *perfect reconstruction* (PR) if the reconstructed signal $\hat{x}(n)$ is a delayed version of the input signal $x(n)$ in Figure 2.12, that is, all the three distortions are zero.

2.4 Polyphase Decomposition

An important advancement in multirate signal processing is the invention of the polyphase representation [3, 36]. This permits great simplification of theoretical results and also leads to computationally efficient implementations of decimation and interpolation filters, as well as filter banks and transmultiplexers.

To explain the basic idea, consider a filter

$$H(z) = \sum_{n=-\infty}^{\infty} h(n)z^{-n}.$$

By separating the even numbered coefficients of $h(n)$ from the odd numbered ones, we can write

$$H(z) = \sum_{n=-\infty}^{\infty} h(2n)z^{-2n} + z^{-1} \sum_{n=-\infty}^{\infty} h(2n+1)z^{-2n}.$$

Defining

$$E_0(z) = \sum_{n=-\infty}^{\infty} h(2n)z^{-n}, \quad E_1(z) = \sum_{n=-\infty}^{\infty} h(2n+1)z^{-n}.$$

we can, therefore, write $H(z)$ as

$$H(z) = E_0(z^2) + z^{-1}E_1(z^2).$$

Extending this idea further, suppose we are given any integer M . We can always decompose $H(z)$ as

$$\begin{aligned} H(z) &= \sum_{n=-\infty}^{\infty} h(nM)z^{-nM} \\ &+ z^{-1} \sum_{n=-\infty}^{\infty} h(nM+1)z^{-nM} \\ &\vdots \\ &+ z^{-(M-1)} \sum_{n=-\infty}^{\infty} h(nM+M-1)z^{-nM}. \end{aligned}$$

This can be compactly written as

$$H(z) = \sum_{l=0}^{M-1} z^{-l} \sum_{n=-\infty}^{\infty} h(Mn+l)z^{-nM}.$$

Defining

$$E_l(z) = \sum_{n=-\infty}^{\infty} e_l(n)z^{-n},$$

where

$$e_l(n) = h(Mn+l), \quad 0 \leq l \leq M-1.$$

We can write $H(z)$ as

$$H(z) = \sum_{l=0}^{M-1} z^{-l} E_l(z^M). \quad (2.8)$$

Equation (2.8) is called the *type 1 polyphase representation* and $E_l(z)$ the *polyphase components* of $H(z)$.

A variation of (2.8) is given by

$$H(z) = \sum_{l=0}^{M-1} z^{-(M-1-l)} R_l(z^M). \quad (2.9)$$

This is called the *type 2 polyphase representation*. The *type 2 polyphase components* $R_l(z)$ are permutations of $E_l(z)$, that is

$$R_l(z) = E_{M-1-l}(z).$$

From above we know that the transfer function of analysis filters $H_k(z)$ can be expressed in the form

$$H_k(z) = \sum_{l=0}^{M-1} z^{-l} E_{kl}(z^M) \quad (\text{type 1 polyphase}), \quad k = 0, 1, \dots, M-1.$$

Then rewrite these in the matrix form:

$$\begin{bmatrix} H_0(z) \\ \vdots \\ H_{M-1} \end{bmatrix} = \begin{bmatrix} E_{00}(z^M) & E_{01}(z^M) & \cdots & E_{0,M-1}(z^M) \\ \vdots & \vdots & \ddots & \vdots \\ E_{M-1,0}(z^M) & E_{M-1,1}(z^M) & \cdots & E_{M-1,M-1}(z^M) \end{bmatrix} \begin{bmatrix} 1 \\ \vdots \\ z^{-(M-1)} \end{bmatrix} \quad (2.10)$$

where

$$E(z) = \begin{bmatrix} E_{00}(z) & E_{01}(z) & \cdots & E_{0,M-1}(z) \\ E_{10}(z) & E_{11}(z) & \cdots & E_{1,M-1}(z) \\ \vdots & \vdots & \ddots & \vdots \\ E_{M-1,0}(z) & E_{M-1,1}(z) & \cdots & E_{M-1,M-1}(z) \end{bmatrix}, \quad (2.11)$$

which is the $M \times M$ *type 1 polyphase matrix* for the analysis bank.

We can express the set of synthesis filters also in a similar manner. Thus

$$F_k(z) = \sum_{l=0}^{M-1} z^{-(M-1-l)} R_{lk}(z^M) \quad (\text{type 2 polyphase}).$$

Using matrix notation we have

$$[F_0(z) \quad \cdots \quad F_{M-1}(z)] = \begin{bmatrix} z^{-(M-1)} & z^{-(M-2)} & \cdots & 1 \\ R_{00}(z^M) & \cdots & R_{0,M-1}(z^M) \\ R_{10}(z^M) & \cdots & R_{1,M-1}(z^M) \\ \vdots & \ddots & \vdots \\ R_{M-1,0}(z^M) & \cdots & R_{M-1,M-1}(z^M) \end{bmatrix}, \quad (2.12)$$

where

$$R(z) = \begin{bmatrix} R_{00}(z) & R_{01}(z) & \cdots & R_{0,M-1}(z) \\ R_{10}(z) & R_{11}(z) & \cdots & R_{1,M-1}(z) \\ \vdots & \vdots & \ddots & \vdots \\ R_{M-1,0}(z) & R_{M-1,1}(z) & \cdots & R_{M-1,M-1}(z) \end{bmatrix}. \quad (2.13)$$

The matrix $R(z)$ is the *type 2 polyphase matrix* for the synthesis bank.

Using these two representations in the filter bank, we obtain the equivalent representation shown in Figure 2.17. It can be simplified to Figure 2.18 using the noble identities, which we refer to as the polyphase representation of the M -channel filter bank.

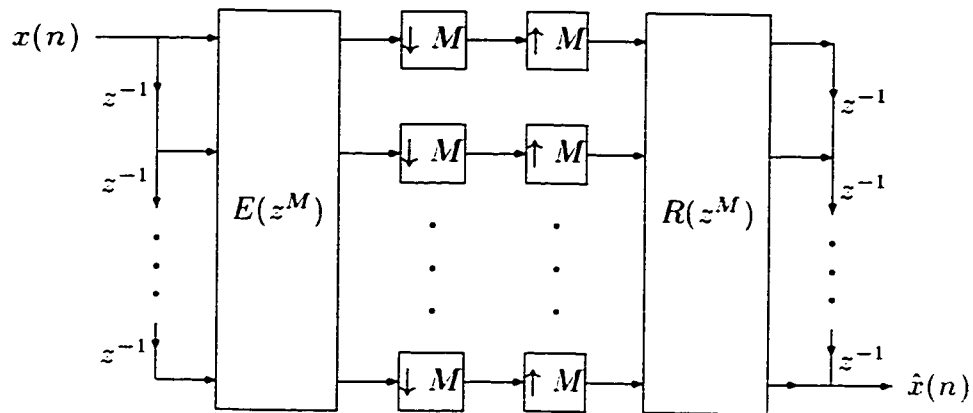


Figure 2.17: Polyphase representation of the M -channel filter bank in Figure 2.12.

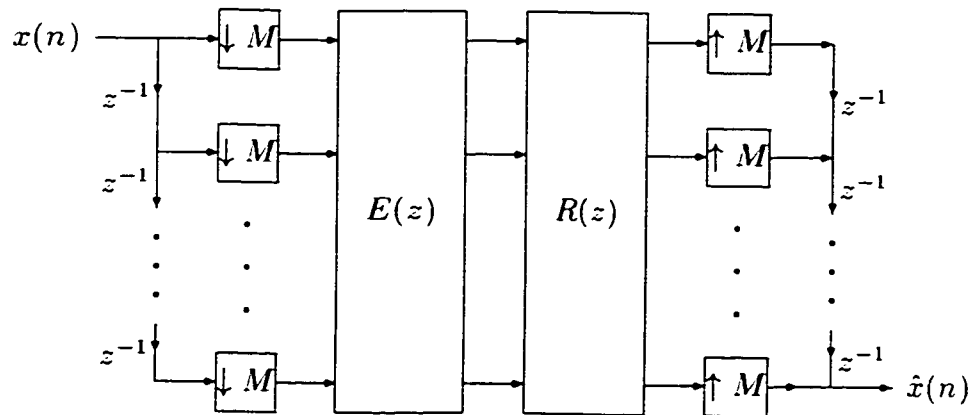


Figure 2.18: Rearrangement using noble identities.

The polyphase decomposition of transmultiplexers is similar, which we will show in Chapter 3.

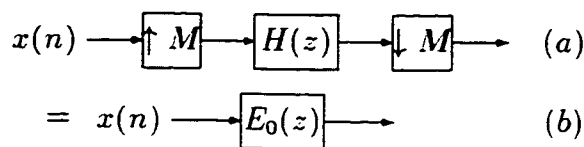


Figure 2.19: The polyphase identity.

Let us consider a very interesting property. Pay attention to the structure of Figure 2.19 which is a cascade of an expander followed by a filter $H(z)$, which in turn is followed by a decimator. Even though the decimator and expander are time-varying building blocks, the above cascaded system happens to be time-invariant. To see this note that the input to the decimator has the z -transform

$$[X(z^M)H(z)]|_{\downarrow M} = X(z)[H(z)|_{\downarrow M}] = X(z)E_0(z),$$

where $E_0(z)$ is the 0-th polyphase component of $H(z)$. Thus Figure 2.19 represents a linear time invariant system with transfer function $E_0(z)$. This property is called the polyphase identity, which is very useful - see the following chapters.

2.5 Perfect Reconstruction of Filter Banks

If a filter bank is free from aliasing, amplitude distortion, and phase distortion, it is said to have the perfect reconstruction (abbreviated PR) property [38, 11]. This is equivalent to the condition $T(z) = cz^{-n_0}$. For a PR filter bank we have

$$\hat{X}(z) = cz^{-n_0}X(z), \quad \text{i.e.,} \quad \hat{x}(n) = cx(n - n_0), \quad c \neq 0.$$

for all possible inputs $x(n)$. In other words, $\hat{x}(n)$ is merely a scaled and delayed version of $x(n)$. This, of course, ignores the coding/decoding error and filter roundoff noise.

From Figure 2.18, it is clear that if

$$R(z)E(z) = I, \tag{2.14}$$

then the output $\hat{x}(n)$ is the same as the input $x(n)$.

The condition (2.14) is sufficient for perfect reconstruction. It is clear that if we replace this with

$$R(z)E(z) = cz^{-m_0}I, \tag{2.15}$$

we still have perfect reconstruction, but now $T(z) = cz^{-(Mm_0+M-1)}$. More generally it can be shown that, the system has perfect reconstruction if and only if the product $R(z)E(z)$ has the form

$$P(z) = R(z)E(z) = cz^{-m_0} \begin{bmatrix} 0 & I_{M-r} \\ z^{-1}I_r & 0 \end{bmatrix}. \quad (2.16)$$

for some integer r with $0 \leq r \leq M - 1$, some integer m_0 , and some constant $c \neq 0$. Under this condition the reconstructed signal is $\hat{x}(n) = cx(n - n_0)$, where $n_0 = Mm_0 + r + M - 1$.

2.6 \mathcal{H}_2 Norm

Norms are widely used in control and signal processing to quantify sizes of signals and systems.

2.6.1 Norms of Signals

We shall use two norms for the signal $v = \{v(0), v(1), \dots\}$ [9]:

$$\begin{aligned} 2 - Norm : \quad \|v\|_2 &= [v(0)^2 + v(1)^2 + \dots]^{1/2} \\ \infty - Norm : \quad \|v\|_\infty &= \sup_k |v(k)| \end{aligned} \quad (2.17)$$

The 2-norm is associated with energy: $\|v\|_2^2$ is interpreted as the energy of the signal $v(k)$. The ∞ -norm is the maximum amplitude of the signal, more precisely, the least upper bound on the amplitude.

2.6.2 Norms of SISO Systems

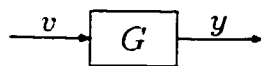


Figure 2.20: A SISO system.

Now we turn to LTI (linear time invariant) systems. Figure 2.20 is a SISO (single-input and single-output) system with input v and output y . The impulse-response function of this system is $g(k)$ and $G(z)$ is the transfer function. There are three norms of interest [9], listed as follows:

$$\begin{aligned}
1 - Norm : \quad \|g\|_1 &= |g(0)| + |g(1)| + \dots \\
2 - Norm : \quad \|G\|_2 &= \left(\frac{1}{2\pi} \int_0^{2\pi} |G(e^{j\omega})|^2 d\omega \right)^{1/2} \\
\infty - Norm : \quad \|G\|_\infty &= \max_\omega |G(e^{j\omega})|
\end{aligned} \tag{2.18}$$

We can see from the expression for the 2-norm of the system that if input is the unit impulse, δ_d , then the 2-norm of output equals the 2-norm of the system G . That is [9]

$$\|G\delta_d\|_2 = \|G(z)\|_2. \tag{2.19}$$

Thus $\|G(z)\|_2^2$ equals the energy of the output for a unit impulse input.

2.6.3 Norms of Multivariable Systems

From the discussions above we know that the 2-norm of the system is an average system gain for known input, while the ∞ -norm is a worst-case system gain for unknown inputs. Let us extend the definitions of norms to MIMO (multi-input and multi-output) systems.

Figure 2.21 is an MIMO system with input v and output y [9]:

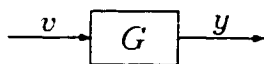


Figure 2.21: An MIMO system.

where $y = Gv$, $v(k) \in \ell^m$, $y(k) \in \ell^p$. ℓ is defined to be the space of discrete-time signals defined on the set of all integers, and ℓ^n is the space of the discrete-time signals with dimension n . We get

$$y(k) = \sum_l g(k, l)v(l)$$

where $g(k, l) \in \ell^{p \times m}$ is the impulse-response function.

The definitions and conclusions of the norms can be extended to the case of multivariable systems: The 2-norm and ∞ -norm of a stable $p \times m$ transfer function matrix

$$G(z) = \begin{bmatrix} \hat{g}_{11} & \hat{g}_{12} & \cdots & \hat{g}_{1m} \\ \hat{g}_{21} & \hat{g}_{22} & \cdots & \hat{g}_{2m} \\ \vdots & \vdots & \ddots & \vdots \\ \hat{g}_{p1} & \hat{g}_{p2} & \cdots & \hat{g}_{pm} \end{bmatrix} = [\hat{g}_1 \quad \hat{g}_2 \quad \cdots \quad \hat{g}_m],$$

are [9]

$$\begin{aligned}
 2 - norm : \quad \|G\|_2 &= \left\{ \frac{1}{2\pi} \int_0^{2\pi} \text{trace} [G(e^{j\omega})^* G(e^{j\omega})] d\omega \right\}^{1/2} \\
 \infty - norm : \quad \|G\|_\infty &= \max_\omega \sigma_{max}[G(e^{j\omega})]
 \end{aligned}
 \tag{2.20}$$

where the *trace* of a square matrix is the sum of the entries on the main diagonal, that is, the sum of the eigenvalues, and σ_{max} is the maximum singular value.

Let $e_i, i = 1, \dots, m$, denote the standard basis vectors in \mathfrak{R}^m . Thus, $\delta_d e_i$ is an impulse applied to the i^{th} input; $G\delta_d e_i$ is the corresponding output. From the definition of the 2-norm we can conclude [9]:

$$\begin{aligned}
 \|G(z)\|_2^2 &= \sum_i \sum_j \|\hat{g}_{ij}\|_2^2 \\
 &= \|\hat{g}_1\|_2^2 + \dots + \|\hat{g}_m\|_2^2 \\
 &= \sum_{i=1}^m \|G\delta_d e_i\|_2^2
 \end{aligned}
 \tag{2.21}$$

That is, similar to the SISO case, the 2-norm of the transfer function G is related to the average 2-norm of the output when impulses are applied at the input channels.

Chapter 3

Optimal Design of Uniform Transmultiplexers

A schematic diagram of an M -channel uniform-band transmultiplexer is depicted in Figure 3.1: M signals x_0, x_1, \dots, x_{M-1} , with the same sampling rate, are combined together (TDM \rightarrow FDM) through the upsamplers by a factor of M , $\uparrow M$, and the synthesis filters $F_0(z), F_1(z), \dots, F_{M-1}(z)$; then the combined signal is coded and transmitted (not modelled), and processed (FDM \rightarrow TDM) through the analysis filters $H_0(z), H_1(z), \dots, H_{M-1}(z)$ and the downsamplers by a factor of M , $\downarrow M$, yielding reconstructed signals $\hat{x}_0, \hat{x}_1, \dots, \hat{x}_{M-1}$.

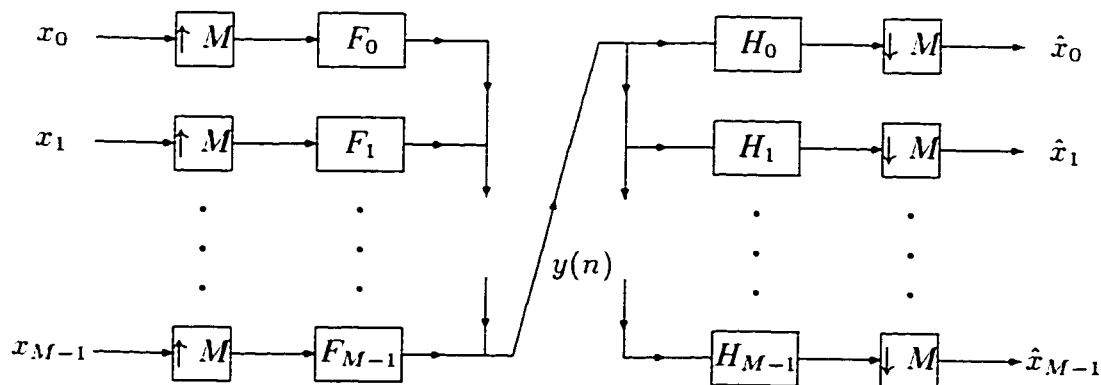


Figure 3.1: An M -channel uniform-band transmultiplexer.

In analogy with the filter bank, we continue to use terms such as “analysis” and “synthesis” filters. Notice the conceptual duality between filter bank and the transmultiplexer. In the former, we first “analyze” and then “synthesis”; this is in reverse order as compared to the transmultiplexer. We will see that the problem of designing filters for “perfect reconstruction transmultiplexer” is similar to the design

of perfect reconstruction filter banks.

3.1 Applications of Transmultiplexers

Transmultiplexers were studied in the early 1970's by Bellanger and Daguet for telephony applications [4]. Their seminal work was one of the first dealing with multirate signal processing, which has matured lately in the signal processing field.

Now, there are several emerging application areas such as discrete multitone (DMT) techniques, spread spectrum orthogonal transmultiplexers for code division multiple access (CDMA) and low probability of intercept (LPI) communications [1, 2].

Let us discuss a few applications used widely in recent years.

- **Spread Spectrum PR-QMF Codes for CDMA**

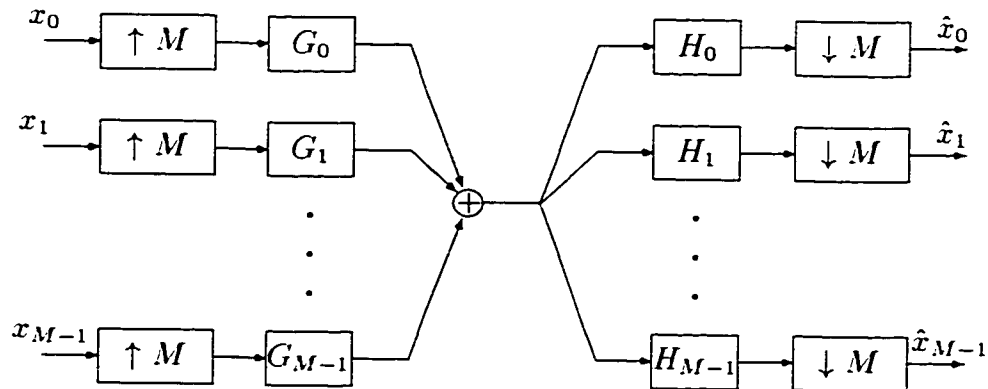


Figure 3.2: M -band transmultiplexer structure for CDMA communications

The CDMA techniques have been proposed as an alternative to the classical multiplexing methods such as TDM and FDM. Figure 3.2 shows the M -band transmultiplexer structure for CDMA communications. Due to the absence of synchronization between the transmitter and receiver, the desired user codes for CDMA communications should jointly satisfy the following time-frequency properties [2]: (1) The orthogonal user codes can not be unit sample functions. (2) The orthogonal user codes are expected to be spread over the full spectrum with minimized intercode and intracode correlations. Several examples have been done to show that the correlation and frequency spreading properties of multivalued spread spectrum PR-QMF code outperform the other codes. There

have been several other subband (wavelet) transform-based CDMA communication configurations reported in the literature [12, 15, 20, 25]. It is predicted that these techniques might find their applications in the next generation of PCS (private communication systems) products.

- **DMT Modulation**

DMT modulation has been widely used in applications such as asymmetric digital subscriber line (ADSL), high bit-rate digital subscriber line (HDSL), and very high bit-rate digital subscriber line (VDSL) communications for the single-user case [1].

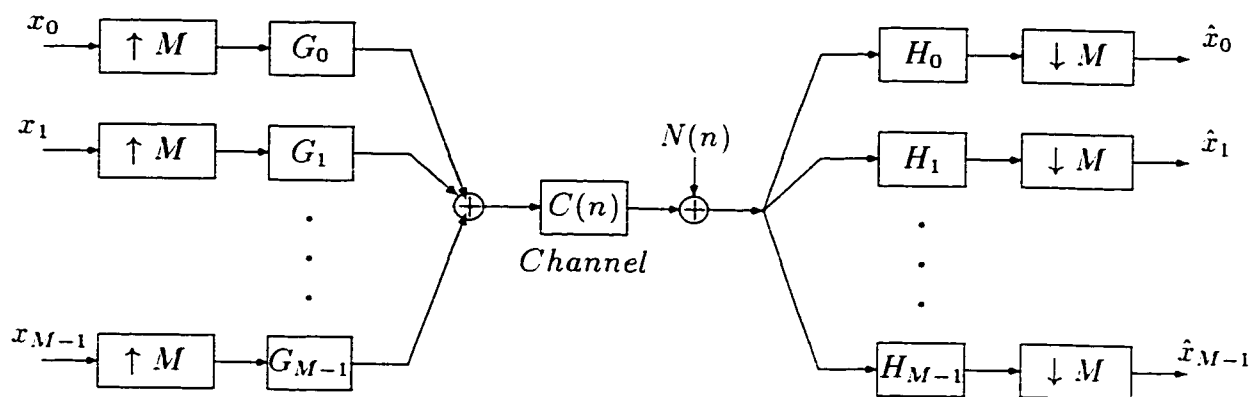


Figure 3.3: A basic structure of a DMT modulation-based digital ADSL transceiver.

The basic structure of a DMT modulation-based digital ADSL transceiver is displayed in Figure 3.3, the DMT-based system uses a set of M frequency-selective orthogonal functions $\{G_i(n)\}$. The subsymbols $\{x_0(n), x_1(n), \dots, x_{M-1}(n)\}$ are formed by grouping blocks of an incoming bit stream via certain constellation schemes like quadrature amplitude modulation (QAM) or pulse amplitude modulation (PAM). The parsing of the incoming bit stream to the subsymbols is determined by the subchannel attenuation level. Therefore, each of the subcarriers (orthogonal functions) carries a different number of bits per symbol commensurate with the corresponding subchannel attenuation [23].

This technology has two advantages [1]: (1) adaptation of the data rates of subchannels based on the possible variations of the channel and noise characteristics, (2) combining different coding schemes including block and trellis-based

modulation in order to increase the system's robustness toward transmission errors.

- **LPI Communications**

Time and frequency spread functions are often used as user codes or signatures to provide LPI communications. Spread spectrum communication is a popular example of this approach with its military and civilian applications [13, 14]. The basic philosophy of these techniques is to distribute the orthogonality conditions of the function set in both the time and frequency domains. This helps the transmitter to hide the information bearing signal in either domain from an interceptor since it can see a fairly low signal-to-noise ratio (SNR). Thus, the time or frequency domain localized interference immunity of the communications system is significantly boosted. The primary advantage of a spread spectrum system is its low transmission power requirements along with its interference resistance. The inherent flexibilities of subband transforms on a time-frequency plane naturally make them very valuable signal processing tools for LPI communications. These flexibilities provide the user with codes that are not easy to detect and recognize by unintended receivers.

In summary, several popular communication applications can be described in terms of synthesis/analysis configuration (transmultiplexer) of subband transforms such as code division multiple access (CDMA), frequency division multiple access (FDMA), and time division multiple access (TDMA) communication. In particular, FDMA or DMT modulation-based systems have been more widely used than others.

3.2 Input-Output Relation for Uniform Transmultiplexers

In Figure 3.1, the components $x_k(n)$ of the TDM version can be recovered by separating the consecutive regions of $Y(e^{j\omega})$ (which are the M message signals) with the help of an analysis bank and then decimating the outputs. Now, if the synthesis filters $F_k(z)$ are non-ideal, the adjacent spectra in Figure 2.13 will actually tend to overlap. Similarly if the analysis filters $H_k(z)$ are non-ideal then the outputs of $H_k(z)$

have contributions from $X_k(e^{j\omega})$ as well as $X_l(e^{j\omega}), l \neq k$. So in general each of the reconstructed signals $\hat{x}_k(n)$ has contributions from the desired signal $x_k(n)$ as well as the “cross-talk” terms $x_l(n), l \neq k$. An obvious approach to reduce the extent of cross-talk is to design $H_k(z)$ and $F_k(z)$ to have very sharp cutoff regions to avoid overlapping in the signals throughout the decimator in Figure 3.4 [38], which requires filters of very high order. From the following it can be shown that the cross-talk terms can be completely eliminated by careful choice of the relation between the analysis and synthesis filters.

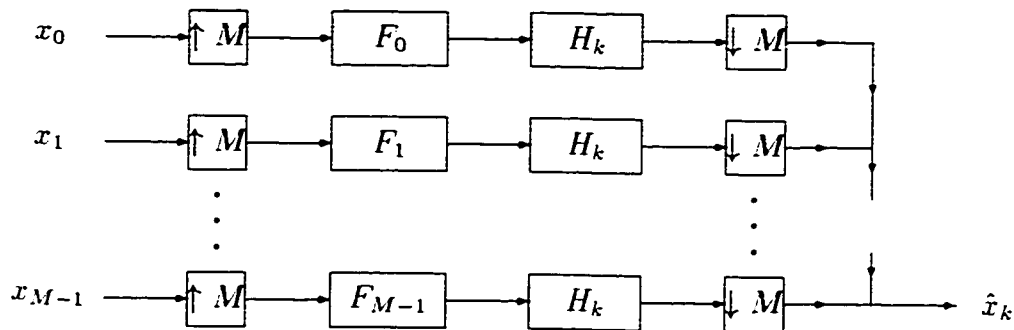


Figure 3.4: The relation between $\hat{x}_k(n)$ and $x_m(n)$.

The relation between $\hat{x}_k(n)$ and $x_m(n)$ can be schematically represented as in Figure (3.4). By using the polyphase identity (Figure 2.19) we see that each branch in this figure is an LTI system. Therefore

$$\hat{X}_k(z) = \sum_{m=0}^{M-1} T_{km}(z)X_m(z), \quad 0 \leq k \leq M-1, \quad (3.1)$$

where $T_{km}(z)$ is the 0-th polyphase component of $H_k(z)F_m(z)$. By defining

$$x(n) = \begin{bmatrix} x_0(n) \\ x_1(n) \\ \vdots \\ x_{M-1}(n) \end{bmatrix}, \quad \hat{x}(n) = \begin{bmatrix} \hat{x}_0(n) \\ \hat{x}_1(n) \\ \vdots \\ \hat{x}_{M-1}(n) \end{bmatrix},$$

we can express (3.1) as

$$\hat{X}(z) = T(z)X(z), \quad (3.2)$$

where

$$T(z) = \begin{bmatrix} T_{00}(z) & T_{01}(z) & \cdots & T_{0,M-1}(z) \\ T_{10}(z) & T_{11}(z) & \cdots & T_{1,M-1}(z) \\ \vdots & \vdots & \ddots & \vdots \\ T_{M-1,0}(z) & T_{M-1,1}(z) & \cdots & T_{M-1,M-1}(z) \end{bmatrix}.$$

So the transmultiplexer is an LTI system with transfer matrix $T(z)$. The system is free from cross-talk if and only if $T(z)$ is diagonal. That is, the 0-th polyphase component of $H_k(z)F_m(z)$ should be zero unless $k = m$. Under this condition, each reconstructed TDM signal $\hat{x}_k(n)$ is related to the original signal $x_k(n)$ according to

$$\hat{X}_k(z) = T_{kk}(z)X_k(z).$$

The transfer functions $T_{kk}(z)$ represent the distortions that remain after cross-talk elimination. If $T_{kk}(z)$ is allpass for all k , there is no amplitude distortion; if $T_{kk}(z)$ has linear phase, there is no phase distortion. That is,

$$T_{kk}(z) = c_k z^{-n_k}, \quad \text{for all } k.$$

So, for well designed transmultiplexers, \hat{x}_i approximates x_i . Ideally, we say the transmultiplexer achieves *perfect reconstruction* [38] if \hat{x}_i is a delayed version of x_i , namely, if there exist positive integers d_i such that

$$\hat{x}_i(n) = c_k x_i(n - d_i), \quad i = 0, 1, \dots, M - 1, \quad (3.3)$$

all the distortions are zero.

3.3 Polyphase Decomposition

The use of polyphase decomposition adds further insight into the operation of the transmultiplexer. As in the filter bank case, we can redraw the analysis and synthesis banks in terms of the polyphase matrices $E(z)$ and $R(z)$. The resulting equivalent transmultiplexer circuit is shown in Figure 3.5. Then it can be simplified into Figure 3.6, after invoking the noble identities. This structure can be further simplified into the equivalent form shown in Figure 3.7. It is, therefore, clear that the transfer matrix $T(z)$ can be expressed as

$$T(z) = E(z)\Gamma(z)R(z), \quad (3.4)$$

where Γ is a fixed function:

$$\Gamma(z) = \begin{bmatrix} 0 & 1 \\ z^{-1}I_{M-1} & 0 \end{bmatrix}.$$

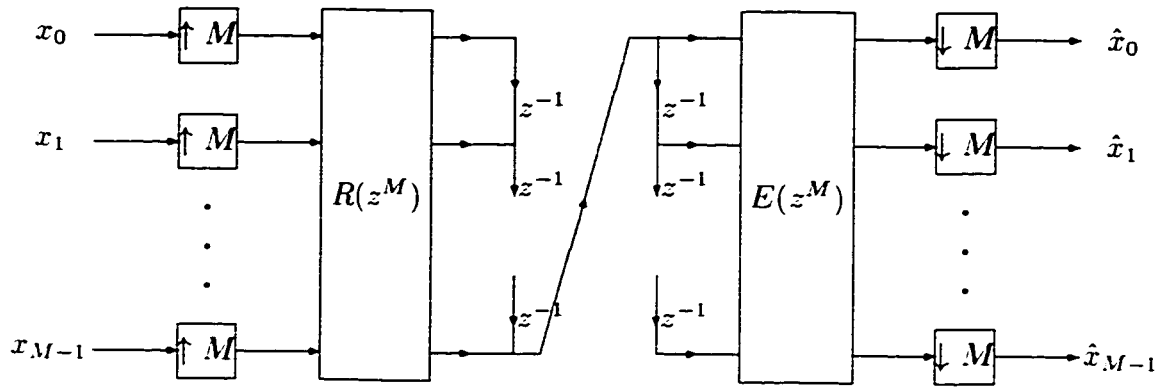


Figure 3.5: Polyphase decomposition of the transmultiplexer in Figure 3.1.

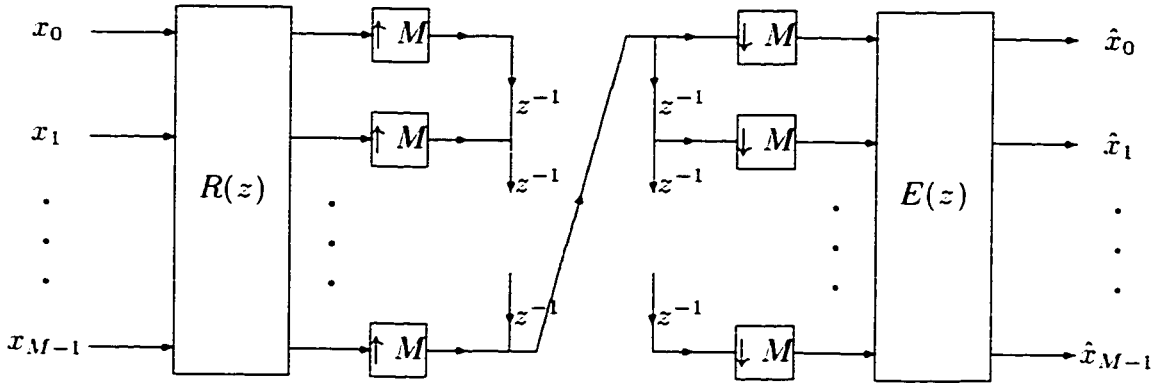


Figure 3.6: Rearrangement using noble identities.

That is

$$\begin{bmatrix} \hat{X}_0(z) \\ \hat{X}_1(z) \\ \vdots \\ \hat{X}_{M-1}(z) \end{bmatrix} = E(z) \begin{bmatrix} 0 & 1 \\ z^{-1} I_{M-1} & 0 \end{bmatrix} R(z) \begin{bmatrix} X_0(z) \\ X_1(z) \\ \vdots \\ X_{M-1}(z) \end{bmatrix}. \quad (3.5)$$

From this expression we can explore the conditions for perfect reconstruction.

3.4 Perfect Reconstruction

3.4.1 The Conditions for Perfect Reconstruction

From Section 3.2 we know that the transmultiplexer achieves perfect reconstruction if and only if \hat{x}_i is a delayed version of x_i , that is, in (3.2), $T(z)$ is a diagonal matrix

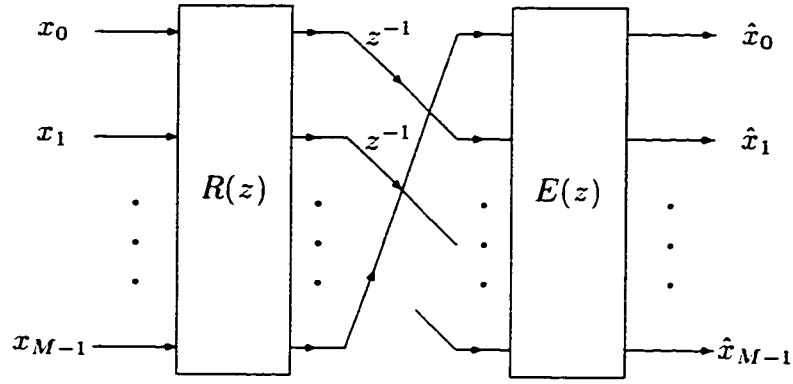


Figure 3.7: The equivalent form of Figure 3.6.

with all the elements on the main diagonal being pure time delays:

$$T(z) = \begin{bmatrix} c_0 z^{-d_0} & 0 & \cdots & 0 \\ 0 & c_1 z^{-d_1} & \cdots & 0 \\ \vdots & \vdots & \ddots & \vdots \\ 0 & 0 & \cdots & c_{M-1} z^{-d_{M-1}} \end{bmatrix}, \quad (3.6)$$

where $c_i \neq 0$ for $i = 0, 1, \dots, M-1$.

From (3.6) it is easy to get a sufficient condition for perfect reconstruction by setting $T(z) = cz^{-n_0} I$ [38]. Now

$$\begin{aligned} T(z) &= cz^{-n_0} I \\ \iff E(z)\Gamma(z)R(z) &= cz^{-n_0} I \\ \iff cE^{-1}(z)R^{-1}(z) &= z^{n_0}\Gamma(z) \\ \iff R(z)E(z) &= cz^{-n_0}\Gamma^{-1}(z) \end{aligned}$$

Substituting for $\Gamma(z)$, this becomes

$$R(z)E(z) = cz^{-n_0} \begin{bmatrix} 0 & I_{M-1} \\ z^{-1} & 0 \end{bmatrix}, \quad (3.7)$$

for appropriate integer n_0 .

3.4.2 Relation to Perfect Reconstruction (PR) Filter Banks

Reference [24] gave us the idea for the connections between QMF banks and transmultiplexers. The following results from [24] are very useful. Note here we use PR QMF banks and PR transmultiplexer instead of aliasing-free QMF bank and crosstalk-free transmultiplexer.

Let $E'(z)$ and $R'(z)$ be the polyphase component matrices of the analysis and synthesis filter banks of an M -channel, maximally decimated QMF circuit $\{H'_i(z), F'_i(z)\}$. A sufficient condition for a PR-QMF bank is that the matrix $P'(z) = R'(z)E'(z)$ should have the form (2.16). If $r = 0$, it will be called a *standard* PR-QMF bank, whereas if it satisfies (2.16) with $r \neq 0$, it will be called an *r -skewed* PR-QMF bank. The following properties relate standard PR-QMF banks and r -skewed PR-QMF banks.

1. An r -skewed PR-QMF bank $\{H''_i(z), F''_i(z)\}$ is always obtainable from a standard PR-QMF bank $\{H'_i(z), F'_i(z)\}$ by choosing the filters as $H''_i(z) = H'_i(z)$ and $F''_i(z) = z^{-r}F'_i(z)$, $0 \leq i \leq M - 1$.
2. Let $\{H'_i(z), F'_i(z)\}$ represent a 1-skewed PR-QMF bank. Define $H_i(z) = H'_i(z)$ and $F_i(z) = F'_i(z)$, $\forall i$. Then $\{H_i(z), F_i(z)\}$ represents a PR transmultiplexer.

Proof of the first property If the PR-QMF bank $\{H'_i(z), F'_i(z)\}$ is a standard PR-QMF bank, from the definition we know that

$$P'(z) = R'(z)E'(z) = cz^{-n_0}I_M.$$

The synthesis filter bank $F'(z)$ corresponding to $R'(z)$ is

$$F'(z) = [F'_0(z) \ F'_1(z) \ \cdots \ F'_{M-1}(z)]^T = R'^T(z^M)e(z), \quad (3.8)$$

where $e(z) = [z^{-(M-1)} \ z^{-(M-2)} \ \cdots \ 1]^T$. Similarly,

$$F''(z) = R''^T(z^M)e(z). \quad (3.9)$$

Since $H''_i(z) = H'_i(z)$, $\forall i$, we have $E''_i(z) = E'_i(z)$. By choosing $F''_i(z) = z^{-r}F'_i(z)$, we can write

$$F''(z) = z^{-r}F'(z). \quad (3.10)$$

Substituting (3.8) and (3.9) into (3.10), we get

$$R''^T(z^M)e(z) = z^{-r}R'^T(z^M)e(z), \quad (3.11)$$

where

$$z^{-r}e(z) = z^{-r} \begin{bmatrix} z^{-(M-1)} \\ z^{-(M-2)} \\ \vdots \\ 1 \end{bmatrix} = \begin{bmatrix} z^{-(M-1+r)} \\ z^{-(M-2+r)} \\ \vdots \\ z^{-r} \end{bmatrix}. \quad (3.12)$$

Note that

$$\begin{bmatrix} 0 & z^{-M}I_r \\ I_{M-r} & 0 \end{bmatrix} e(z) = \begin{bmatrix} z^{-(M-1+r)} \\ z^{-(M-2+r)} \\ \vdots \\ z^{-r} \end{bmatrix}. \quad (3.13)$$

From (3.12) and (3.13) we know

$$z^{-r}e(z) = \begin{bmatrix} 0 & z^{-M}I_r \\ I_{M-r} & 0 \end{bmatrix} e(z). \quad (3.14)$$

Substitute (3.14) into (3.11) and get

$$R''^T(z^M)e(z) = R'^T(z^M) \begin{bmatrix} 0 & z^{-M}I_r \\ I_{M-r} & 0 \end{bmatrix} e(z).$$

That is

$$R''(z) = \begin{bmatrix} 0 & I_{M-r} \\ z^{-1}I_r & 0 \end{bmatrix} R(z). \quad (3.15)$$

From (3.15) we can conclude

$$R''(z)E''(z) = \begin{bmatrix} 0 & I_{M-r} \\ z^{-1}I_r & 0 \end{bmatrix} R(z)E(z) = cz^{-n_0} \begin{bmatrix} 0 & I_{M-r} \\ z^{-1}I_r & 0 \end{bmatrix}.$$

this proves the first property. \square

Proof of the second property By definition, the matrix $P'(z)$ of the 1-skewed PR-QMF bank $\{H'_i(z), F'_i(z)\}$ satisfies

$$P'(z) = R'(z)E'(z) = cz^{-n_0} \begin{bmatrix} 0 & I_{M-1} \\ z^{-1} & 0 \end{bmatrix}. \quad (3.16)$$

So, for the transmultiplexer filters, the matrix $P(z)$ satisfies $P(z) = R(z)E(z)$. Hence, from (3.16), we can write

$$R(z) = cz^{-n_0} \begin{bmatrix} 0 & I_{M-1} \\ z^{-1} & 0 \end{bmatrix} E^{-1}(z). \quad (3.17)$$

Using (3.17) in (3.5), we get $\hat{X}(z) = z^{-1}cz^{-n_0}X(z), \forall i$. Thus, $\{H_i(z), F_i(z)\}$ represents a PR transmultiplexer in which all the $T_i(z)$ are equal and are given by $T_i(z) = z^{-1}T'(z), \forall i$. \square

From the two propositions above, we can get a PR transmultiplexer directly from a 1-skewed PR-QMF bank just by switching the synthesis and analysis part. On the other hand, if the PR-QMF bank is not 1-skewed, that is, $r \neq 1$, then we can insert appropriate amount of delay in front of the filters $F_k(z)$ to force $r = 1$. The amount of delay to be introduced can be judged as follows: If $r = 0$, the amount of delay to be inserted is $M - 1$ (M here is to make the filters causal); otherwise, it is $r - 1$.

3.5 Distortion Measures

In order to quantify errors incurred in signal reconstruction in the transmultiplexer of Figure (2.16), we need a mathematical model. It is a fact that the system in Figure (2.16) represents a linear, time-invariant (LTI) system, though multirate building elements are involved; but it is multi-input, multi-output (MIMO).

In the frequency domain the transmultiplexer is modelled by the $M \times M$ transfer matrix $T(z)$ relating $X(z)$ to $\hat{X}(z)$ (see Section 3.2): $\hat{X}(z) = T(z)X(z)$. This transfer matrix can be computed based on (3.4) [38]:

$$T(z) = E(z)\Gamma(z)R(z). \quad (3.18)$$

Writing

$$T(z) = \begin{bmatrix} T_{00}(z) & T_{01}(z) & \cdots & T_{0,M-1}(z) \\ T_{10}(z) & T_{11}(z) & \cdots & T_{1,M-1}(z) \\ \vdots & \vdots & \ddots & \vdots \\ T_{M-1,0}(z) & T_{M-1,1}(z) & \cdots & T_{M-1,M-1}(z) \end{bmatrix}. \quad (3.19)$$

we can re-express the condition for perfect reconstruction in (3.3) as follows: There exist positive integers d_0, d_1, \dots, d_{M-1} such that $T(z)$ equals the ideal system $T_d(z)$ defined by

$$T_d(z) = \begin{bmatrix} z^{-d_0} & 0 & \cdots & 0 \\ 0 & z^{-d_1} & \cdots & 0 \\ \vdots & \vdots & \ddots & \vdots \\ 0 & 0 & \cdots & z^{-d_{M-1}} \end{bmatrix}. \quad (3.20)$$

Note that in this case, $T(z)$ is diagonal (no cross-talk distortion) and the diagonal elements are time delays (no magnitude and phase distortions).

In cases of non-perfect reconstruction, we shall discuss ways to quantify the three distortions. First, cross-talk distortion exists if there is at least one non-zero off-

diagonal element in $T(z)$. The energy of all the off-diagonal terms in $T(z)$ can be used to quantify cross-talk distortion; so we define

$$\text{CD} = \left[\frac{1}{2\pi} \int_0^{2\pi} \sum_{i,j(i \neq j)} |T_{ij}(e^{j\omega})|^2 d\omega \right]^{1/2}$$

as a measure for cross-talk distortion. Note that $(\text{CD})^2$ is the overall cross-talk energy present in the system. Even if $\text{CD} = 0$, the channel transfer functions $T_{ii}(z)$ may still have errors in magnitude and phase compared with the ideal time delay z^{-d_i} ; define the following quantities

$$\text{MD}_i = \left[\frac{1}{2\pi} \int_0^{2\pi} (|T_{ii}(e^{j\omega})| - 1)^2 d\omega \right]^{1/2}, \quad (3.21)$$

$$\text{PD}_i = \left\{ \frac{1}{2\pi} \int_0^{2\pi} \sin^2 [\angle T_{ii}(e^{j\omega}) + d_i\omega] d\omega \right\}^{1/2}. \quad (3.22)$$

Note that MD_i and PD_i are defined across all frequencies for the i -th channel: $(\text{MD}_i)^2$ is the energy of the magnitude distortion, and PD_i the energy of sine of the phase distortion $\phi(\omega) = \angle T_{ii}(e^{j\omega}) + d_i\omega$. There are two reasons why we use sine in the definition of PD_i : First, if $\phi(\omega)$ is within $\pm\pi/2$, which is usually the case, $\sin^2[\phi(\omega)]$ is a good indicator of the size of $\phi(\omega)$; second, the PD_i defined in (4.16) connects well with the new distortion measure to be proposed later. From MD_i and PD_i , we can introduce ways to quantify magnitude and phase distortions for the transmultiplexer:

$$\text{MD} = \left(\sum_i \text{MD}_i^2 \right)^{1/2}, \quad \text{PD} = \left(\sum_i \text{PD}_i^2 \right)^{1/2}. \quad (3.23)$$

Note that $(\text{MD})^2$ is the overall energy of magnitude distortion, and $(\text{PD})^2$ the overall energy of the sine of phase distortion.

Alternatively, one can use maximum magnitude instead of overall energy to quantify cross-talk, magnitude and phase distortions:

$$\begin{aligned} \text{CD}_{\max} &= \max_{i,j(i \neq j)} \max_{\omega} |T_{ij}(e^{j\omega})|, \\ \text{MD}_{\max} &= \max_i \max_{\omega} \left| |T_{ii}(e^{j\omega})| - 1 \right|, \\ \text{PD}_{\max} &= \max_i \max_{\omega} |\angle T_{ii}(e^{j\omega}) + d_i\omega|. \end{aligned}$$

These are useful and relevant in design based on minimizing the ∞ -norm, see the connections in filter banks [10, 30].

In summary, either $\{CD, MD, PD\}$ or $\{CD_{\max}, MD_{\max}, PD_{\max}\}$ can be used as a complete set of distortion measures for the transmultiplexer in Figure 3.1; the first set reflects overall energy, whereas the second measures maximum magnitudes. Here, the first set is more relevant for the criterion we propose for design later.

We will put forward a single distortion measure for perfect reconstruction with the following two desirable properties: First, it captures the three traditional distortions in one in the sense that small values in this measure result in low CD, MD and PD defined earlier; second, it is relatively easy to optimize this measure in transmultiplexer design. The new distortion measure to be proposed depends on 2-norms of transfer matrices which we define next.

Let $T(z)$ be any stable, $(M-1) \times (M-1)$ transfer matrix of the same form given in (3.19). The 2-norm of $T(z)$ is defined as

$$\|T(z)\|_2 = \left\{ \frac{1}{2\pi} \int_0^{2\pi} \text{trace} [T(e^{j\omega})^* T(e^{j\omega})] d\omega \right\}^{1/2},$$

where $T(e^{j\omega})^*$ is the complex conjugate transpose of $T(e^{j\omega})$. It is straightforward to verify that

$$\|T(z)\|_2^2 = \sum_{i,j} \|T_{ij}(z)\|_2^2, \quad (3.24)$$

where the 2-norm of the scalar function $T_{ij}(z)$ is given by

$$\|T_{ij}(z)\|_2 = \left[\frac{1}{2\pi} \int_0^{2\pi} |T_{ij}(e^{j\omega})|^2 d\omega \right]^{1/2}. \quad (3.25)$$

This norm applied to a transfer matrix of an LTI system can be interpreted in terms of the impulse responses or the white noise responses of the system, see, e.g., [9].

Returning to the transmultiplexer problem, perfect reconstruction is achieved if $T(z) = T_d(z)$, where $T_d(z)$ is the desired ideal system given in (3.20). Comparing $T(z)$ with $T_d(z)$, we arrive at the error system depicted in Figure 3.8, where e_i is the error signal in reconstruction for the i -th channel. The transfer matrix for the error system taking input vector $x(n)$ to the error vector $e(n)$, defined in the obvious way, is clearly $T(z) - T_d(z)$. The new distortion measure we propose for reconstruction is the 2-norm of the error transfer matrix:

$$J = \|T(z) - T_d(z)\|_2.$$

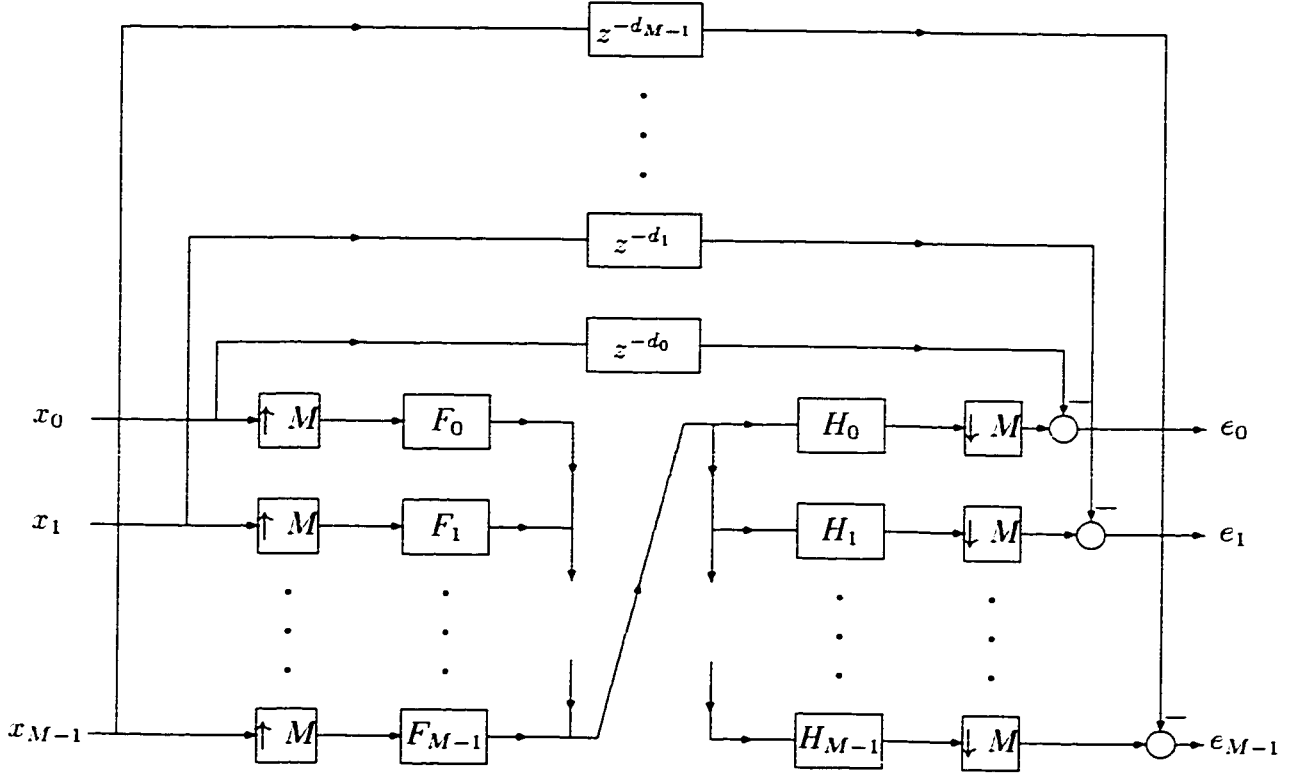


Figure 3.8: The error system between the transmultiplexer and the ideal system.

The reasons why this measure is appropriate are given in the next proposition which establishes simple connections between J and the three distortions CD, MD, and PD.

Proposition 1 *CD and MD relate to J via*

$$CD^2 + MD^2 \leq J^2; \quad (3.26)$$

whereas CD and PD relate to J via

$$CD^2 + PD^2 \leq J^2. \quad (3.27)$$

Proof From the representations for $T(z)$ and $T_d(z)$ in (3.19) and (3.20), respectively, we get

$$T(z) - T_d(z) = \begin{bmatrix} T_{00}(z) - z^{-d_0} & T_{01}(z) & \cdots & T_{0,M-1}(z) \\ T_{10}(z) & T_{11}(z) - z^{-d_1} & \cdots & T_{1,M-1}(z) \\ \vdots & \vdots & \ddots & \vdots \\ T_{M-1,0}(z) & T_{M-1,1}(z) & \cdots & T_{M-1,M-1}(z) - z^{-d_{M-1}} \end{bmatrix}.$$

The 2-norm formula in (3.24-3.25) gives

$$J^2 = \frac{1}{2\pi} \int_0^{2\pi} \sum_{i,j(i \neq j)} |T_{ij}(e^{j\omega})|^2 d\omega + \frac{1}{2\pi} \int_0^{2\pi} \sum_i |T_{ii}(e^{j\omega}) - e^{-jd_i\omega}|^2 d\omega.$$

We know that

$$CD^2 = \left[\frac{1}{2\pi} \int_0^{2\pi} \sum_{i,j(i \neq j)} |T_{ij}(e^{j\omega})|^2 d\omega \right].$$

which means the first term of J^2 is CD^2 . Write

$$A_i(\omega) = |T_{ii}(e^{j\omega}) - e^{-jd_i\omega}|$$

to get

$$J^2 = CD^2 + \frac{1}{2\pi} \int_0^{2\pi} \sum_i [A_i(\omega)]^2 d\omega, \quad (3.28)$$

$A_i(\omega)$ is a more natural distortion index capturing both magnitude and phase distortions together.

Since $A_i(\omega) \geq ||T_{ii}(e^{j\omega})| - 1|$, it follows that

$$\frac{1}{2\pi} \int_0^{2\pi} \sum_i [A_i(\omega)]^2 d\omega \geq \frac{1}{2\pi} \int_0^{2\pi} \sum_i ||T_{ii}(e^{j\omega})| - 1|^2 d\omega = MD^2.$$

Substituting this into (3.28) gives (3.26).

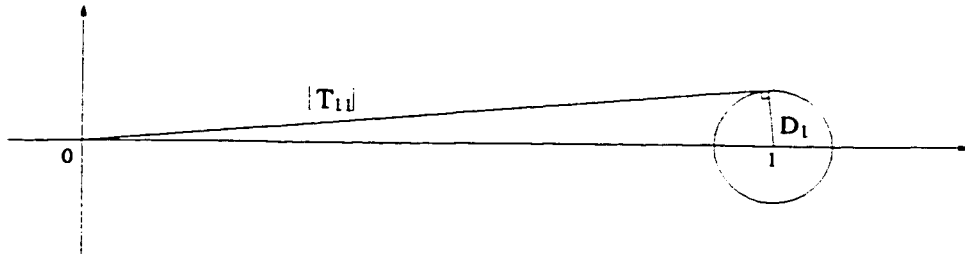


Figure 3.9: $\sin^{-1} A_i$.

For the definition of A_i , write

$$|T_{ii}(e^{j\omega})| = |T_{ii}|e^{j\mathcal{L}T_{ii}}.$$

Then

$$\begin{aligned} A_i(\omega) &= |T_{ii}(e^{j\omega}) - e^{-jd_i\omega}| \\ &= \left| |T_{ii}|e^{j\mathcal{L}T_{ii}} - e^{-jd_i\omega} \right| \\ &= \left| |T_{ii}|e^{j(\mathcal{L}T_{ii}+d_i\omega)} - 1 \right|. \end{aligned}$$

which says that the point $|T_{ii}|e^{j(\angle T_{ii} + d_i\omega)}$ lies on a circle with centre $(1, 0)$ and radius A_i (refer to Figure 3.9). Therefore,

$$|\angle T_{ii} + d_i\omega| \leq \sin^{-1} A_i,$$

That is,

$$\sin^2 [\angle T_{ii}(e^{j\omega}) + d_i\omega] \leq [A_i(\omega)]^2. \quad (3.29)$$

Hence (3.27) is proven. \square

Based on Proposition 1, it is clear that all the three distortions, CD, MD, and PD, are bounded above by J . Therefore it makes sense to minimize J in transmultiplexer design because this suboptimizes all CD, MD, and PD simultaneously.

3.6 Optimal Design Procedures

In this section we formulate the optimal design problem for transmultiplexers based on the distortion criterion J and develop the design procedure.

In view of the transmultiplexer in Figure 3.1, our design is divided into two steps: First, FIR synthesis filters $F_i(z)$ are designed based on frequency band combining requirement; next, FIR analysis filters $H_i(z)$ of a fixed length are designed to minimize J . This two-step design process has several advantages:

- It guarantees that the analysis filters designed have the optimal reconstruction property for a given set of synthesis filters. This is useful in cases where one can select synthesis filters from other approaches, e.g., Johnston's filters [22] as we will study in Example 1, and then redesign the analysis filters for optimality.
- By Proposition 1, the quantity J captures all three distortions CD, MD, and PD; minimizing J in design allows the reconstruction error to be distributed evenly across CD, MD, and PD.
- The design scenario provides an easy framework for studying tradeoffs among several important design factors, including filter complexity, reconstruction time delay, and reconstruction performance (J).

With reference to Figure 3.8, the design problem can be stated as follows:

Given the desired reconstruction time delays d_0, d_1, \dots, d_{M-1} and the FIR synthesis filters $F_0(z), F_1(z), \dots, F_{M-1}(z)$, design FIR analysis filters $H_0(z), H_1(z), \dots, H_{M-1}(z)$ of a given length to minimize J .

Note from (3.18) that $J = \|E(z)\Gamma(z)R(z) - T_d(z)\|_2$. Here, $\Gamma(z)$, $R(z)$, and $T_d(z)$ are all FIR and given and only $E(z)$, the FIR polyphase matrix of the analysis filters [38], is designable. Define $Q(z) = \Gamma(z)R(z)$ to get that $Q(z)$ is again FIR and given: and the equivalent design problem is:

$$J_{opt} = \min_{E(z)} \|E(z)Q(z) - T_d(z)\|_2, \quad (3.30)$$

where the minimization is over the class of FIR $E(z)$ of some fixed length.

To reduce the latter minimization problem to a solvable matrix problem, we look at the impulse response matrix of the MIMO system $P := EQ - T_d$. Let the orders of $Q(z)$ and $E(z)$ be m and l , respectively, and define

$$Q(z) = \sum_{i=0}^m z^{-i} Q_i, \quad E(z) = \sum_{i=0}^l z^{-i} E_i.$$

The matrices Q_0, Q_1, \dots, Q_m can be computed from the given data; but E_0, E_1, \dots, E_l are designable. If we have $0 \leq d_i \leq m + l$, $i = 0, 1, \dots, M - 1$, then the impulse response matrix of P is FIR with order $m + l$:

$$P(z) = \sum_{i=0}^{m+l} z^{-i} P_i.$$

By Parseval's equality,

$$J = \|P(z)\|_2 = \left[\sum_{i=0}^{m+l} \text{trace}(P_i P_i') \right]^{1/2} = [\text{trace}(\underline{P} \underline{P}')]^{1/2},$$

where we have defined the row matrix

$$\underline{P} = [P_0 \quad P_1 \quad \dots \quad P_{m+l}].$$

Since $P(z) = E(z)Q(z) - T_d(z)$, it can be verified that

$$\underline{P} = \underline{E} \underline{M} - \underline{D},$$

where \underline{D} relates to $T_d(z)$ just as \underline{P} does to $P(z)$,

$$\underline{E} = [E_0 \quad E_1 \quad \dots \quad E_l],$$

and \underline{M} is an $(l + 1) \times (m + l + 1)$ block matrix depending on only known matrices Q_0, Q_1, \dots, Q_m . So the problem in (3.30) reduces to the following matrix problem:

$$J_{opt} = \min_{\underline{E}} \{ \text{trace} [(\underline{E} \underline{M} - \underline{D})(\underline{E} \underline{M} - \underline{D})'] \}^{1/2}.$$

If the matrix \underline{M} has full row rank, or equivalently $\underline{M} \underline{M}'$ is invertible, the optimal solution can be obtained as

$$\underline{E}_{opt} = \underline{D} \underline{M}' (\underline{M} \underline{M})^{-1}.$$

From here we can recover the optimal analysis filters $H_0(z), H_1(z), \dots, H_{M-1}(z)$.

3.7 Design Examples

Next, we discuss two design examples based on the optimization just described. We will obtain the synthesis filters from some existing filter bank systems in the literature which achieve close-to-perfect reconstruction and compare two sets of analysis filters: The first set is obtained in the *normal* way from the filter bank system (using traditional method); and the second set in the *optimal* way proposed in this paper.

Example 1 In this two-channel example, we consider a filter bank with analysis filters $\hat{H}_0(z)$ and $\hat{H}_1(z)$ and synthesis filters $\hat{F}_0(z)$ and $\hat{F}_1(z)$ satisfying $\hat{H}_1(z) = \hat{H}_0(-z)$, $\hat{F}_0(z) = \hat{H}_0(z)$, and $\hat{F}_1(z) = -\hat{H}_0(-z)$, where $\hat{H}_0(z)$ is taken to be the Johnston's FIR filter (48D) [22] with 48 coefficients. Such a filter bank removes aliasing and phase distortions but has small magnitude distortion. For the two-channel transmultiplexer, we take the synthesis filters to be $F_0(z) = z^{-1} \hat{H}_0(z)$ and $F_1(z) = -z^{-1} \hat{H}_0(-z)$. (The factor z^{-1} is introduced because the corresponding filter bank is 1-skewed.) Their magnitude responses are given in Figure 3.10.

By the normal approach, we get the analysis filters for the transmultiplexer from the filter bank: $H_0(z) = \hat{H}_0(z)$ and $H_1(z) = \hat{H}_0(-z)$.

By the optimal approach we redesign FIR $H_0(z)$ and $H_1(z)$ of order 47 by minimizing J when the desired ideal system is of the form

$$T_d(z) = \begin{bmatrix} z^{-d} & 0 \\ 0 & z^{-d} \end{bmatrix}.$$

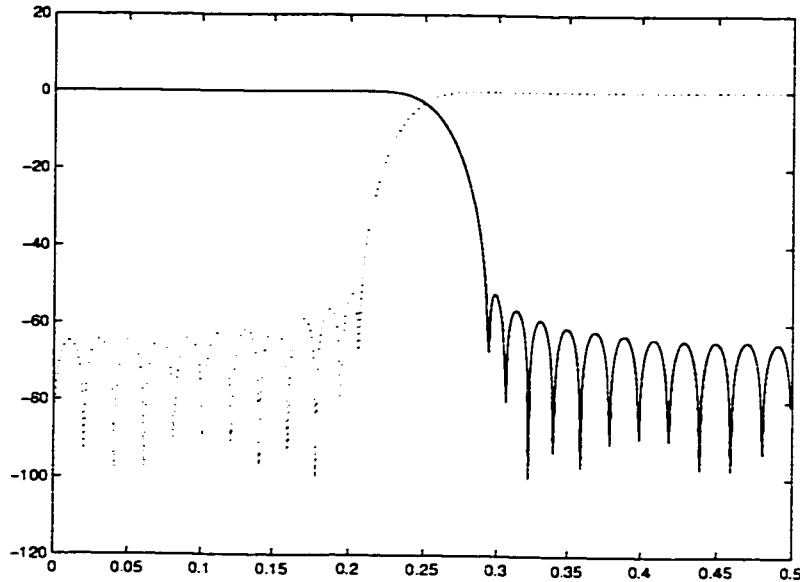


Figure 3.10: Example 1: The magnitude responses for F_0 (solid) and F_1 (dotted): dB versus $\omega/2\pi$.

The optimal distortion performance J_{opt} as a function of the time delay d is given in Figure 3.11. Figure 3.11 shows that there is a unique optimal choice for d : $d = 25$. With this optimal value for d , the optimal analysis filters $H_0(z)$ and $H_1(z)$ are computed, with their magnitude responses given in Figure 3.13: the corresponding J_{opt} is 6.044×10^{-4} . Figure 3.12 presents the simulation results, with the two inputs to be:

$$\begin{aligned} u_1 &= 2 \sin(0.3\pi t) + \cos(0.4\pi t), \\ u_2 &= 1.5 \cos(0.2\pi t) + \sin(0.6\pi t). \end{aligned}$$

We find that the outputs of the error system are very small: The maximal magnitude of the errors is 3.679×10^{-4} . This means the outputs of the designed system approximate the inputs very well.

In terms of the distortion measures defined in Section 3.2, performance comparison of the two transmultiplexers via the normal and optimal approaches is given in Table 3.1. We note that the optimal design outperforms the normal design in MD at the cost of slight CD. Both designs remove PD completely.

Example 2 This three-channel example is based on a filter bank system designed in [37], where the FIR analysis and synthesis filters are all of order 14, and the magnitude responses for the synthesis filters are given in Figure 3.14; for the transmultiplexer

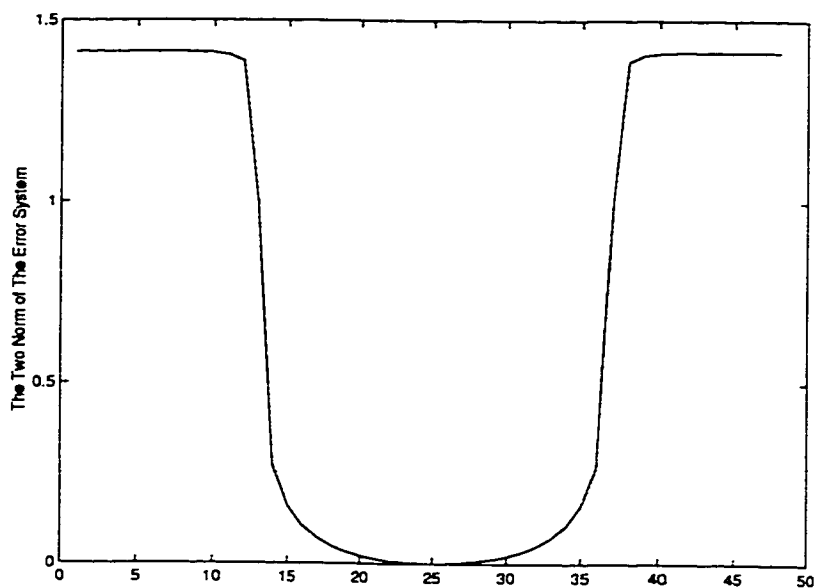


Figure 3.11: Example 1: J_{opt} versus the reconstruction delay d .

Table 3.1: Example 1: Distortion performance comparison.

Distortion	Normal	Optimal
CD	0	4.59×10^{-5}
MD	6.14×10^{-4}	6.02×10^{-4}
PD	0	0
CD _{max}	0	7.35×10^{-5}
MD _{max}	1.23×10^{-3}	1.13×10^{-3}
PD _{max}	0	0

application, we modify the synthesis filters by multiplying by the factor z^{-3} to handle the skewedness condition [24]. The filter bank system does not achieve perfect reconstruction but removes phase distortion completely. Again, the normal approach is to use these filters in the transmultiplexer; and the optimal approach is to redesign the analysis filters of the same length by optimizing J , taking the reconstruction time delays to be the same: $d_0 = d_1 = d_2$. It is found that the minimum J_{opt} is 1.67×10^{-4} when the reconstruction time delay is 6. For this delay value, the optimal analysis filters are computed. Their magnitude responses are depicted in Figure 3.15, and the simulation results are given in Figure 3.16, the maximal magnitude of the errors is

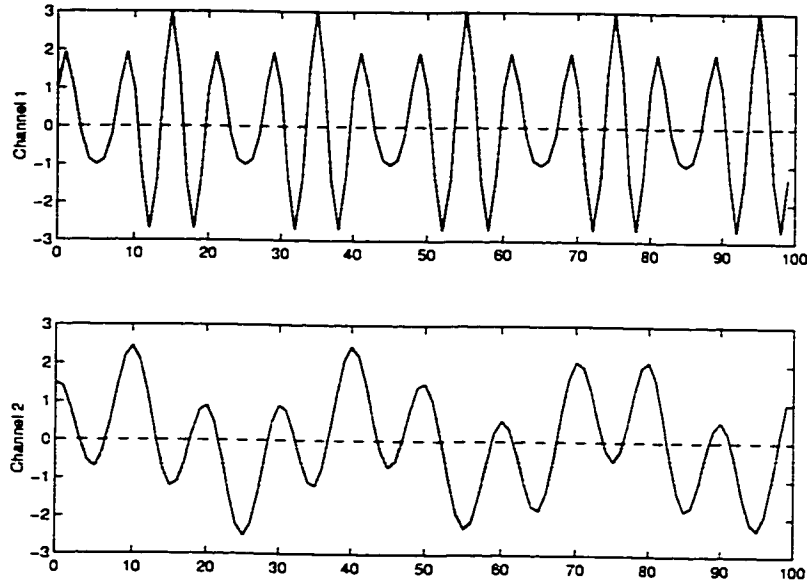


Figure 3.12: Example 1: The simulation results of the error system with inputs (solid) and outputs (dotted).

2.805×10^{-4} , with the three inputs to be

$$\begin{aligned} u_1 &= \sin(0.3\pi t) + \cos(0.2\pi t), \\ u_2 &= 2\sin(0.2\pi t) + \sin(0.1\pi t), \\ u_3 &= \cos(0.1\pi t) + 2\sin(0.2\pi t). \end{aligned}$$

The performance of the two transmultiplexers designed by the normal and optimal approaches are compared in Table 3.2. (Note that PD_{\max} in the table is measured in radians.)

Table 3.2: Example 2: Distortion performance comparison.

Distortion	Normal	Optimal
CD	2.05×10^{-3}	1.14×10^{-4}
MD	1.35×10^{-3}	8.67×10^{-5}
PD	0	8.65×10^{-5}
CD_{\max}	1.34×10^{-3}	1.13×10^{-4}
MD_{\max}	1.79×10^{-3}	1.20×10^{-4}
PD_{\max}	0	1.25×10^{-4}

The merit of the optimal approach is evident: By tolerating a slight phase distortion, one can *significantly* improve the cross-talk and magnitude distortions. Note

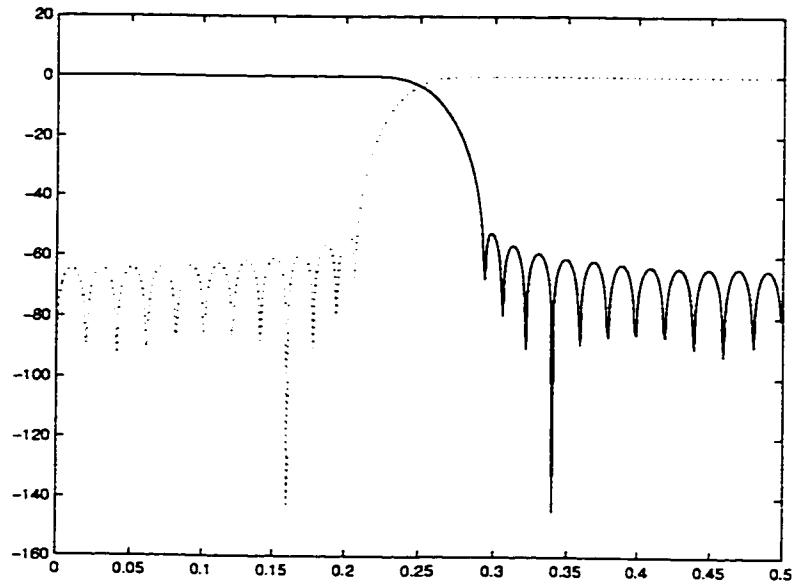


Figure 3.13: Example 1: The magnitude responses for the optimal H_0 (solid) and H_1 (dotted): dB versus $\omega/2\pi$.

that the conclusion is the same no matter we use CD, MD, and PD (energy) or CD_{\max} , MD_{\max} , and PD_{\max} (peak value).

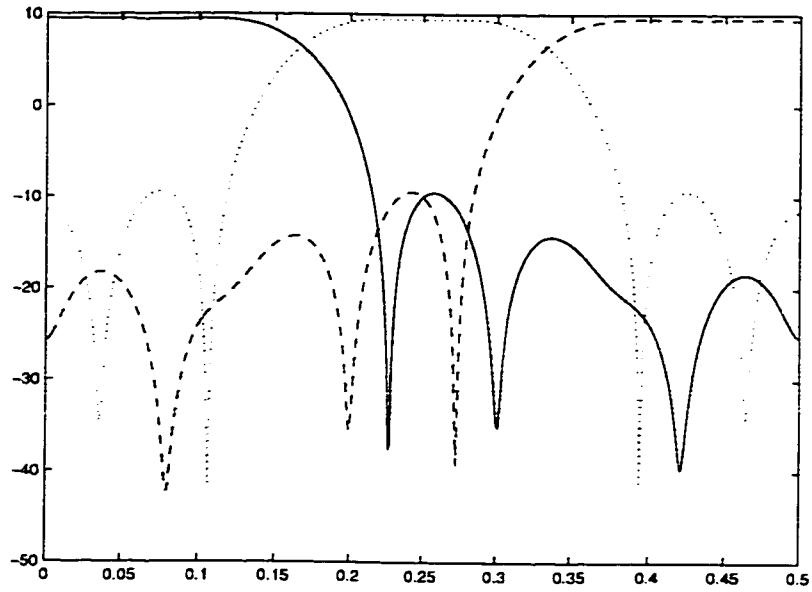


Figure 3.14: Example 2: The magnitude responses for F_0 (solid), F_1 (dotted) and F_2 (dashed): dB versus $\omega/2\pi$.

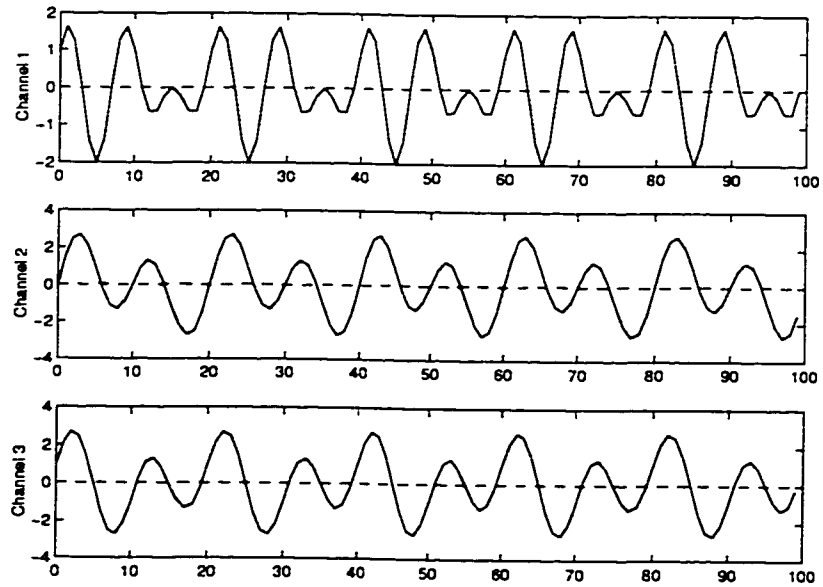


Figure 3.15: Example 2: The simulation results of the error system with inputs (solid) and outputs (dashed).

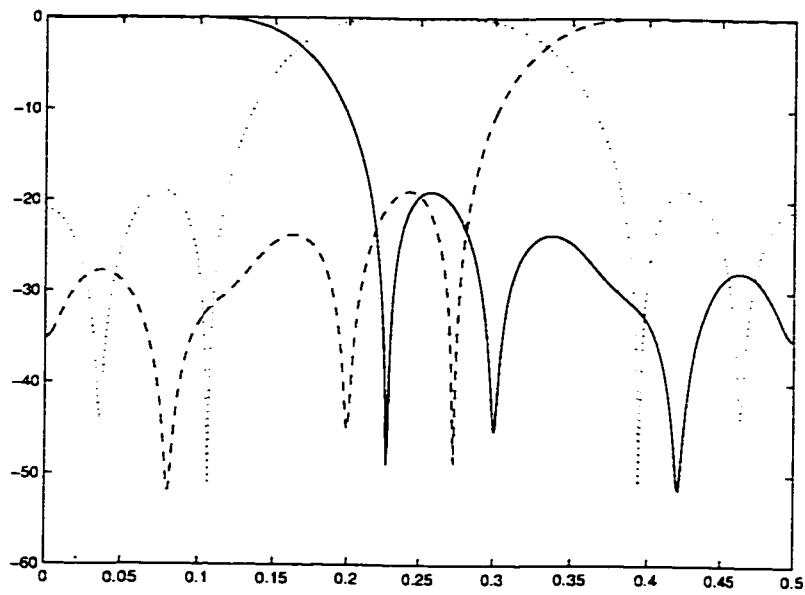


Figure 3.16: Example 1: The magnitude responses for the optimal H_0 (solid), H_1 (dotted) and H_2 (dashed): dB versus $\omega/2\pi$.

Chapter 4

Optimal Design of Nonuniform Transmultiplexers Using General Building Blocks

4.1 Introduction

Typical studies of transmultiplexers focus on uniform-band structures in which incoming data signals are assumed to have the same sampling rate and are upsampled at the same integer factor. In this chapter, our goal is to study nonuniform transmultiplexers where incoming signals have possibly different sampling rates and thus are upsampled at different fractional ratios. A general nonuniform transmultiplexer built with traditional blocks is shown in Figure 4.1, where m signals x_i ($i = 0, 1, \dots, m-1$).

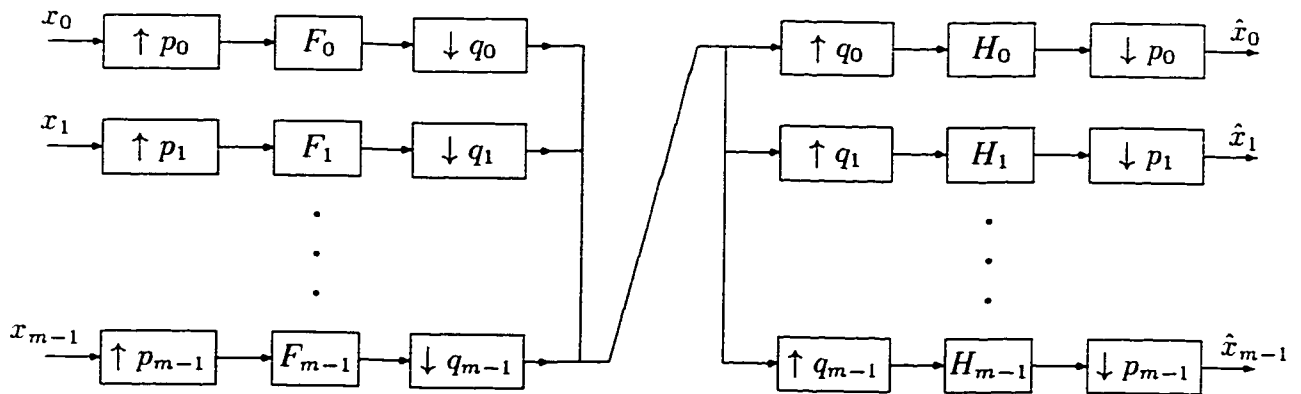


Figure 4.1: A nonuniform transmultiplexer using traditional building blocks.

with different sampling rates, are synthesized by m synthesis subsystems formed by upsampler $\uparrow p_i$, LTI filter F_i , and downsampler $\downarrow q_i$ ($q_i < p_i$). Then these signals are combined into a single channel, and are coded and transmitted (not modelled). In the

other end, the combined signal is analyzed through m analysis subsystems consisting of upsampler $\uparrow q_i$, LTI filter H_i , and downsampler $\downarrow p_i$, and hence generating the reconstructed signals \hat{x}_i ($i = 0, 1, \dots, m - 1$).

Note that each subsystems is a sample-rate changer as depicted in Figure 4.2. where the output sample rate is m/n times the input sample rate. We say it is a dual-rate system with the input-output property that shifting the input (u) by n samples results in shifting the output (y) by m samples. Such a property is defined as (m, n) -shift invariance [6]. If $m = n = 1$, a linear, (m, n) -shift invariant system reduced to an LTI system.



Figure 4.2: A sample-rate changer.

Let f_i be the sampling rate for the incoming signal x_i . Since after synthesis the signals are combined (and hence have the same sampling rate), we have

$$\frac{p_0}{q_0} f_0 = \frac{p_1}{q_1} f_1 = \dots = \frac{p_{m-1}}{q_{m-1}} f_{m-1}.$$

Thus the sampling rates for the incoming signals are rationally related. Usually integers p_i and q_i are coprime; even if they are not, this structure does not lead to more general systems [8, 35]. To fully use the channel, we assume the critical sampling ratios, i.e.,

$$\sum_{i=0}^{m-1} \frac{q_i}{p_i} = 1. \quad (4.1)$$

Same as in the uniform case, we say the transmultiplexer achieves *perfect reconstruction* [38] if \hat{x}_i is a delayed version of x_i , namely, if there exist nonnegative integers d_i such that

$$\hat{x}_i(k) = x_i(k - d_i), \quad i = 0, 1, \dots, m - 1. \quad (4.2)$$

Note that in this case there are no cross-talk, magnitude and phase distortions.

However, according to the analogy of transmultiplexers and filter banks established in [39, 32, 24], in general, it is impossible to remove cross-talk distortion using causal LTI filters F_i and H_i , let alone perfect reconstruction. As in the filter bank case, this is due to the incompatibility of the upsampling ratios p_i/q_i involved.

As suggested in [35, 8], more general building blocks should be used to allow more design freedom in order to achieve perfect reconstruction. The system proposed as a general building block in [8] for multirate signal processing is the linear, dual-rate system depicted in Figure 4.3, and is represented by $G : (p, q)$, where p and q are positive integers. This system has the (p, q) -shift invariance property in that shifting the input by q samples results in shifting the output by p samples; thus the output sampling rate is p/q times the input sampling rate. The dual-rate system in Figure 4.3 is more general than the structure in Figure 4.2, and it can be realized by Figure 4.2 only if the two integers p and q are coprime [6]. Such system allows more design freedom if p and q have nontrivial common factors. In this case, they can be implemented by the cascade combination of upsamplers, certain linear switching time-varying (LSTV) systems, and downsamplers [8]—see Section 4.3 for details.

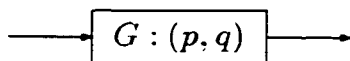


Figure 4.3: A dual-rate system.

The synthesis and analysis subsystems in Figure 4.1 are such dual-rate systems, e.g., the i -th synthesis subsystem is (p_i, q_i) -shift invariant. Replacing the synthesis and analysis subsystems in Figure 4.1 by appropriate dual-rate systems gives rise to a more general transmultiplexer. Let n be the least common multiple of integers p_0, p_1, \dots, p_{m-1} ; define

$$r_i = \frac{nq_i}{p_i}, \quad i = 0, 1, \dots, m-1. \quad (4.3)$$

It follows that r_i is integer-valued. The more general transmultiplexer using dual-rate structures as building blocks is shown in Figure 4.4. Note that each synthesis or analysis subsystem in Figure 4.1 is replaced by a (possibly) more general dual-rate system in Figure 4.3, but the output-to-input sampling rate conversion ratio is kept the same, e.g., for the i -th synthesis subsystem, we have

$$\frac{n}{r_i} = \frac{p_i}{q_i},$$

which follows easily from (4.3).

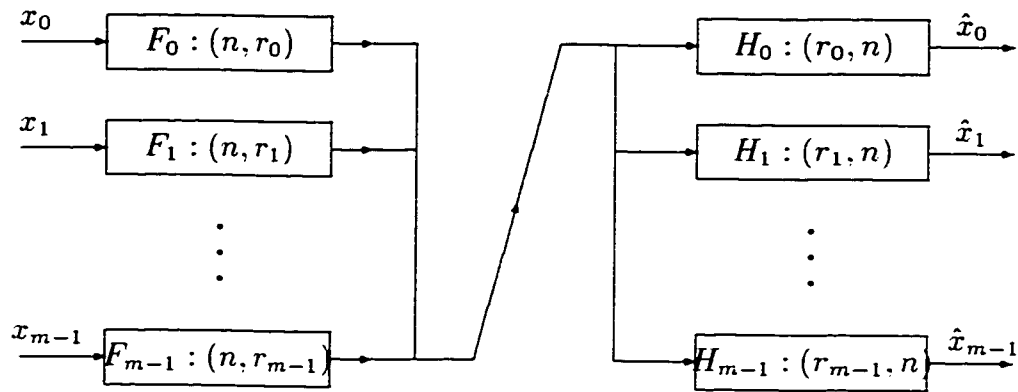


Figure 4.4: A nonuniform transmultiplexer using general building blocks.

As in the filter bank case [35, 8], perfect reconstruction is possible to achieve in Figure 4.4.

Different from uniform transmultiplexers, the structure in Figure 4.4 is not time-invariant in general, e.g., the system from x_i to \hat{x}_i is linear periodically time-varying (LPTV) with period r_i . Hence, in addition to the usual cross-talk, magnitude, and phase distortions, which are similar to the uniform case [39, 38, 26], there exists a new *aliasing distortion* from x_i to \hat{x}_i - see Section 4.5 for details. Coping with this new distortion is effectively done later.

The chapter is organized as follows. In Section 4.2 we introduce blocking and develop a blocked model for the transmultiplexer in Figure 4.4. Section 4.3 relates the blocked model to the LSTV structure for implementation. Section 4.4 states a necessary and sufficient condition for perfect reconstruction based on the blocked model. In Section 4.5 we propose measures for cross-talk, aliasing, magnitude, and phase distortions, and a composite new measure. Section 4.6 develops an iterative design procedure for the transmultiplexer aiming at minimizing the composite distortion measure. Finally in Section 4.7 this method is illustrated in details with a three-channel example.

4.2 Blocked Models

Blocking is a standard technique for treating periodic/multirate systems in signal processing [28, 29, 40]. Relating it to the polyphase decomposition in the frequency domain provides deep insight for multirate systems.

4.2.1 Blocking Signals

As in Chapter 3, ℓ is the space of discrete-time signals defined on the set of all integers. A signal x in ℓ is written

$$\{\cdots, x(-2), x(-1) \mid x(0), x(1), x(2), \cdots\},$$

the vertical bar separating the time from $k = 0$. For an integer $n > 0$, defining L_n to be the n -fold *blocking operator*, $\underline{x} = L_n x$ is the blocked signal (underlining denotes blocking):

$$\{\cdots \mid x(0), x(1), \cdots\} \mapsto \left\{ \cdots \left| \begin{array}{c} x(0) \\ x(1) \\ \vdots \\ x(n-1) \end{array} \right|, \begin{array}{c} x(n) \\ x(n+1) \\ \vdots \\ x(2n-1) \end{array} \right|, \cdots \right\}. \quad (4.4)$$

L_n maps ℓ to ℓ^n , the external direct sum of n copies of ℓ . The underlying period for the blocked signal \underline{x} is nh if the underlying period for x is h . The vector representation of the equation $\underline{x} = L_n x$ when $n = 2$ is: (see [9] for details)

$$\begin{bmatrix} \vdots \\ \underline{x}(0) \\ \underline{x}(1) \\ \underline{x}(2) \\ \vdots \end{bmatrix} = \begin{bmatrix} \vdots & \vdots & \vdots & \vdots & \vdots & \vdots & \vdots \\ \cdots & I & 0 & 0 & 0 & 0 & \cdots \\ \cdots & 0 & I & 0 & 0 & 0 & \cdots \\ \cdots & 0 & 0 & I & 0 & 0 & \cdots \\ \cdots & 0 & 0 & 0 & I & 0 & \cdots \\ \cdots & 0 & 0 & 0 & 0 & I & \cdots \\ \cdots & 0 & 0 & 0 & 0 & 0 & \cdots \\ \vdots & \vdots & \vdots & \vdots & \vdots & \vdots & \vdots \end{bmatrix} \begin{bmatrix} \vdots \\ v(0) \\ v(1) \\ v(2) \\ \vdots \end{bmatrix}.$$

For the partition shown, the system L is non-causal and time-varying since L is neither lower-triangular nor Toeplitz, namely, constant along all diagonals.

The inverse L^{-1} , mapping ℓ^n to ℓ , amounts to reversing the operation in (4.4). It is defined as follows [9]: If

$$y = \left\{ \cdots \left| \begin{array}{c} y_1(0) \\ y_2(0) \\ \vdots \\ y_n(0) \end{array} \right|, \begin{array}{c} y_1(1) \\ y_2(1) \\ \vdots \\ y_n(1) \end{array} \right|, \cdots \right\},$$

and

$$x = L^{-1}y,$$

then

$$x = \{\dots | y_1(0), y_2(0), \dots, y_n(0), y_1(1), \dots, y_n(1), \dots\}.$$

The corresponding matrix for $n = 2$ is [9]:

$$[L^{-1}] = \begin{bmatrix} & \vdots & \vdots & \vdots & \vdots & \vdots & \vdots & \vdots \\ \dots & I & 0 & 0 & 0 & 0 & \dots & \\ \dots & 0 & I & 0 & 0 & 0 & \dots & \\ \dots & 0 & 0 & I & 0 & 0 & \dots & \\ \dots & 0 & 0 & 0 & I & 0 & \dots & \\ \dots & 0 & 0 & 0 & 0 & I & \dots & \\ \vdots & \vdots & \vdots & \vdots & \vdots & \vdots & & \end{bmatrix}.$$

Clearly, L^{-1} is causal but time-varying.

4.2.2 Blocking Systems

For a linear discrete-time system G mapping ℓ to ℓ , blocking of its input and output signals induces another linear system, denoted \underline{G} . That is, $\underline{G} = L_n G L_n^{-1}$, mapping \underline{x} to \underline{y} . \underline{G} has n inputs and n outputs if G maps x to y and is single-input and single-output (SISO).

The following facts hold based on [6] and [9].

1. \underline{G} is time-invariant if and only if G is n -periodic.
2. If G is n -periodic, the transfer matrix $\hat{\underline{G}}$ of \underline{G} is $n \times n$ and satisfies $\hat{\underline{y}}(z) = \hat{\underline{G}}(z)\hat{\underline{x}}(z)$, where $\hat{\underline{x}}$ and $\hat{\underline{y}}$ are polyphase vectors of the input and output.
3. The norms of the two transfer function \hat{G} and $\hat{\underline{G}}$ satisfy: $\|\hat{G}\|_2^2 = \|\hat{\underline{G}}\|_2^2/n$ and $\|\hat{G}\|_\infty = \|\hat{\underline{G}}\|_\infty$.
4. If G is LTI with the transfer function

$$\hat{G}(z) = \sum_{i=0}^{n-1} z^{-i} \hat{G}_i(z^n),$$

\underline{G} is also LTI and its transfer matrix is

$$\hat{\underline{G}}(z) = \begin{bmatrix} \hat{G}_0(z) & z^{-1}\hat{G}_{n-1}(z) & z^{-1}\hat{G}_{n-2}(z) & \dots & z^{-1}\hat{G}_1(z) \\ \hat{G}_1(z) & \hat{G}_0(z) & z^{-1}\hat{G}_{n-1}(z) & \dots & z^{-1}\hat{G}_2(z) \\ \hat{G}_2(z) & \hat{G}_1(z) & \hat{G}_0(z) & \dots & z^{-1}\hat{G}_3(z) \\ \vdots & \vdots & \vdots & \ddots & \vdots \\ \hat{G}_{n-1}(z) & \hat{G}_{n-2}(z) & \hat{G}_{n-3}(z) & \dots & \hat{G}_0(z) \end{bmatrix}. \quad (4.5)$$

Note that the matrix in (4.5) is the n -fold polyphase matrix associated with G . It is Toeplitz and is determined by only n functions: the n -fold polyphase components of $\hat{G}(z)$.

4.2.3 Blocking Analysis Subsystems

From Figure 4.1 we know that all the analysis subsystems have similar structures. In general, Figure 4.5 is an analysis subsystem by dropping the subscripts. Note the system $A = D_q H E_p$ changes sampling rates by a factor of p/q [6], where D_q is the q -fold decimator ($\downarrow q$) and E_p is the p -fold expander ($\uparrow p$).

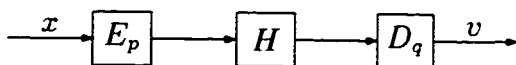


Figure 4.5: An analysis subsystem.

The sampling periods of the input and output are not equal. If the sampling period of x is h , the v 's is qh/p . So in general, A is not n -periodic. For the blocked system to have the same rate at the input and output, we should block v by the np/q -fold blocking operator and x should be blocked by n . This suggests blocking A this way [6],

$$\underline{A} := L_{np/q} A L_n^{-1}.$$

This \underline{A} is LTI. Reference [6] gives the method to calculate the transfer matrix for \underline{A} :

Let $\hat{H}(z)$ be the (np) -fold polyphase matrix of H :

$$\hat{H}(z) = \begin{bmatrix} \hat{H}_0(z) & z^{-1} \hat{H}_{np-1}(z) & \cdots & z^{-1} \hat{H}_1(z) \\ \hat{H}_1(z) & \hat{H}_0(z) & \cdots & z^{-1} \hat{H}_2(z) \\ \vdots & \vdots & \ddots & \vdots \\ \hat{H}_{np-1}(z) & \hat{H}_{np-2}(z) & \cdots & \hat{H}_0(z) \end{bmatrix}.$$

Then the $(np/q) \times n$ transfer matrix for \underline{A} is obtained by retaining every q -th row and every p -th column of \hat{H} starting from the upper-left corner:

$$\hat{A}(z) = \begin{bmatrix} \hat{H}_0(z) & z^{-1} \hat{H}_{np-p}(z) & \cdots & z^{-1} \hat{H}_p(z) \\ \hat{H}_q(z) & \hat{H}_{q-p}(z) & \cdots & z^{-1} \hat{H}_{q+p}(z) \\ \vdots & \vdots & \ddots & \vdots \\ \hat{H}_{np-q}(z) & \hat{H}_{np-q-p}(z) & \cdots & \hat{H}_{np-q+p}(z) \end{bmatrix}.$$

(assuming $q > p$).

Note that the matrix \hat{A} is no longer Toeplitz.

In general, n is a multiple of q . We can write $\hat{v}(z) = \hat{A}(z)\hat{x}(z)$, where \hat{x} and \hat{v} are the n -fold and (np/q) -fold polyphase vectors of $x(z)$ and $v(z)$ in Figure 4.5.

4.2.4 Blocking Synthesis Subsystems

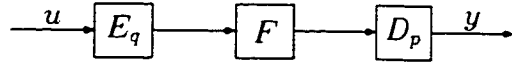


Figure 4.6: A synthesis subsystem.

The synthesis subsystems are the dual of the analysis subsystems studied before, see the system $u \rightarrow y$ shown in Figure 4.6. where F is LTI. We wish to block y by L_n and block u by np/q , where n is a multiple of q , so we define the blocked S to be [6]:

$$\underline{S} = L_n S L_{np/q}^{-1}.$$

This \underline{S} is LTI. The following result from [6] gives the way to calculate the transfer matrix for the blocked synthesis subsystem \underline{S} :

Let $\hat{F}(z)$ be the (np) -fold polyphase matrix of F :

$$\hat{F}(z) = \begin{bmatrix} \hat{F}_0(z) & z^{-1}\hat{F}_{np-1}(z) & \cdots & z^{-1}\hat{F}_1(z) \\ \hat{F}_1(z) & \hat{F}_0(z) & \cdots & z^{-1}\hat{F}_2(z) \\ \vdots & \vdots & \ddots & \vdots \\ \hat{F}_{np-1}(z) & \hat{F}_{np-2}(z) & \cdots & \hat{F}_0(z) \end{bmatrix}.$$

Then the $n \times (np/q)$ transfer matrix for \underline{A} is obtained by retaining every p -th row and every q -th column of \hat{F} starting from the upper-left corner:

$$\hat{S}(z) = \begin{bmatrix} \hat{F}_0(z) & z^{-1}\hat{F}_{np-q}(z) & \cdots & z^{-1}\hat{F}_q(z) \\ \hat{F}_p(z) & \hat{F}_{np-q+p}(z) & \cdots & z^{-1}\hat{F}_{q+p}(z) \\ \vdots & \vdots & \ddots & \vdots \\ \hat{F}_{np-p}(z) & \hat{F}_{np-p-q}(z) & \cdots & \hat{F}_{q-p}(z) \end{bmatrix}.$$

(assuming $p > q$).

Again, in general \hat{S} is no longer Toeplitz but it contains all (np) -fold polyphase components of F if p and q are coprime.

4.2.5 Blocking the Transmultiplexer System

Putting together the results above, it is not difficult to get the blocked system for Figure 4.1. We consider the more general transmultiplexer in Figure 4.4 represented by

$$T = \begin{bmatrix} H_0 \\ H_1 \\ \vdots \\ H_{m-1} \end{bmatrix} \begin{bmatrix} F_0 & F_1 & \cdots & F_{m-1} \end{bmatrix}. \quad (4.6)$$

Since the m channels have different downsampling ratios, we need to block them differently to get an LTI model. In view of (4.6), the blocked transmultiplexer, \underline{T} , is defined as follows:

$$\begin{aligned} \underline{T} &= \begin{bmatrix} L_{r_0} & & & \\ & L_{r_1} & & \\ & & \cdots & \\ & & & L_{r_{m-1}} \end{bmatrix} T \begin{bmatrix} L_{r_0}^{-1} & & & \\ & L_{r_1}^{-1} & & \\ & & \cdots & \\ & & & L_{r_{m-1}}^{-1} \end{bmatrix} \\ &= \begin{bmatrix} L_{r_0} & & & \\ & L_{r_1} & & \\ & & \cdots & \\ & & & L_{r_{m-1}} \end{bmatrix} \begin{bmatrix} H_0 \\ H_1 \\ \vdots \\ H_{m-1} \end{bmatrix} \\ &\quad \begin{bmatrix} F_0 & F_1 & \cdots & F_{m-1} \end{bmatrix} \begin{bmatrix} L_{r_0}^{-1} & & & \\ & L_{r_1}^{-1} & & \\ & & \cdots & \\ & & & L_{r_{m-1}}^{-1} \end{bmatrix} \\ &= \begin{bmatrix} L_{r_0} H_0 L_n^{-1} \\ L_{r_1} H_1 L_n^{-1} \\ \vdots \\ L_{m-1} H_{m-1} L_n^{-1} \end{bmatrix} \begin{bmatrix} L_n F_0 L_{r_0}^{-1} & L_n F_1 L_{r_1}^{-1} & \cdots & L_n F_{m-1} L_{r_{m-1}}^{-1} \end{bmatrix} \end{aligned}$$

Defining the blocked subsystems

$$\underline{F}_i = L_n F_i L_{r_i}^{-1}, \quad \underline{H}_i = L_{r_i} H_i L_n^{-1}, \quad i = 0, 1, \dots, m-1,$$

and the blocked synthesis and analysis matrices, respectively,

$$\underline{F} = \begin{bmatrix} \underline{F}_0 & \underline{F}_1 & \cdots & \underline{F}_{m-1} \end{bmatrix}, \quad (4.7)$$

$$\underline{H} = \begin{bmatrix} \underline{H}_0 \\ \underline{H}_1 \\ \vdots \\ \underline{H}_{m-1} \end{bmatrix}, \quad (4.8)$$

we can write \underline{T} as

$$\underline{T} = \underline{H} \underline{F}.$$

All the blocked systems defined are LTI because of the shift invariant properties of the subsystems: e.g., since F_0 is (n, r_0) -shift invariant, it follows that the blocked system \underline{F}_0 is $(1, 1)$ -shift invariant and hence LTI. Therefore, \underline{F} and \underline{H} are LTI, and so is \underline{T} ; the frequency-domain model using transfer matrices is

$$\underline{T}(z) = \underline{H}(z)\underline{F}(z).$$

For a dimensional count, note that \underline{F}_i has r_i inputs and n outputs (because the way blocking is introduced); thus \underline{F} has $\sum_{i=0}^{m-1} r_i$ inputs and n outputs. It follows from (4.3) and (4.1) that

$$n = \sum_{i=0}^{m-1} r_i.$$

Hence \underline{F} is a square system with n inputs and outputs. Similarly, \underline{H} is square with n inputs and outputs and so is \underline{T} .

4.3 Realization of Dual-Rate Systems via Linear Switching Time-Varying Structures

We know that if p and q are already coprime, any (p, q) -shift invariant system can be implemented by the structure in Figure 4.2 using only the traditional decimator and expander. If p and q are not coprime, we can also make use of a similar structure with traditional decimator and expander and some SISO system F , where F belongs to a special class of LPTV systems, which are called linear switching time-varying (LSTV) systems (see [8] for details).

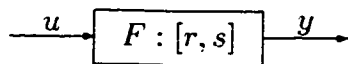


Figure 4.7: An $[r, s]$ -LSTV system.

An $[r, s]$ -LSTV system F is represented in Figure 4.7, which consists of r LTI subsystems, F_0, F_1, \dots, F_{r-1} , and a switching device as depicted in Figure 4.8. The switching device switches the input u to each subsystem for exactly s samples starting from F_0 to F_{r-1} and then repeats [8].

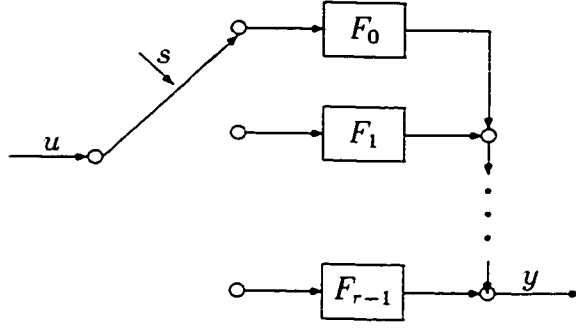


Figure 4.8: The structure of an $[r, s]$ -LSTV system.

It is obvious that the LSTV system F is LPTV with period rs . Blocking the input and output by a factor of rs , we get an LTI MIMO system $\underline{F} := L_{rs} F L_{rs}^{-1}$, whose dimension is $(rs) \times (rs)$. Reference [8] gave the way for calculating the transfer function of the blocked system \underline{F} :

Let $\underline{F}_j = L_{rs} F_j L_{rs}^{-1}$, $j = 0, 1, \dots, r-1$; partition each transfer matrix as follows:

$$\underline{F}_j(z) = \begin{bmatrix} \underline{F}_j^0(z) & \underline{F}_j^1(z) & \dots & \underline{F}_j^{r-1}(z) \end{bmatrix},$$

every submatrix being $(rs) \times s$. Then the transfer matrix for the blocked LSTV system, $\underline{F} = L_{rs} F L_{rs}^{-1}$, is given by

$$\underline{F}(z) = \begin{bmatrix} \underline{F}_0^0(z) & \underline{F}_1^0(z) & \dots & \underline{F}_{r-1}^0(z) \end{bmatrix}.$$

Each submatrix in $\underline{F}(z)$ is pseudo-circulant column-wise only.

To see clearly how to write down this transfer matrix, let us consider the case with $r = 2, s = 3$; then $\hat{\underline{F}}(z)$ is 6×6 . Using the discussion above we get the blocked systems

$$\underline{F}_j(z) = \begin{bmatrix} \hat{F}_j^0(z) & z^{-1} \hat{F}_j^5(z) & z^{-1} \hat{F}_j^4(z) & z^{-1} \hat{F}_j^3(z) & z^{-1} \hat{F}_j^2(z) & z^{-1} \hat{F}_j^1(z) \\ \hat{F}_j^1(z) & \hat{F}_j^0(z) & z^{-1} \hat{F}_j^5(z) & z^{-1} \hat{F}_j^4(z) & z^{-1} \hat{F}_j^3(z) & z^{-1} \hat{F}_j^2(z) \\ \hat{F}_j^2(z) & \hat{F}_j^1(z) & \hat{F}_j^0(z) & z^{-1} \hat{F}_j^5(z) & z^{-1} \hat{F}_j^4(z) & z^{-1} \hat{F}_j^3(z) \\ \hat{F}_j^3(z) & \hat{F}_j^2(z) & \hat{F}_j^1(z) & \hat{F}_j^0(z) & z^{-1} \hat{F}_j^5(z) & z^{-1} \hat{F}_j^4(z) \\ \hat{F}_j^4(z) & \hat{F}_j^3(z) & \hat{F}_j^2(z) & \hat{F}_j^1(z) & \hat{F}_j^0(z) & z^{-1} \hat{F}_j^5(z) \\ \hat{F}_j^5(z) & \hat{F}_j^4(z) & \hat{F}_j^3(z) & \hat{F}_j^2(z) & \hat{F}_j^1(z) & \hat{F}_j^0(z) \end{bmatrix}, \quad j = 0, 1.$$

$\hat{\underline{F}}(z)$ can be formed by putting together the first three columns of $\hat{\underline{F}}_0(z)$ and the last three columns of $\hat{\underline{F}}_1(z)$:

$$\underline{E}(z) = \begin{bmatrix} \hat{F}_0^0(z) & z^{-1}\hat{F}_0^5(z) & z^{-1}\hat{F}_0^4(z) & z^{-1}\hat{F}_1^3(z) & z^{-1}\hat{F}_1^2(z) & z^{-1}\hat{F}_1^1(z) \\ \hat{F}_0^1(z) & \hat{F}_0^0(z) & z^{-1}\hat{F}_0^5(z) & z^{-1}\hat{F}_1^4(z) & z^{-1}\hat{F}_1^3(z) & z^{-1}\hat{F}_1^2(z) \\ \hat{F}_0^2(z) & \hat{F}_0^1(z) & \hat{F}_0^0(z) & z^{-1}\hat{F}_1^5(z) & z^{-1}\hat{F}_1^4(z) & z^{-1}\hat{F}_1^3(z) \\ \hat{F}_0^3(z) & \hat{F}_0^2(z) & \hat{F}_0^1(z) & \hat{F}_1^0(z) & z^{-1}\hat{F}_1^5(z) & z^{-1}\hat{F}_1^4(z) \\ \hat{F}_0^4(z) & \hat{F}_0^3(z) & \hat{F}_0^2(z) & \hat{F}_1^1(z) & \hat{F}_1^0(z) & z^{-1}\hat{F}_1^5(z) \\ \hat{F}_0^5(z) & \hat{F}_0^4(z) & \hat{F}_0^3(z) & \hat{F}_1^2(z) & \hat{F}_1^1(z) & \hat{F}_1^0(z) \end{bmatrix}.$$

From Section 4.2 we know that if in Figure 4.4 the blocked systems $\underline{F}_i(z)$ and $\underline{H}_i(z)$ is computed, we can construct from (4.7) and (4.8) the two $n \times n$ matrices $\underline{E}(z)$ and $\underline{H}(z)$, and hence $\underline{T}(z)$. How do we compute the blocked systems $\underline{F}_i(z)$ and $\underline{H}_i(z)$? If the general transmultiplexer in Figure 4.4 reduces to the traditional transmultiplexer in Figure 4.1, procedures discussed in section 3.3 can be used directly. Otherwise, we adopt the structure studied before using LSTV systems in Figure 4.8 for implementation of the general blocks in Figure 4.4.

Consider the general dual-rate system G in Figure 4.3 which is (p, q) -shift invariant. Write $p = l\bar{p}$ and $q = l\bar{q}$ so that l is the common factor and \bar{p} and \bar{q} are relative prime. From [8] we know that the dual-rate system is realizable by the cascade structure of the expander $\uparrow \bar{p}$, some $[l, \bar{p}\bar{q}]$ -LSTV system G' , and the decimator $\downarrow \bar{q}$. So we can represent G in Figure 4.9 using LSTV system shown in Figure 4.8, where G_0, G_1, \dots, G_{l-1} are LTI systems. The periodic switch connects each channel for $\bar{p}\bar{q}$ samples starting from time $k = 0$ and system G_0 [8]. In terms of the LTI systems

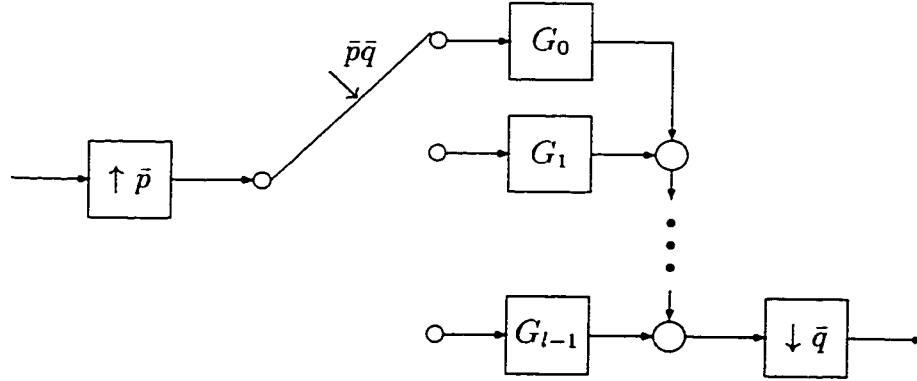


Figure 4.9: Implementation of a (p, q) -shift invariant system via an LSTV structure.

G_i , the following procedure is summarized based on earlier discussions (also see the proof of Theorem 3 in [8]) to compute the transfer matrix for $\underline{G} = L_p G L_q^{-1}$:

1. Compute the type-1 polyphase representations [38] for G_i :

$$G_i(z) = \sum_{j=0}^{\bar{p}\bar{q}l-1} z^{-j} G_i^j(z^{\bar{p}\bar{q}l}), \quad i = 0, 1, \dots, l-1.$$

2. Form the $(\bar{p}\bar{q}l) \times (\bar{p}\bar{q}l)$ pseudocirculant matrices

$$\underline{G}_i(z) = \begin{bmatrix} G_i^0(z) & z^{-1}G_i^{\bar{p}\bar{q}l-1}(z) & \dots & z^{-1}G_i^1(z) \\ G_i^1(z) & G_i^0(z) & \dots & z^{-1}G_i^2(z) \\ \vdots & \vdots & \ddots & \vdots \\ G_i^{\bar{p}\bar{q}l-1}(z) & G_i^{\bar{p}\bar{q}l-2}(z) & \dots & G_i^0(z) \end{bmatrix}, \quad i = 0, 1, \dots, l-1.$$

3. Form an $(\bar{p}\bar{q}l) \times (\bar{p}\bar{q}l)$ matrix $M(z)$ as follows: The first $\bar{p}\bar{q}$ columns are taken from the first $\bar{p}\bar{q}$ columns of $\underline{G}_0(z)$, the next $\bar{p}\bar{q}$ columns are from the corresponding columns of $\underline{G}_1(z)$, and so on, and the last $\bar{p}\bar{q}$ columns are taken from the last $\bar{p}\bar{q}$ columns of $\underline{G}_{l-1}(z)$.
4. $\underline{G}(z)$ is obtained by exacting a $p \times q$ matrix from $M(z)$ by taking rows numbered $0, \bar{q}, 2\bar{q}, \dots, (p-1)\bar{q}$ and columns numbered $0, \bar{p}, 2\bar{p}, \dots, (q-1)\bar{p}$.

With this procedure, we can compute the blocked transmultiplexer.

From above we know that all $(\bar{p}\bar{q}l)$ -fold polyphase components of the subsystems $G_j, j = 0, 1, \dots, q-1$, appear exactly once in \hat{G} . Hence, there exists a one-to-one correspondence between the dual-rate G and the set of subsystems of G_0, G_1, \dots, G_{q-1} . As was observed, using general dual-rate systems provides more design freedom: All the $n \times n$ elements of the matrices $\underline{F}(z)$ and $\underline{H}(z)$ can be designed freely. Thus it is always possible to achieve perfect reconstruction by properly designing the subsystems in Figure 4.4.

Let us summarize as follows. With respect to the general transmultiplexer in Figure 4.4, first we represent each dual-rate subsystem by the LSTV structure in Figure 4.9; based on this we derive the blocked subsystems $\underline{F}_i(z)$ and $\underline{H}_i(z)$, using the above procedure; next, we form the synthesis and analysis matrix $\underline{F}(z)$ and $\underline{H}(z)$ as in (4.7) and (4.8); and finally, the blocked transmultiplexer has an $n \times n$ transfer matrix given by $\underline{T}(z) = \underline{H}(z)\underline{F}(z)$. This transfer matrix will be used for analysis and design in the sequel.

4.4 Perfect Reconstruction

As we saw in the preceding section, the blocked transmultiplexer is LTI with $\underline{T}(z) = \underline{H}(z)\underline{F}(z)$. In view of (4.7) and (4.8), we can write $\underline{T}(z)$ as a $m \times m$ block matrix:

$$\underline{T}(z) = \begin{bmatrix} T_{00}(z) & T_{01}(z) & \cdots & T_{0,m-1}(z) \\ T_{10}(z) & T_{11}(z) & \cdots & T_{1,m-1}(z) \\ \vdots & \vdots & & \vdots \\ T_{m-1,0}(z) & T_{m-1,1}(z) & \cdots & T_{m-1,m-1}(z) \end{bmatrix}, \quad (4.9)$$

where

$$T_{ij}(z) = \underline{H}_i(z)\underline{F}_j(z), \quad i, j = 0, 1, \dots, m-1.$$

The transmultiplexer achieves perfect reconstruction if in Figure 4.4 \hat{x}_i is a delayed version of x_i , i.e., if there exist nonnegative integers d_i such that $T = T_d$ with

$$T_d = \begin{bmatrix} D_{d_0} & 0 & \cdots & 0 \\ 0 & D_{d_1} & \cdots & 0 \\ \vdots & \vdots & & \vdots \\ 0 & 0 & \cdots & D_{d_{m-1}} \end{bmatrix}, \quad (4.10)$$

D_{d_i} being the time-delay system with transfer function $D_{d_i}(z) = z^{-d_i}$. Blocking T_d the same way as we blocked T , we can state a condition for perfect reconstruction in terms of the blocked transfer matrices.

Theorem 1 *The transmultiplexer in Figure 4.4 achieves perfect reconstruction if and only if*

$$\underline{H}(z)\underline{F}(z) = \begin{bmatrix} T_{00d}(z) & 0 & \cdots & 0 \\ 0 & T_{11d}(z) & \cdots & 0 \\ \vdots & \vdots & & \vdots \\ 0 & 0 & \cdots & T_{m-1,m-1,d}(z) \end{bmatrix},$$

where $T_{i;d}(z)$ is $r_i \times r_i$ and is of the form

$$T_{i;d}(z) = z^{-k_i} \begin{bmatrix} 0 & z^{-1}I_{s_i} \\ I_{r_i-s_i} & 0 \end{bmatrix} \quad (4.11)$$

for some integers k_i and s_i satisfying $k_i \geq 0$ and $0 \leq s_i \leq r_i - 1$. (Note that I_{s_i} is the $s_i \times s_i$ identity matrix; similarly for $I_{r_i-s_i}$.)

Proof From the previous discussion, perfect reconstruction is obtained if and only if for some integers d_i , \underline{T} equals the blocked T_d in (4.10), or equivalently,

$$\underline{H}(z)\underline{E}(z) = \begin{bmatrix} \underline{D}_{d_0}(z) & 0 & \cdots & 0 \\ 0 & \underline{D}_{d_1}(z) & \cdots & 0 \\ \vdots & \vdots & & \vdots \\ 0 & 0 & \cdots & \underline{D}_{d_{m-1}}(z) \end{bmatrix},$$

where \underline{D}_{d_i} is the blocked time-delay system $L_{r_i} D_{d_i} L_{r_i}^{-1}$. The transfer matrix for \underline{D}_{d_i} can be readily derived: Write $d_i = k_i r_i + s_i$ for $k_i \geq 0$ and $0 \leq s_i \leq r_i - 1$; then the polyphase components of D_{d_i} are given by

$$\hat{G}_j(z) = \begin{cases} z^{-k_i}, & j = s_i, \\ 0, & j \neq s_i. \end{cases}$$

Thus $\underline{D}_{d_i}(z)$ equals to the right-hand side of (4.11), see Property 4 on page 53. The theorem is therefore proven. \square

4.5 Distortion Measures

Many practical transmultiplexers do not achieve perfect reconstruction, or achieve close to perfect reconstruction. In order to measure the degree of closeness to perfect reconstruction, we shall introduce four quantities to measure sources of distortions: cross-talk distortion, aliasing distortion, magnitude and phase distortions. The aliasing distortion is unique and new in the nonuniform case and does not occur in the uniform case. These distortion measures are based on the blocked model $\underline{T}(z)$ in (4.9).

First, cross-talk exists if there is any signal leakage from one channel to another, or equivalently, if there is at least one non-zero off-diagonal block in $\underline{T}(z)$. We use the 2-norm of $T_{ij}(z)$ to measure its size:

$$\|T_{ij}(z)\|_2 = \left\{ \frac{1}{2\pi} \int_0^{2\pi} \text{trace} [T_{ij}(e^{j\omega})^* T_{ij}(e^{j\omega})] d\omega \right\}^{1/2}.$$

Here $T_{ij}(e^{j\omega})^*$ is the complex conjugate transpose of $T_{ij}(e^{j\omega})$. So $\|T_{ij}(z)\|_2^2$ is the energy of this block. The energy of all the off-diagonal blocks in $\underline{T}(z)$ can be used to quantify cross-talk distortion; so we define

$$\text{CD} = \left[\sum_{i,j(i \neq j)} \|T_{ij}(z)\|_2^2 \right]^{1/2}$$

as a measure for cross-talk distortion. Note that $(\text{CD})^2$ is the overall cross-talk energy present in the system.

If CD is zero, $\underline{T}(z)$ becomes a block-diagonal matrix; but the diagonal blocks arise from LPTV (instead of LTI) systems in general. This means that in Figure 4.4 the system from x_i to \hat{x}_i , namely, $H_i F_i$, is in general LPTV with period r_i , and $T_{ii}(z)$ is its blocked transfer matrix. This fact separates the transmultiplexer in Figure 4.4 from the uniform ones: A new aliasing distortion may be present in the system.

To quantify this effect, the following result from [7] is useful.

Lemma 1 *An LPTV system G with period r can be uniquely decomposed into*

$$G = G^{ti} + G^{tv}$$

satisfying the two properties

(i) G^{ti} is the optimal LTI approximation of G in the sense that it minimizes $\|\underline{G}(z) - \underline{Q}(z)\|_2$ over the class of LTI Q 's (\underline{G} denotes the blocked system $L_r G L_r^{-1}$; similarly for \underline{Q}).

(ii) $\|\underline{G}(z)\|_2^2 = r \|G^{ti}(z)\|_2^2 + \|G^{tv}(z)\|_2^2$.

The factor r in (ii) is due to the fact that we used the LTI system G^{ti} instead of \underline{G}^{ti} . How to compute this decomposition is given in [7]. Based on this lemma, the quantity $\|G^{tv}(z)\|_2$ can be used to measure aliasing in G .

Back to our transmultiplexer problem, the system from x_i to \hat{x}_i ($H_i F_i$) is LPTV with period r_i ; decompose this into $G_i^{ti} + G_i^{tv}$, where G_i^{ti} is the LTI component and G_i^{tv} the time-varying component. Thus we have

$$T_{ii}(z) = \underline{G}_i^{ti}(z) + \underline{G}_i^{tv}(z). \quad (4.12)$$

Aliasing distortion in the i -th channel is measured by

$$\text{AD}_i = \|\underline{G}_i^{tv}(z)\|_2. \quad (4.13)$$

The overall aliasing distortion is defined as

$$\text{AD} = \left(\sum_{i=0}^{m-1} \text{AD}_i^2 \right)^{1/2}. \quad (4.14)$$

Even if both CD and AD are zero, the i -th channel $H_i F_i$ which reduces to an LTI system G_i^{ti} may still have errors in magnitude and phase compared with the ideal time delay z^{-d_i} ; define the following quantities

$$\text{MD}_i = \left[\frac{1}{2\pi} \int_0^{2\pi} (|G_i^{ti}(e^{j\omega})| - 1)^2 d\omega \right]^{1/2}, \quad (4.15)$$

$$\text{PD}_i = \left\{ \frac{1}{2\pi} \int_0^{2\pi} \sin^2 [\angle G_i^{ti}(e^{j\omega}) + d_i \omega] d\omega \right\}^{1/2}. \quad (4.16)$$

Note that MD_i and PD_i are defined across all frequencies for the i -th channel: $(\text{MD}_i)^2$ is the energy of the magnitude distortion, and PD_i the energy of sine of the phase distortion $\phi(\omega) = \angle G_i^{ti}(e^{j\omega}) + d_i \omega$.

In summary, CD measures the cross-talk distortion of the transmultiplexer, AD_i , MD_i , and PD_i measure aliasing, magnitude, and phase distortions in the i -th channel.

Next, we propose a composite distortion measure which captures all the four types of distortions and is relatively easy to use in design. Comparing the transmultiplexer T with the ideal system T_d in (4.10), we get the error system $T - T_d$; the new distortion measure is the 2-norm of the blocked error transfer matrix:

$$J = \|\underline{T}(z) - \underline{T}_d(z)\|_2.$$

Such a measure is appropriate because in the next theorem we establish connections between J and the four types of distortions discussed earlier.

Theorem 2 *CD, AD, and MD_i relate to J via*

$$CD^2 + AD^2 + \sum_{i=0}^{m-1} r_i \text{MD}_i^2 \leq J^2; \quad (4.17)$$

whereas CD, AD, and PD_i relate to J via

$$CD^2 + AD^2 + \sum_{i=0}^{m-1} r_i \text{PD}_i^2 \leq J^2. \quad (4.18)$$

Proof From the representations for $\underline{T}(z)$ and T_d in (4.9) and (4.10), respectively, we get

$$\underline{T}(z) - \underline{T}_d(z) = \begin{bmatrix} T_{00}(z) - \underline{D}_{d_0}(z) & T_{01}(z) & \cdots & T_{0,m-1}(z) \\ T_{10}(z) & T_{11}(z) - \underline{D}_{d_1}(z) & \cdots & T_{1,m-1}(z) \\ \vdots & \vdots & \ddots & \vdots \\ T_{m-1,0}(z) & T_{m-1,1}(z) & \cdots & T_{m-1,m-1}(z) - \underline{D}_{d_{m-1}}(z) \end{bmatrix}.$$

From the 2-norm definition it is not hard to get

$$J^2 = \sum_{i,j(i \neq j)} \|T_{ij}(z)\|_2^2 + \sum_{i=0}^{m-1} \|T_{ii}(z) - \underline{D}_{d_i}(z)\|_2^2. \quad (4.19)$$

The first term is CD^2 . From (4.12) and Lemma 1 we get

$$\begin{aligned} \|T_{ii}(z) - \underline{D}_{d_i}(z)\|_2^2 &= \|\underline{G}_i^{ti}(z) + \underline{G}_i^{tv}(z) - \underline{D}_{d_i}(z)\|_2^2 \\ &= r_i \|G_i^{ti}(z) - z^{-d_i}\|_2^2 + \|\underline{G}_i^{tv}(z)\|_2^2 \\ &= r_i \|G_i^{ti}(z) - z^{-d_i}\|_2^2 + AD_i^2 \end{aligned}$$

Substitute this into (4.19) and note (4.14) to get

$$J^2 = CD^2 + AD^2 + \sum_{i=0}^{m-1} r_i \|G_i^{ti}(z) - z^{-d_i}\|_2^2.$$

The proof is complete by noting the following two inequalities which have been used in the uniform case (see Chapter 3):

$$\begin{aligned} \|G_i^{ti}(z) - z^{-d_i}\|_2 &\geq MD_i, \\ \|G_i^{ti}(z) - z^{-d_i}\|_2 &\geq PD_i. \end{aligned}$$

□

In view of Theorem 2, one can define the overall magnitude and phase distortions for the transmultiplexer in Figure 4.4 as follows:

$$MD = \left(\sum_{i=0}^{m-1} r_i MD_i^2 \right)^{1/2}, \quad PD = \left(\sum_{i=0}^{m-1} r_i PD_i^2 \right)^{1/2}.$$

Then it is clear from Theorem 2 that all distortions (CD , AD , MD , and PD) are bounded above by J . Therefore it makes sense to minimize J in transmultiplexer design because this suboptimizes the four distortions simultaneously.

4.6 Design Procedures

In view of Figure 4.4 and the new distortion measure J discussed in the preceding section, we wish to design synthesis and analysis subsystems to minimize J . The subsystems are implemented via the LSTV structure in Figure 4.9 with LTI systems which are FIR of a given length. Thus our optimal transmultiplexer design problem using FIR subsystems can be stated as follows:

Given the desired reconstruction time delays d_0, d_1, \dots, d_{m-1} , design FIR synthesis and analysis subsystems of some given lengths to minimize J .

Such an optimal design problem can be recast using the blocked model: Given $\underline{T}_d(z)$, design $\underline{F}(z)$ and $\underline{H}(z)$ of some given lengths to minimize

$$J = \|\underline{H}(z)\underline{F}(z) - \underline{T}_d(z)\|_2.$$

(Of course, for this design to be practical, one should impose some constraint to guarantee that the synthesis subsystems have certain frequency limiting properties; this can be achieved by incorporating some penalty on the stop-band ripples in the synthesis subsystems – see the design example later for more details.) Because both $\underline{F}(z)$ and $\underline{H}(z)$ are designable, this optimization problem is in general nonlinear and difficult to solve. Thus we propose the following iterative design procedure which turns out to be very effective in the design example to follow.

Step 1 Design synthesis subsystems to satisfy desired frequency limiting properties (without considering reconstruction performance); these are used to initiate the iteration.

Step 2 Given the synthesis subsystems, design FIR analysis subsystems by minimizing J ; using the blocked models, this is equivalent to

$$\min_{\underline{H}(z)} \|\underline{H}(z)\underline{F}(z) - \underline{T}_d(z)\|_2.$$

Step 3 Fixing the analysis subsystems just designed, now redesign FIR synthesis subsystems by minimizing J ; using the blocked models, this is equivalent to

$$\min_{\underline{F}(z)} \|\underline{H}(z)\underline{F}(z) - \underline{T}_d(z)\|_2.$$

Step 4 Repeat Steps 2 and 3 until J is sufficiently small.

We note that the idea of iteratively designing analysis and synthesis filters was used effectively in uniform filter bank design in [41]. The advantage of this procedure is evident: By fixing either $\underline{F}(z)$ or $\underline{H}(z)$ in Steps 2 and 3, the optimization problems

become mathematically tractable; in fact, they are finite-dimensional, convex optimization with a quadratic cost function, whose global optimal solution can be always computed. Even analytical solutions can be obtained.

For example, looking at the optimal design problem in Step 2, we define

$$P(z) = \underline{H}(z)\underline{E}(z) - \underline{T}_d(z).$$

This system is FIR and hence can be represented by its finitely coefficient matrices P_i . By Parseval's equality,

$$J = \|P(z)\|_2 = \left[\sum_i \text{trace}(P_i P_i') \right]^{1/2}. \quad (4.20)$$

Since $\underline{E}(z)$ and $\underline{T}_d(z)$ are given and thus $P(z)$ depends on $\underline{H}(z)$ in an affine manner, it follows that P_i relates to the coefficients of $\underline{H}(z)$ (to be designed) too in an affine manner. Therefore, we can rewrite the quantity in (4.20) in the following way:

$$J = [(Mx - b)'(Mx - b)]^{1/2}.$$

Here, x is a column vector containing all the parameters in $\underline{H}(z)$ to be designed, b is a column vector depending on only $\underline{T}_d(z)$, and M is a matrix depending on $\underline{E}(z)$ and the way x is formed. Both b and M can be computed and are independent of the design parameters (x). Now the optimal design problem in Step 2 becomes a least square problem:

$$\min_x [(Mx - b)'(Mx - b)]^{1/2}.$$

If the matrix M has full column rank, or equivalently $M'M$ is invertible, the optimal solution can be obtained to be

$$x_{opt} = (M'M)^{-1} M'b.$$

From here we can recover the optimal analysis subsystems. The optimal design problem in Step 3 can be solved similarly.

4.7 A Design Example

Let us now illustrate with a design example. Consider the three-channel nonuniform transmultiplexer depicted in Figure 4.10, built with traditional blocks (The filters involved are all causal and LTI). A dual structure in the filter bank case is impossible to

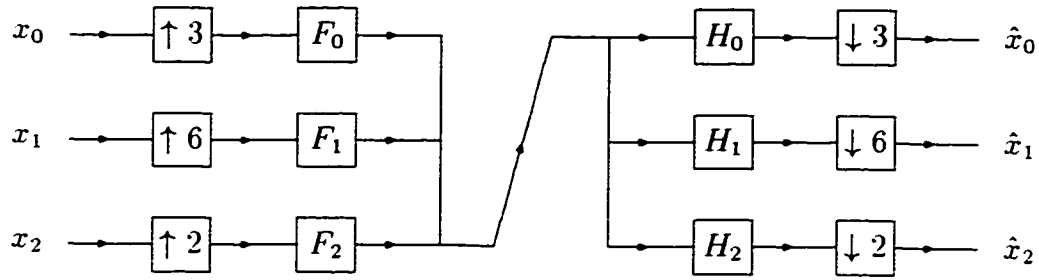


Figure 4.10: A three-channel nonuniform transmultiplexer using traditional building blocks.

achieve perfect reconstruction no matter how the causal LTI filters are designed [21]; hence perfect reconstruction is too impossible for the transmultiplexer in Figure 4.10 with causal LTI filters [39, 32, 24]. Nevertheless, we proceed by applying the iterative design procedure to see how close we can get to perfect reconstruction; and we shall compare the result with that of using general building blocks later.

How do we initiate the iterative procedure? One idea is to get the initial synthesis filters from the ideal, brick-wall ones. If we choose $H_i = F_i$ and F_0, F_1 , and F_2 to be ideal filters with passband, $[0, \pi/3)$, $[\pi/3, \pi/2)$, and $[\pi/2, \pi)$, respectively, it is readily verified that perfect reconstruction is achieved with $\hat{x}_i = x_i$; but these ideal filters do not satisfy the stability and causality properties. Suppose that FIR and causal synthesis filters of order 35 are to be designed; we initially use truncated and shifted ideal filters to start the iterative procedure. The magnitude responses of these initial synthesis filters (FIR and causal with order 35) are given in Figure 4.11.

Next we apply the iterative design procedure to the example in Figure 4.10. Shifting the truncated ideal filters for causality introduces time delays in the reconstruction; it is easy to calculate that these are $d_0 = 12$, $d_1 = 6$, and $d_2 = 18$, which are fixed in the design steps. The analysis and synthesis filters involved in design are all FIR and causal with a fixed order of 35.

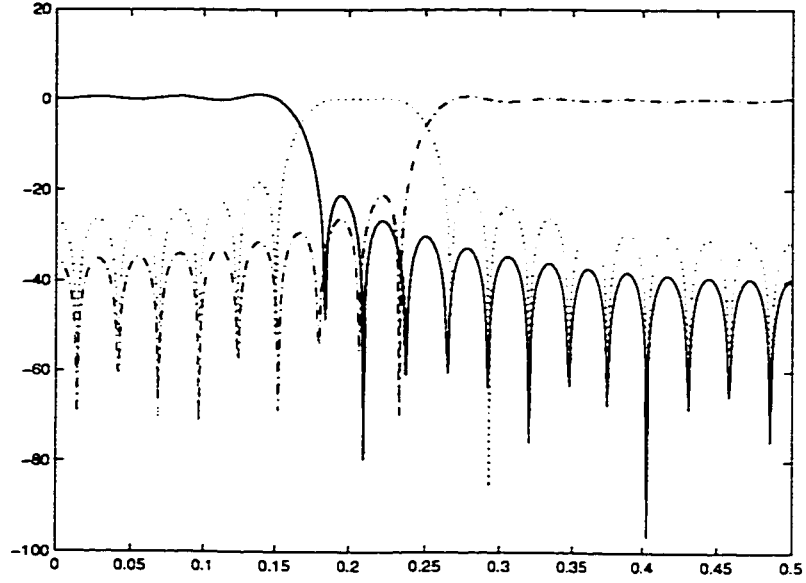


Figure 4.11: The magnitude responses for the initial F_0 (solid), F_1 (dotted) and F_2 (dash-dot): dB versus $\omega/2\pi$

It is easily to compute the expressions for the blocked subsystems:

$$\underline{H} = \begin{bmatrix} H_{00} & z^{-1}H_{05} & z^{-1}H_{04} & z^{-1}H_{03} & z^{-1}H_{02} & z^{-1}H_{01} \\ H_{03} & H_{02} & H_{01} & H_{00} & z^{-1}H_{05} & z^{-1}H_{04} \\ H_{10} & z^{-1}H_{15} & z^{-1}H_{14} & z^{-1}H_{13} & z^{-1}H_{12} & z^{-1}H_{11} \\ H_{20} & z^{-1}H_{25} & z^{-1}H_{24} & z^{-1}H_{23} & z^{-1}H_{22} & z^{-1}H_{21} \\ H_{22} & H_{21} & H_{20} & H_{00} & z^{-1}H_{25} & z^{-1}H_{24} \\ H_{24} & H_{23} & H_{22} & H_{21} & H_{20} & z^{-1}H_{25} \end{bmatrix},$$

and

$$\underline{F} = \begin{bmatrix} F_{00} & z^{-1}F_{03} & F_{10} & F_{20} & z^{-1}F_{24} & z^{-1}F_{22} \\ F_{01} & z^{-1}F_{04} & F_{11} & F_{21} & z^{-1}F_{25} & z^{-1}F_{23} \\ F_{02} & z^{-1}F_{05} & F_{12} & F_{22} & F_{20} & z^{-1}F_{24} \\ F_{03} & F_{00} & F_{13} & F_{23} & F_{21} & z^{-1}F_{25} \\ F_{04} & F_{01} & F_{14} & F_{24} & F_{22} & F_{20} \\ F_{05} & F_{02} & F_{15} & F_{25} & F_{23} & F_{21} \end{bmatrix}.$$

Because there are many structural constraints among the elements of \underline{H} and \underline{F} , we can not design \underline{H} or \underline{F} freely using the same method as we stated in Chapter 3. Some equality conditions must be included besides the object function. By changing the variables of the optimization problem, analytical method can still be used.

For example, in Step 3, note that the columns of \underline{F} are not independent. The second column has the same elements as the first one; they differ by inserting some delays and changing the order of the elements. Similarly for the last three columns. So,

instead of defining the whole matrix as the variable, we define three vector variables:

$$x_1 = \begin{bmatrix} F_{00} \\ F_{01} \\ F_{02} \\ F_{03} \\ F_{04} \\ F_{05} \end{bmatrix} \quad x_2 = \begin{bmatrix} F_{10} \\ F_{11} \\ F_{12} \\ F_{13} \\ F_{14} \\ F_{15} \end{bmatrix} \quad x_3 = \begin{bmatrix} F_{20} \\ F_{21} \\ F_{22} \\ F_{23} \\ F_{24} \\ F_{25} \end{bmatrix}.$$

By the properties of the 2-norm (2.21):

$$\begin{aligned} J^2 = \|\underline{H}(z)\underline{F}(z) - \underline{T}_d(z)\|_2^2 &= \|\underline{H}(z)x_1 - \underline{T}_d(z)^1\|_2^2 + \|\underline{H}_1(z)x_1 - \underline{T}_d(z)^2\|_2^2 \\ &+ \|\underline{H}(z)x_2 - \underline{T}_d(z)^3\|_2^2 + \|\underline{H}(z)x_3 - \underline{T}_d(z)^4\|_2^2 \\ &+ \|\underline{H}_2(z)x_3 - \underline{T}_d(z)^5\|_2^2 + \|\underline{H}_3(z)x_3 - \underline{T}_d(z)^6\|_2^2. \end{aligned}$$

where $\underline{H}_1(z)$, $\underline{H}_2(z)$ and $\underline{H}_3(z)$ are the matrices satisfying:

$$\begin{aligned} \underline{H}_1(z)x_1 &= \underline{H}(z)\underline{F}(z)^2, \\ \underline{H}_2(z)x_3 &= \underline{H}(z)\underline{F}(z)^5, \\ \underline{H}_3(z)x_3 &= \underline{H}(z)\underline{F}(z)^6. \end{aligned}$$

$\underline{T}_d(z)^i$ and $\underline{F}(z)^i$ are the i th column of \underline{T}_d and \underline{F} respectively.

Define

$$\begin{aligned} J_1 &= \|\underline{H}x_1 - \underline{T}_d^1\|_2^2 + \|\underline{H}_1x_1 - \underline{T}_d^2\|_2^2, \\ J_2 &= \|\underline{H}(z)x_2 - \underline{T}_d(z)^3\|_2^2, \\ J_3 &= \|\underline{H}(z)x_3 - \underline{T}_d(z)^4\|_2^2 + \|\underline{H}_2(z)x_3 - \underline{T}_d(z)^5\|_2^2 + \|\underline{H}_3(z)x_3 - \underline{T}_d(z)^6\|_2^2. \end{aligned}$$

Then the optimization problem is: Design x_i to minimize J_i , $i = 1, 2, 3$. Note that x_1 , x_2 and x_3 can be designed independently. The former optimization problem is changed into three sub-optimization problems. For each problem, the method we proposed in the uniform case is applicable except the variable is vector now instead of matrix.

After a good number of iterations, J converges to the value $J = 0.8038$: the corresponding synthesis and analysis filters are shown in Figures 4.12 and 4.13, respectively, for their magnitude responses; the distortions achieved for this design are summarized in Table 4.1. From there, it is clear that the the procedure produces a design with errors distributed fairly evenly among CD, AD, MD, and PD; but the limitation of using traditional building blocks is also evident: The distortions are relatively large. (Perfect reconstruction in this case is impossible to achieve as we commented before.)

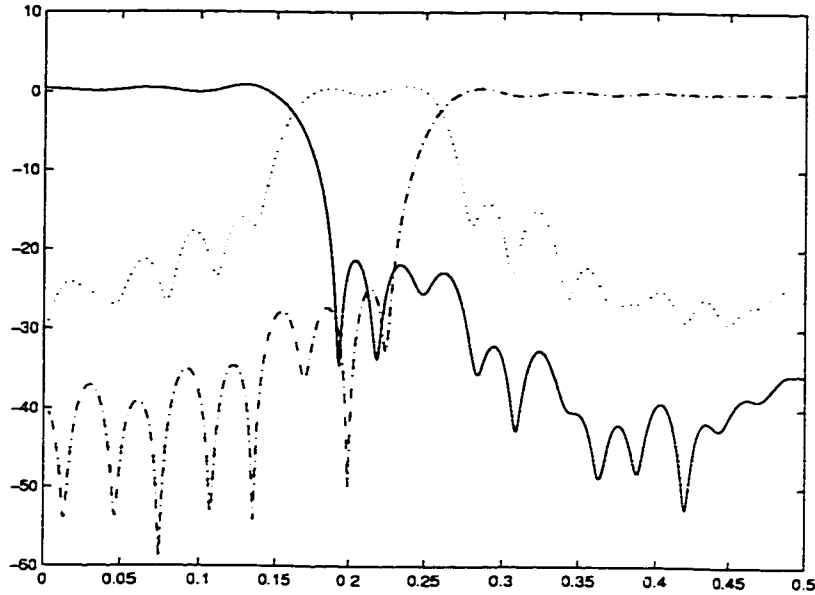


Figure 4.12: The magnitude responses for the designed F_0 (solid), F_1 (dotted) and F_2 (dash-dot): dB versus $\omega/2\pi$

Table 4.1: Distortions for design using traditional blocks.

J	0.8038
CD	0.2224
AD	0.2007
MD	0.2749
PD	0.2075

Now we adopt general building blocks for analysis subsystems as shown in Figure 4.14. This structure is interesting because it is mixed in that the synthesis part is built with traditional blocks, whereas the analysis part with general blocks. As we shall see later, such structure can produce substantially improved design in terms of reconstruction performance.

We use the same initial synthesis filters as in the previous design, obtained by truncating and shifting the ideal filters. The general blocks for analysis are represented by the LSTV structure in Figure 4.9: $H_0 : (2, 6)$ is implemented by an LSTV system with two LTI systems denoted by $H_{0,0}$ and $H_{0,1}$ followed by $\downarrow 3$; $H_1 : (1, 6)$ is implemented by a single LTI system ($H_{1,0}$) followed by $\downarrow 3$; and $H_2 : (3, 6)$ is implemented by an LSTV system with three LTI systems denoted by $H_{2,0}$, $H_{2,1}$, and $H_{2,2}$

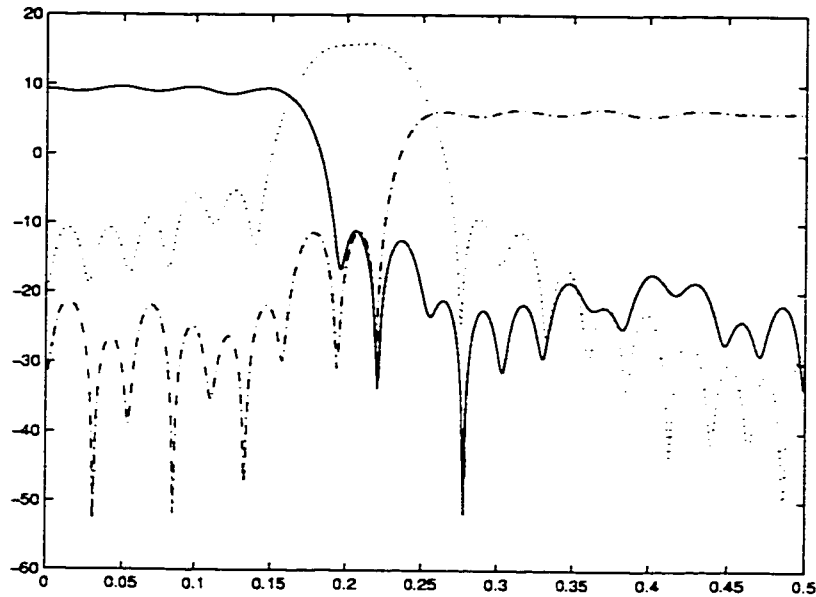


Figure 4.13: The magnitude responses for the designed H_0 (solid), H_1 (dotted) and H_2 (dash-dot): dB versus $\omega/2\pi$

followed by $\downarrow 2$. Thus for the analysis part, there are six LTI filters to be designed: $H_{0,0}, H_{0,1}, H_{1,0}, H_{2,0}, H_{2,1}$, and $H_{2,2}$. All the six LTI filters are causal and FIR with order 35 in the design exercise.

In order to have some control of the band limiting properties of the synthesis filters, in Step 3 of the iterative design procedure presented earlier we include penalties on the stopband ripples in the synthesis filters (F_0, F_1 , and F_2) to be designed: Instead

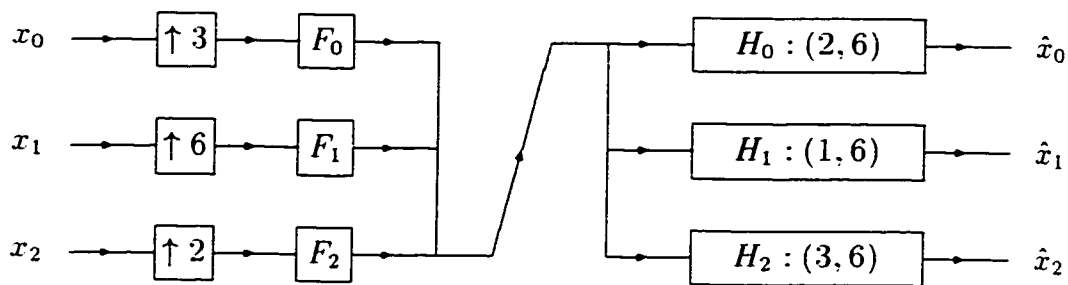


Figure 4.14: A three-channel nonuniform transmultiplexer using general analysis building blocks.

of minimizing J to design synthesis filters, we minimize the quantity

$$J^2 + \alpha_0 J_0^2 + \alpha_1 J_1^2 + \alpha_2 J_2^2,$$

where

$$\begin{aligned} J_0 &= \left\{ \left[\int_{-\pi}^{-\pi/3} + \int_{\pi/3}^{\pi} \right] |F_0(e^{j\omega})|^2 d\omega \right\}^{1/2}, \\ J_1 &= \left\{ \left[\int_{-\pi}^{-\pi/2} + \int_{-\pi/3}^{\pi/3} + \int_{\pi/2}^{\pi} \right] |F_1(e^{j\omega})|^2 d\omega \right\}^{1/2}, \\ J_2 &= \left[\int_{-\pi/2}^{\pi/2} |F_2(e^{j\omega})|^2 d\omega \right]^{1/2}. \end{aligned}$$

The constants α_0 , α_1 , and α_2 are tuned in the design which reflect relative weightings among multiple objectives: In our design of FIR synthesis filters of order 35, these are taken to be

$$\alpha_0 = 0.02, \quad \alpha_1 = 0.02, \quad \alpha_2 = 0.04.$$

The iterative procedure then generates a design with J converging to the value $J = 0.003050$, several order of magnitude better than the previous design using traditional building blocks. The Bode magnitude plots for the three synthesis filters and six analysis filters designed are given in Figures 4.15-4.18, and distortions achieved are given in Table 4.2. Note the significant reduction of distortions – an advantage of using general building blocks. Note also that the synthesis filters are band limiting: F_0 is lowpass, F_1 bandpass, and F_2 highpass. Similarly, the LTI filters in LSTV structures of the analysis end are frequency selective: $H_{0,0}$ and $H_{0,1}$ are lowpass. $H_{1,0}$ is bandpass, and $H_{2,0}$, $H_{2,1}$, and $H_{2,2}$ are highpass.

Table 4.2: Distortions for design using general blocks.

J	0.003050
CD	0.001031
AD	0.001933
MD	0.0001821
PD	0.0002117

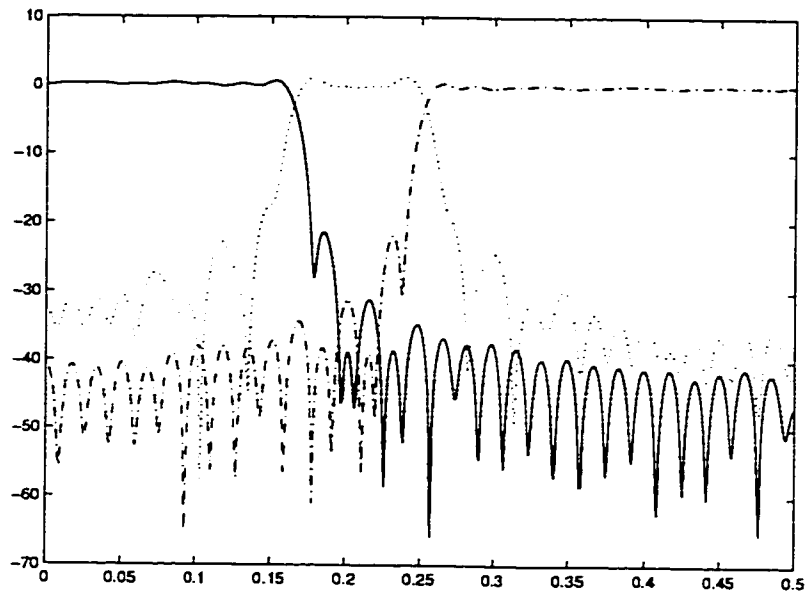


Figure 4.15: The magnitude responses for the designed F_0 (solid), F_1 (dotted) and F_2 (dash-dot): dB versus $\omega/2\pi$

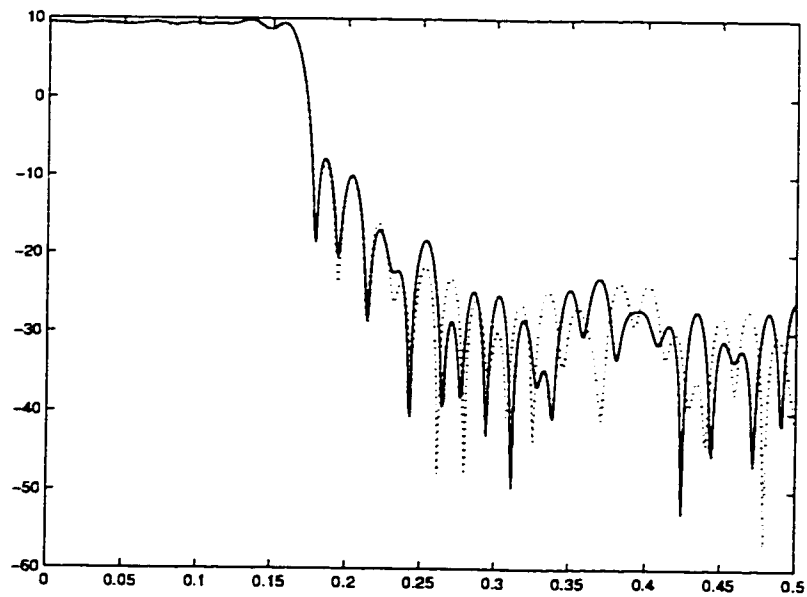


Figure 4.16: The magnitude responses for the designed $H_{0,0}$ (solid), $H_{0,1}$ (dotted): dB versus $\omega/2\pi$

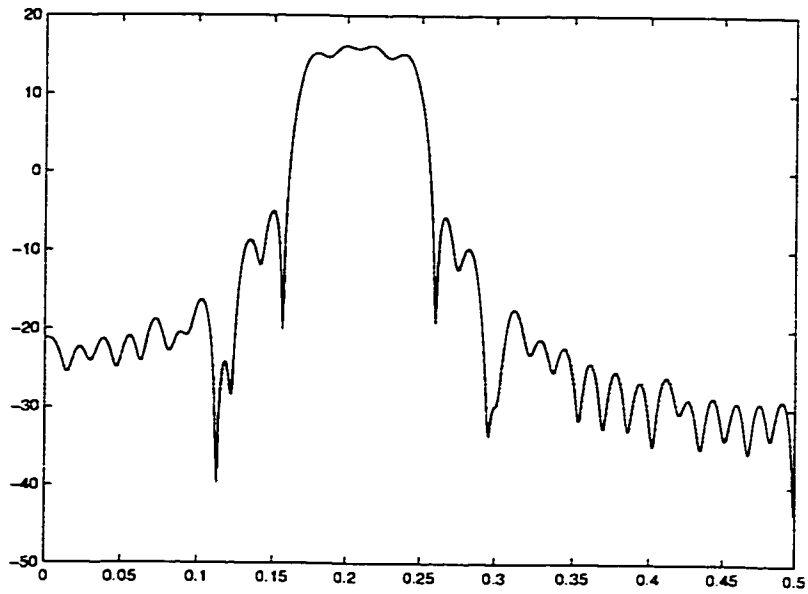


Figure 4.17: The magnitude responses for the designed $H_{1,0}$: dB versus $\omega/2\pi$

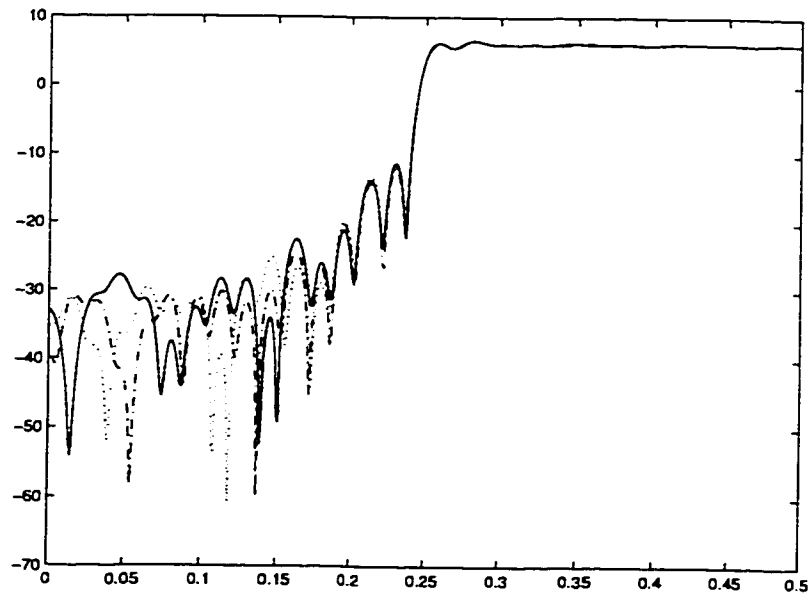


Figure 4.18: The magnitude responses for the designed $H_{2,0}$ (solid), $H_{2,1}$ (dotted) and $H_{2,2}$ (dash-dot): dB versus $\omega/2\pi$

Chapter 5

Conclusions

For both uniform and nonuniform transmultiplexers, we proposed ways to measure the distortions associated with a non-perfect reconstruction, and a new distortion criterion (J): 2-norm of the error system (or blocked error system for the nonuniform case). This new criterion has the merit of capturing the distortions all in one. Then we developed the related optimal design procedures.

The uniform case is a little easier according to its simple structure. The optimization problem in Step 2 of the design procedure in Chapter 3 can be solved analytically and it guarantees that the analysis filters designed have the optimal reconstruction property for a given set of synthesis filters. Two examples are presented. The performance is compared with the normal design approach.

The design of nonuniform transmultiplexers is more complicated. Unlike uniform case, the following points are observed:

- It is already known that normally perfect reconstruction is not achievable, so general dual-rate systems are introduced to allow more design freedom. In this case, the incompatibility for alias cancellation and structural dependency constraint for design, both due to fractional decimation ratios in different channels, are eliminated. The LSTV systems are used to realize the general building blocks.
- The whole system is no longer LTI. So we employ the blocking technique, and derive a blocked LTI model for the transmultiplexer in Figure 4.4. The transfer

matrix for the LTI model is calculated and the condition for perfect reconstruction is given.

- In Figure 4.4 from each input to its corresponding output is in general LPTV. So a new aliasing distortion is present.
- An optimal iterative design procedure based on the new error criterion is developed for FIR subsystems, which turns out to be very effective. At each iteration step, an optimal FIR design problem is solved by fixing the synthesis or analysis subsystems. In order to get the good band limiting characteristics for the synthesis subsystems, in Step 3 of the iterative design procedure we include penalties on the stopband ripples in the synthesis filters to be designed.

Possible extensions of this work are as follows:

- The design framework proposed for transmultiplexers could be made more useful if other design constraints are incorporated; in these cases, numerical optimization techniques would be necessary.
- An alternative distortion measure is the ∞ -norm of the error system or blocked error system for the nonuniform case; such a measure relates naturally to CD_{\max} , MD_{\max} , and PD_{\max} (or including AD_{\max}), which we proposed in Chapter 3. Design based on minimizing this measure will have direct control over CD_{\max} , MD_{\max} , and PD_{\max} (or AD_{\max} as well).

Bibliography

- [1] A.N. Akansu, P. Duhamel, X. Lin, and M. de Courville. "Orthogonal transmultiplexers in communication: a review," *IEEE Trans. on Signal Processing*, vol. 46, no. 4, pp. 979-995, 1998.
- [2] A.N. Akansu, M.V. Tazebay, and R.A. Haddad, "A new look at digital orthogonal transmultiplexers for CDMA communications," *IEEE Trans. on Signal Processing*, vol. 45, no. 1, pp. 263-267, 1997.
- [3] M. Bellanger, G. Bonnerot and M. Coudreuse, "Digital filtering by polyphase network: application to sample rate alteration and filter banks," *IEEE Trans. on Acoust. Speech and Signal Proc.* vol. ASSP-24, pp. 109-114, April 1976.
- [4] M. G. Bellanger and J. L. Daguet, "TDM-FDM transmultiplexer: Digital polyphase and FFT," *IEEE Trans. Commun.* , vol. COMM-22, pp. 1199-1205. Sept. 1974
- [5] J. Cioffi. "A multicarrier primer," *Amati Commun. Corp*, Stanford Univ. . Tutorial.
- [6] T. Chen, "Nonuniform multirate filter banks: analysis and design with an H-infinity performance measure," *IEEE Trans. on Signal Processing*, vol. 45, no. 3, pp. 572-582, 1997.
- [7] T. Chen and L. Qiu, "Linear periodically time-varying discrete-time systems: aliasing and LTI approximations," *Systems and Control Letters*, vol. 30, pp. 225-235, 1997.
- [8] T. Chen, L. Qiu, and E. Bai, "General multirate building structures with application to nonuniform filter banks," the Special Issue on Multirate Systems,

- Filter Banks, Wavelets, and Applications, *IEEE Trans. on Circuits and Systems II: Analog and Digital Signal Processing*, vol. 45, no. 8, pp. 948-958, 1998.
- [9] T. Chen and B.A. Francis, *Optimal Sampled-Data Control Systems*, Springer, 1995.
- [10] T. Chen and B.A. Francis, "Design of multirate filter banks by \mathcal{H}_∞ optimization", *IEEE Trans. on Signal Processing*, vol. 43, no. 12, pp. 2822-2830. 1995.
- [11] Ronald E. Crochiere and Lawrence R. Rabiner. *Multirate Digital Signal Processing*, Prentice-Hall. Englewood Cliffs, NJ, 1983.
- [12] D. Cochran and C. Wei, "Bandlimited orthogonal wavelet symbols," *Proc. 27th Asilomar Conf. Signals, Syst. Comput.*, Nov. 1993, pp. 528-532.
- [13] R. C. Dixon, *Spread Spectrum Systems*. New York: Wiley, 1976.
- [14] R. A. Dillard and G. M. Dillard, *Detectability of Spread Spectrum Signals*. Boston, MA: Artech House, 1976.
- [15] F. Daneshgaran and M. Mondin, "Coded modulation and coherent frequency-hopped CDMA with wavelets." *Proc. IEEE MILCOM*, Nov. 1995.
- [16] S. L. Freeny, J. G. Kaiser, and H. S. McDonald, "Some Applications of Digital Signal Processing in Telecommunication," in *Applications of Digital Signal Processing* (A. V. Oppenheim, Ed.) Englewood Cliffs, N.J.: Prentice-Hall, 1978. pp. 1-28.
- [17] S. L. Freeny, R. B. Kiebertz, K. V. Mina, and S. K. Tewksbury, "Design of Digital Filters for an All Digital Frequency Division Multiplex-Time Division Multiplex Translator," *IEEE Trans. Circuit Theory*, Vol. CT-18, No. 6, pp. 702-711, Nov. 1971.
- [18] D. J. Goodman and J. L. Flanagan, "Direct Digital Conversion between Linear and Adaptive Delta Modulation Formats," *Proc. IEEE Int. Comm. Conf.*, Montreal, June 1971.

- [19] John Hartung, "Architecture For The Real-Time Implementation of Three-Dimensional Sub-band Video Coding," *IEEE Trans. ICASSP*, vol. 3, pp. 225-228, 1992.
- [20] K. Hetling, G. Saulnier, and P. Das, "PR-QMF based codes for multipath/multiuser communications," *Proc. IEEE Blobecom.*, Oct. 1995.
- [21] P. Hong and P.P. Vaidyanathan, "Non-uniform multirate filter banks: theory and design," *ISCAS*, pp. 371-374, 1989.
- [22] J. Johnston, "A filter family designed for use in quadrature mirror filter banks," in *Proc. IEEE Int. Conf. Acoust. Speech and Signal Processing*, pp. 291-294, April 1980.
- [23] I. Kalet, "The multitone channel," *IEEE Trans. Commun.*, vol. 37, pp. 119-124, Feb. 1989.
- [24] R.D. Koilpillai, T.Q. Nguyen and P.P. Vaidyanathan, "Some results in the theory of crosstalk-free transmultiplexers," *IEEE Trans. on Signal Processing*, vol. 39, no. 10, pp. 2174-2183, 1991.
- [25] J. Linfner, "MC-CDMA and its relation to general multiuser/multisubchannel transmission systems," *Proc. Int. Symp. Spread Spectrum Tech. Applicat.*, Mainz, Germany, Sept. 1996.
- [26] C.-W. Lin and B.-S. Chen, "State space model and noise filtering design in transmultiplexer systems," *Signal Processing*, vol. 43, pp. 65-78, 1995.
- [27] X. Lin and R. Steele, "High Quality Audio Coding Using Analysis-By-Synthesis Technique," *IEEE Trans. ICASSP*, vol. 5, pp. 3617-3620, 1991.
- [28] R. A. Meyer and C. S. Burrus, "A unified analysis of multirate and periodically timevarying digital filters," *IEEE Trans. Circuits and Systems*, vol. 22, pp. 162-168, 1975.
- [29] T. Mirabbasi and C. W. Barnes, "Multirate recursive digital filters - a general approach and block structures," *IEEE Trans. Acoustics, Speech, Signal Processing*, vol. 31, pp. 1148-1154, 1983.

- [30] S. Mirabbasi, B. A. Francis, and T. Chen, "Controlling distortions in maximally decimated filter banks," *IEEE Trans. on Circuits and Systems II: Analog and Digital Signal Processing*, vol. 44, no. 7, pp. 597-600, 1997.
- [31] M. R. Portnoff, "Time-Frequency Representation of Digital Signals and Systems Based on Short-Time Fourier Analysis," *IEEE Trans. Acoust. Speech Signal Process.*, vol. ASSP-28, no. 1, pp. 55-69, February 1980.
- [32] R.P. Ramachandran and P. Kabal, "Transmultiplexers: perfect reconstruction and compensation of channel distortion," *Signal Processing*, vol. 21, pp. 261-274, 1990.
- [33] R.P. Ramachandran and P. Kabal, "Bandwidth efficient transmultiplexers. part 1: synthesis," *IEEE Trans. on Signal Processing*, vol. 40, no. 1, pp. 70-84, 1992.
- [34] R.P. Ramachandran and P. Kabal, "Bandwidth efficient transmultiplexers. part 2: subband complements and performance aspects," *IEEE Trans. on Signal Processing*, vol. 40, no. 5, pp. 1108-1121, 1992.
- [35] R.G. Shenoy, "Multirate specifications via alias-component matrices," *IEEE Trans. on Circuits and Systems II: Analog and Digital Signal Processing*, vol. 45, pp. 314-320, 1998.
- [36] P. Vary, "On the design of digital filter banks based on a modified principle of polyphase," *AEU*, vol. 6, pp. 97-112, April 1984.
- [37] P.P. Vaidyanathan, "Theory and design of M -channel maximally decimated quadrature mirror filters with arbitrary M , having the perfect-reconstruction property," *IEEE Trans. on Acoustics, Speech, and Signal Processing*, vol. 35, no. 4, pp. 476-492, 1987.
- [38] P.P. Vaidyanathan, *Multirate Systems and Filter Banks*, Prentice-Hall, Englewood Cliffs, NJ, 1993.
- [39] M. Vetterli, "Perfect transmultiplexers," *Proc. IEEE Int. Conf. Acoust. Speech and Signal Processing*, pp. 2567-2570, Tokyo, Japan, April 1986.

- [40] P. P. Vaidyanathan and S. K. Mitra, "Polyphase networks, block digital filtering, LPTV systems, and alias-free QMF banks: a unified approach based on pseudocirculants," *IEEE Trans. Acoustics, Speech, Signal Processing*, vol. 36, pp. 381-391, 1988.
- [41] H. Xu, W. Lu, and A. Antoniou, "Improved iterative method for the design of quadrature mirror-image filter banks." *IEEE Trans. on Circuits and Systems II: Analog and Digital Signal Processing*, vol. 43, no. 5, pp. 363-371. 1996.
- [42] Special Issue on TDM-FDM Conversion, *IEEE Trans. on Comm.*, vol. COM-26, no. 5, May 1978.